Chapter 15

ATMOSPHERIC TEMPERATURES, DENSITY, AND PRESSURE

Section 15.1 I.I. Gringorten, A.J. Kantor, Y. Izumi, and P.I. Tattelman
Section 15.2 A.J. Kantor and A.E. Cole
Section 15.3 A.J. Kantor and A.E. Cole

The three physical properties of the earth's atmosphere, temperature T, density ρ, and pressure P are related by the ideal gas law $P = \rho\ TR$ where R is known as the gas constant for air. Except for the one thousandth of 1% of the atmosphere by mass above 80 km, various gases comprise the atmosphere in essentially constant proportions. The principal exception is water vapor discussed in Chapters 16 and 21.

15.1 THERMAL PROPERTIES, SURFACE TO 90 KM

In the following sections the units of measurement are metric. Abbreviations are used whenever quantitative measures are presented. The temperature is in degrees Kelvin (K), density in kilograms per cubic meter (kg/m^3), pressure in millibars (mb), time in seconds (s) or hours (h), length in centimeters (cm), meters (m) or kilometers (km), and speed in meters per second (m/s) or kilometers per hour (km/h). The main unit of energy is the calorie (cal):

$$1 \text{ cal} = 4.1860 \text{ joules (J)}$$
$$= 1.163 \times 10^{-3} \text{ watt-hours (Wh)}.$$

For energy per unit area an additional unit, the Langley (L), is introduced:

$$1 \text{ L} = 1 \text{ cal/cm}^2$$
$$= 11.62 \text{ Wh/m}^2$$
$$= 41.84 \text{ kJ/m}^2.$$

The main unit of power is the watt (W), but the unit of solar power per unit area is given as Langleys per hour (L/H). In terms of the British Thermal Unit (BTU) 1 L/H = 3.686 BTU $\cdot$ ft^{-2} $\cdot$ h^{-1}.

15.1.1 Energy Supply and Transformation

The prime source of energy that produces and maintains atmospheric motions and the spatial and temporal variations of meteorological elements is the solar radiation intercepted by the earth. In comparison with solar radiation, other energy sources such as heat from the interior of the earth, radiation from other celestial bodies, or the tidal forces of the moon and sun are practically negligible. Manmade sources, such as the heat island of a city, can be neglected although their by-products, such as the increasing amounts of carbon dioxide in the atmosphere, have been subjected to intense scrutiny in recent years with respect to heat balance and climatic trends.

The rate at which solar energy is received on a plane surface perpendicular to the incident radiation outside of the atmosphere at the earth's mean distance from the sun is the *solar constant;* the approximate value used in this section is 2.0 L/min, or about 1400 W/m^2. (A detailed description of the solar constant and its empirically determined value is given in Chapters 1 and 2. The rate at which direct solar energy is received on a unit horizontal plane at the earth's surface or in the atmosphere above the earth's surface is called the *insolation*. The planetary *albedo,* which is the reflected radiation divided by the total incident solar radiation, varies primarily with angle of incidence of the radiation, the type of surface, and the amount of cloudiness. On the average, 30% to 40% of the incident solar energy is reflected back to space by the cloud surfaces, the clear atmosphere, the earth/air interface, and particles such as dust and ice crystals suspended in the atmosphere. The remaining 60% to 70% of the solar radiation is available as the energy source for maintaining and driving atmospheric processes.

Less than twenty years ago we could confidently consider the earth and its surrounding atmosphere as a self-contained thermodynamic system. No major energy changes in the system within the 50 to 100 year period of our climatological records were apparent. Globally there had been no obvious systematic short-term change in (1) heating of the earth's surface or the atmosphere, (2) the intensity of the atmospheric circulation, or (3) the balance between evaporation and precipitation. The processes affecting the internal and latent heat and the mechanical energy within the earth-atmosphere system had appeared virtually balanced.

Over the past twenty years there has been much agonizing by many experts and authors over the possibility of climatic change. Since there have been changes in the climate throughout geological history, it is inevitable that there will be long-term and large-scale changes in the future. Man-produced local changes through the use of fossil fuels, destruction of forests and desertification, irrigation on one hand and drainage of swamps on the other hand, urbanization and the introduction of pollutants in the air all have telling effects on local climate. The broader implications, however, over large regions and over decades or centuries have been the subject of many extensive and ongoing investigations by agencies worldwide with only one universally accepted conclusion. The carbon dioxide content of the atmosphere is increasing, which may lead to a global warming [WMO, 1979]. The next 5 to 10 years might produce a valid prediction.

A consensus among climatologists on heating or cooling of large regions of the earth or changes in rainfall patterns in response to natural or manmade influences is lacking. For this chapter the climate is considered to be stationary stochastic. It is stochastic because there is much variability in weather events and conditions that can be fitted into probability distributions assuming partially random processes. It is stationary because derived statistics or parameters, such as averages and standard deviations, are assumed to be unchanging. Their true values are constant and are best estimated by large samples.

The main features of the global energy transformation are summarized in a flow chart, Figure 15-1, from which the relative importance of the major energy cycles within the earth-atmosphere thermodynamic system can be determined. The numerical data presented in this figure are useful for various quantitative estimates. For example, if all energy inputs for the system ceased and rates of energy expenditure were maintained, the reservoir of mechanical energy (momentum) would be depleted in about 3 days, the reservoir of latent heat (precipitable water) in about 12 days, and the reservoir of internal energy (heat) in about 100 days.

Although an absolutely dry and motionless atmosphere is conceivable, it is difficult to imagine an atmosphere at zero degrees K. It is perhaps more appropriate to interpret the above time intervals as fictitious cycles of turnover of the atmospheric properties. The relative magnitudes of these life cycles show that, in comparison with rainfall and winds, temperature is the most conservative and will exhibit the relatively smallest, and thus most regular, temporal and spatial large-scale variation.

The solar energy input into the atmosphere at any one point varies during the earth's rotation about its axis and revolution about the sun. A consistent feature of this variation on a global scale is the driving force produced by differential latitudinal solar heating of the earth's surface. The reaction of the atmosphere to the solar driving force on an hourly, a daily, or an annual basis is observed most easily in the temperature field at low levels.

The solar energy input varies according to season, latitude, orientation of terrain to the incident energy, soil structure, all of which can change the balance between the incoming solar and sky radiation (*short wave*) and the outgoing atmosphere-terrestrial radiation (*long wave*). The difference between short-wave and long-wave radiation is the *net radiation*. Locally, net radiation is decreased primarily by atmospheric moisture (vapor and clouds). Evaporation of soil moisture diminishes by the latent heat required the portion of net radiation available for heating air and soil at the ground. The importance of moisture in establishing general climatic zones is shown by comparing desert climates with adjacent climates at roughly the same latitude. Table 15-1 gives the effect of soil moisture on the heat budget of the earth/air interface.

Slopes facing south receive maximum solar energy. Slopes facing west are usually warmer and drier than those facing east because the time of maximum insolation on a west slope is shifted to the afternoon when the general level of air temperature is higher than in the forenoon.

The energy balance of the earth/air interface requires that net radiation equals the sum of heat fluxes into the air and soil plus the heat equivalent of evaporation. In general, the maximum of heat flux into the soil precedes the maximum of heat flux into the air. The temperature maximum at standard instrument height (about 1.8 m) follows the maximum of heat flux into the air by roughly one to two hours.

15.1.2 Surface Temperature

15.1.2.1 Official Station Temperature. The standard station temperature used in meteorology [NWS, 1979] is measured by a thermometer enclosed within a white-painted, louvered instrument shelter or Stevenson Screen. The shelter has a base about 1 m (1.7 to 2.0 m in Central Europe) above the ground and is mounted in an open field (close-cropped grass surface). The standardized height of the thermometer is about 1.8 m. The shelter permits air circulation past the thermometer and is designed to exclude direct solar and terrestrial radiation. However, the shelter unavoidably absorbs and radiates some heat energy which, although minimal, causes some deviation of the thermometer reading from the "true" air temperature. On calm, sunny days the recorded daytime shelter temperature will normally be 0.5 to 1 K higher than the free air temperature outside the shelter at the same level. On calm, clear nights it will most likely

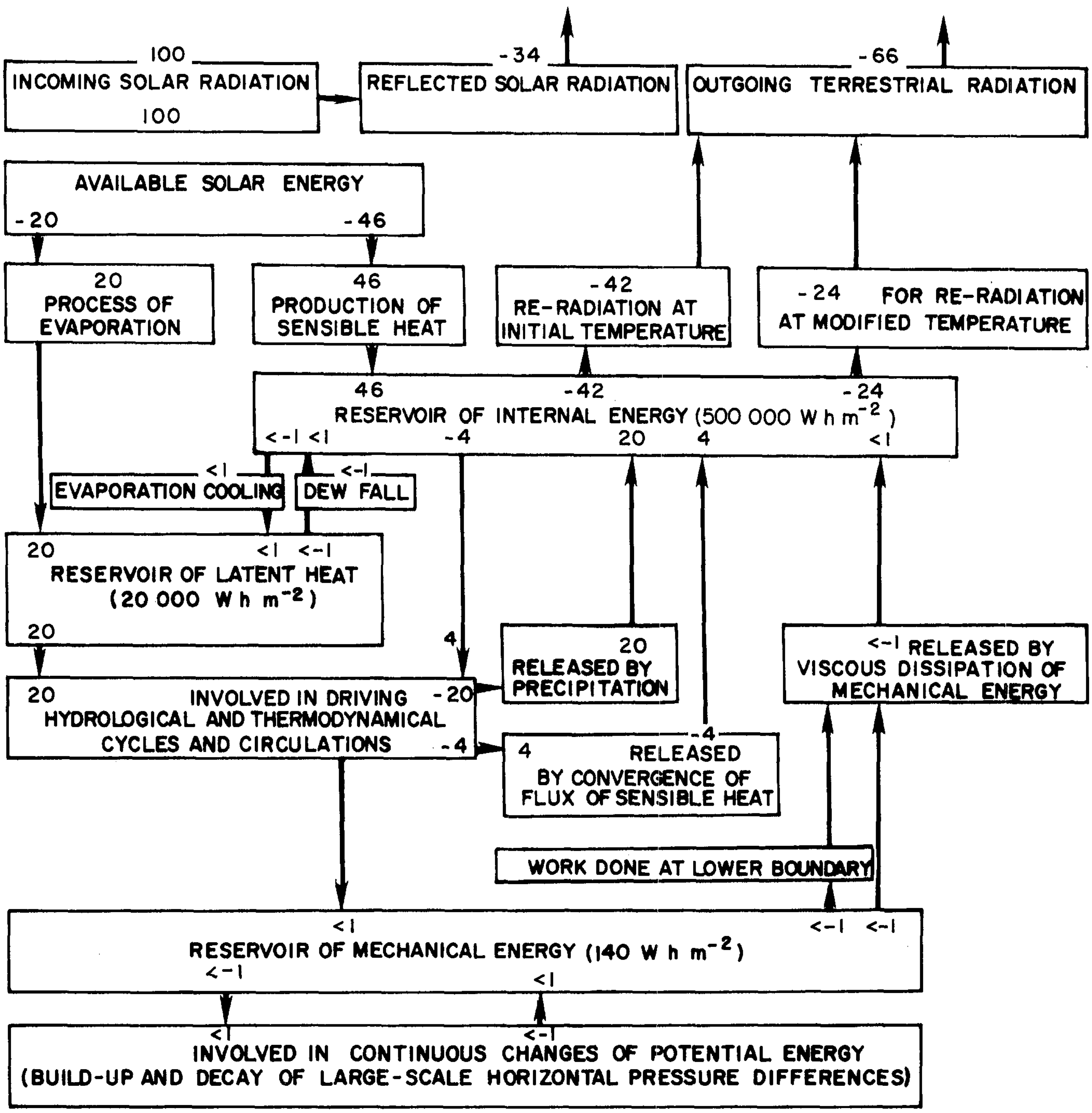

Figure 15-1. Global mean energy cycles of the atmosphere. All values are relative to 100 units of incoming solar radiation, which average 350 W/m^2, or 1/4 of the solar constant. [Revised from Lettau, 1954a].

be cooler by 0.5 K. Therefore, the thermometer should be artificially ventilated. Spatial variations of the ambient air temperature, especially in the first meter above the ground, are dependent upon the type of soil and ground cover. Ground effects decrease with height and for this reason the international standard heights of temperature measurement are a compromise between suppressing ground-cover effects and maintaining ease of access.

15.1.2.2 Daily Temperature. The official station temperature taken every hour on the hour reveals a fairly regular diurnal cycle. This is true despite several superimposed phenomena such as frontal passages and thunderstorms. Usually there is a temperature maximum in midafternoon and a temperature minimum near sunrise. The amplitude of the diurnal cycle varies with location and season from as little as 1 K to more than 17 K.

Table 15-1. Short-wave radiation on horizontal plane, net radiation, and estimated constituents of heat budget at the earth/air interface showing effect of difference in soil moisture caused by rains before 9 August and a dry spell before 7 September 1953 [Davidson and Lettau, 1957].

Radiation (W/m^2)									
Mean Local Time	04h	06h	08h	10h	12h	14h	16h	18h	20h
9 August 1953*									
Short-wave	0	141	544	733	796	823	537	144	—
Net	−59	47	364	497	540	525	273	−13	—
Flux into soil	−40	29	186	63	74	73	28	−65	—
Flux into air	−11	—	81	158	176	190	64	−17	—
Heat of evap.	−8	—	97	276	290	262	181	69	—
7 September 1953**									
Short-wave	0	54	441	765	870	735	407	44	0
Net	−54	−32	181	403	488	398	154	−69	−77
Flux into soil	−44	−25	36	84	95	66	13	−29	−28
Flux into air	−6	−6	98	230	303	299	114	−30	−39
Heat of evap.	−4	−1	47	89	90	33	27	−10	−10

*Mean soil moisture in 0 to 10 cm layer, about 10% wet weight basis.
**Mean soil moisture to 0 to 10 cm layer, about 4% wet weight basis.

The annual cycle of daily mean temperature ranges from practically zero near the equator to as much as 40 K in the temperate zone. As an example, Figure 15-2 shows temperatures at Hanscom AFB, Mass. The middle curve reveals the annual cycle of the daily mean temperature (actually the monthly mean is plotted) and shows an annual range of 25 K. The diurnal range, given here by the difference between mean daily maximum and minimum in Figure 15-2, is fairly uniform throughout the year, averaging 12 K.

Superimposed on both the diurnal and the annual cycles of temperature are many influences including cloudiness, precipitation, wind speed and direction, type of soil, ground cover, and aerodynamic roughness of the terrain. In the example of Figure 15-2, there is a range from the uppermost 1% of the daily maximum to the lowermost 1% of the daily minimum that is 3 times the mean diurnal cycle. The standard deviation of hourly temperature averages 5 K. The range from the uppermost 1% of the maximum temperature of the hottest month to the lowermost 1% of the minimum temperature of the coldest month in Figure 15-2 is about 2 1/2 times the mean annual cycle.

The pattern of surface temperature varies with geographic location. This is illustrated by the statistics of some widely scattered stations and even by the statistics of neighboring stations (Table 15-2). The annual mean temperature is generally lowest in the polar regions and highest in the equatorial belt. In addition, the mean temperature decreases generally with elevation. The diurnal range is greatest in desert climates and least in oceanic or maritime climates. The mean annual range tends to be greatest in temperate climates and least in equatorial climates.

In polar regions, where continuous darkness (daylight) endures for several months of the year, the 24-h cycle is minimal and the small diurnal variations are controlled primarily by changing winds and cloudiness. In summer, nearly all of the solar energy is expended in melting ice; hence, the maximum temperature seldom exceeds 273 K. Extra-

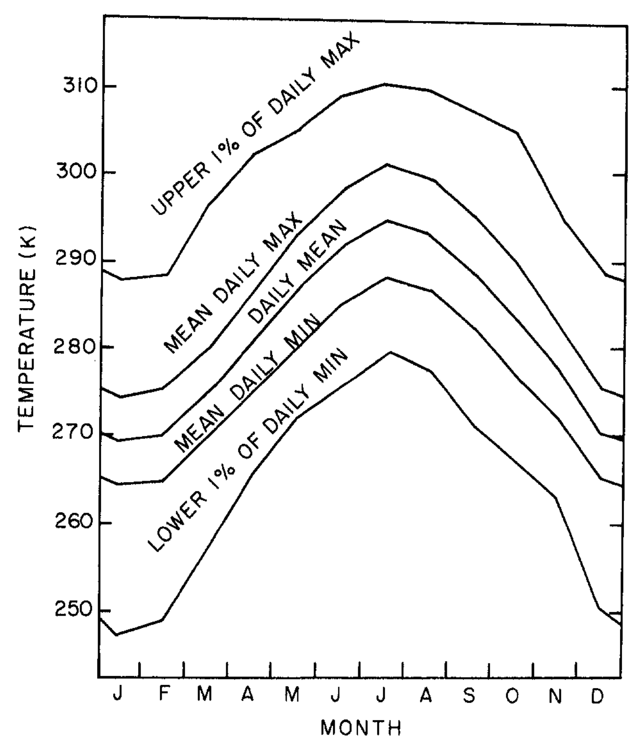

Figure 15-2. Surface temperature at Hanscom AFB, Mass. throughout the year.

Table 15-2. Temperatures at various stations around the world.

Station	Lat	Long	Elev. m	Annual Mean K	Mean Diurnal Range K	Mean Annual Range K	Hottest Month 1% of Daily Max K	Coldest Month 1% of Daily Min K
Hanscom AFB, Mass.	42°28'N	71°17'W	43	282.3	11.7	25.6	311	247
Boston, Mass.	42°22'N	71°02'W	5	283.8	8.6	24.3	—	—
Blue Hill Obs., Mass.	42°13'N	71°07'W	192	282.3	9.6	24.4	—	—
Nantucket, Mass.	41°15'N	70°04'W	13	282.7	7.2	20.4	—	—
Pittsfield, Mass.	42°26'N	73°18'W	357	280.2	11.4	25.6	—	—
Worcester, Mass.	42°16'N	71°52'W	301	281.2	9.5	25.4	—	—
Thule, Greenland	76°32'N	68°42'W	59	261.8	6.4	31.9	289	233
Eielson AFB, Alaska	64°41'N	147°05'W	170	270.2	10.8	39.6	303	224
Keflavik, Iceland	63°58'N	22°36'W	50	278.1	4.4	11.2	291	258
Goose Bay, New Foundland	53°19'N	60°25'W	44	273.2	9.5	33.7	307	237
Berlin, Germany	52°28'N	13°26'E	50	282.8	7.2	20.6	307	254
Limestone, Maine	46°57'N	67°53'W	230	276.9	9.4	29.4	308	241
Bolling AFB, Wash. D.C.	38°49'N	76°51'W	20	287.0	10.2	23.0	311	259
Scott AFB, Ill.	38°33'N	89°51'W	138	286.1	6.2	26.3	311	250
Blytheville, Ark.	35°58'N	89°57'W	81	278.4	6.8	17.9	312	255
Riverside, Calif.	33°54'N	117°15'W	461	292.7	16.8	14.4	314	269
Tucson, Arizona	32°10'N	110°53'W	809	289.4	11.7	19.0	316	267
Ft. Huachuca, Arizona	31°25'N	110°20'W	1439	290.0	14.8	17.0	312	264
Dharan, Saudi Arabia	26°17'N	50°09'E	22	299.8	11.8	19.8	321	276
Wheeler, Hawaii	21°29'N	158°02'W	256	295.8	7.5	4.0	305	283
Honolulu, Hawaii	21°20'N	153°55'W	12	297.7	6.7	4.2	308	291
Guam, Phillipines	13°29'N	144°48'E	82	300.8	1.7	1.7	306	297
Diego Garcia Island	07°18'S	72°24'E	2	300.7	3.9	2.0	305	296
Canton Island	02°46'S	171°43'W	3	300.7	1.2	0.8	305	297

tropical regions characteristically have distinct diurnal and annual cycles. These cycles are superimposed over temperature variations caused by shifting air masses and frontal passages. In tropical regions, the diurnal range rarely exceeds 6 K.

Depending on circumstances and ground characteristics, the surface air temperature could differ by several degrees over short distances ranging from a few meters to a few kilometers. Also, vertical temperature variations are observed from a few millimeters above the ground to the top of the instrument shelter. On windy, cloudy days or nights, the differences between thermometer readings, within short distances of one another in either the horizontal or the vertical, will be minimal. In high temperature regimes, however, with a bright sun and light winds, the ground surface, especially if dry sand, can attain temperatures 17 to 33 K higher than the free air. The temperature of air layers within a few centimeters of the surface will differ only slightly from the ground, but the decrease with height is rapid. The temperature at 0.5 to 1 m above the ground will be only slightly warmer than that observed in the instrument shelter at 1 or 1.5 m above the ground. Conversely, on calm, clear nights the ground radiation can produce a temperature inversion, as much as 4 or 5 K, in the air within several feet of the ground.

The induced temperature in military equipment exposed to the sun's heat will vary greatly with physical properties such as heat conductivity, reflectivity, capacity, and type of exposure. Surface and internal temperatures, such as are induced in a boxcar, make the reading of the shelter thermometer only the beginning of the engineering problem.

Table 15-2 is only an initial guide to the effects of various influences on station temperature. Detailed temperature information should be obtained from the climatological record of each station or of stations close by. The latter should be modified for the influences of terrain proximity to water, and elevation.

5.1.2.3 Horizontal Extent of Surface Temperature. Horizontal differences in surface temperature can arise both from large-scale weather disturbances and from local influences. Weather disturbances such as cold and warm fronts, thunderstorms, and squall lines account for unsystematic changes in the horizontal temperature gradient. Nonuniform radiational heating and cooling of the ground also contribute to turbulent mixing, cloudiness, and vertical motions in the

Table 15-3. Estimates of the horizontal scale of certain local meteorological conditions.

Local Conditions	Horizontal Scale (km)	Temperature Differences (K)
Changes in Air Mass	160 to 1600	3 to 22
Weather Fronts	16 to 160	3 to 22
Squall Lines	8 to 80	3 to 17
Thunderstorms	8 to 24	3 to 17
Sea Breezes	8 to 16	1 to 11
Land Breezes	3 to 8	1 to 6

lower troposphere, resulting in constantly changing temperatures at the surface.

Horizontal transport by air currents, referred to as advection, is a key factor in surface temperature differences. Large-scale advection will bring both the relatively dry cold arctic air masses and the relatively moist warm tropical air masses alternately to the temperature zones. This can produce large changes in the day's mean and the diurnal range of temperature.

Table 15-3 gives estimates of surface temperature differences over varying horizontal distances associated with several kinds of weather phenomena. Large-scale differences are greatest in winter due to the more substantial differential heating by solar radiation from equator to pole and, consequently, the more intense large-scale motion of the atmosphere. In summer the north-south gradients in solar insolation are much less, but the general increase in the amount of insolation results in more thunderstorms and other air-mass activity.

Systematic differences in the surface temperature between neighboring stations are due to five prime factors: (1) aspect or orientation of the terrain with respect to incident solar radiation, (2) type of surface structure and of soil cover underlying the stations, (3) proximity to the moderating influences of large water bodies, (4) elevation, and (5) difference in solar time for stations that are several hundred kilometers apart. Sometimes the topography permits "pools" of cold air to drain locally at night into lower basins or valleys. Also nonuniform distribution of water vapor and cloudiness will result in uneven distributions of short-wave and long-wave radiation and, consequently, uneven cooling and heating at the surface.

A striking example of local influences on surface temperature gradients is found in the temperature contrasts between cities and the surrounding countryside. The sheltering effect of buildings, their heat storage, products of fuel combustion, smog, rain water drainage, and snow removal all act to make the city a relative heat source. Thus, the city's nightly minimum temperature might be 5 to 14 K higher than that of surrounding suburbs. As another example, in hilly or mountainous terrain the valley floor could have a diurnal temperature range 2 to 4 times as great as that over the peaks, and a temperature minimum from 5 to 17 K lower. Also, some pronounced horizontal temperature gradients occur along coastlines in temperate latitudes due to the cooling effect of coastal sea breezes.

Generally, temperatures between two stations become more independent of one another with increasing distance (Figure 15-3). One model curve [Gringorten, 1979] for fitting the correlation coefficient ρ as a function of distance s between stations is given by

$$\rho = \frac{2}{\pi}[(\cos^{-1}\alpha) - \sqrt{1-\alpha^2}]\,, \qquad (15.1)$$

where

$$\alpha = \frac{s}{128r}, \qquad (15.2)$$

where r is the model parameter and is in the same units as the distance s. The value of r is, in fact, the distance over which the correlation coefficient is 0.99. For the curve in Figure 15-3, r = 17.7 km. While this curve could be fitted by other models, the given model curve has the quality that

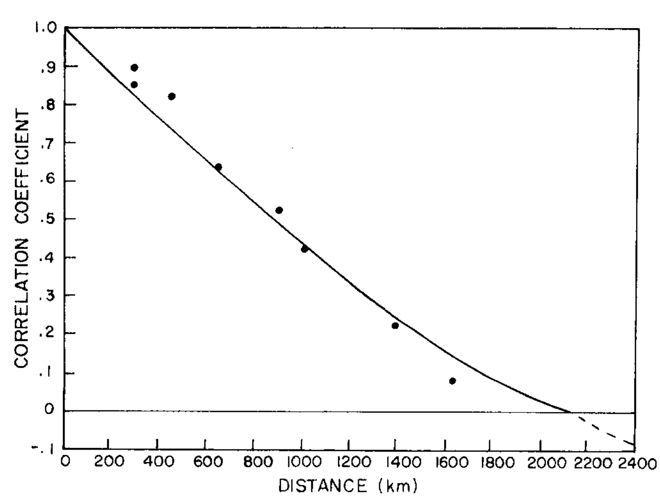

Figure 15-3. The correlation coefficient of the daily mean temperature of Columbus, Ohio with that of nine other U.S. stations at indicated distances from Columbus.

the correlation coefficient decreases exponentially with distance between stations for the first few kilometers of separation. Eventually, the correlation coefficient drops to zero at distance 128r.

In the United States the separation between weather stations averages about 160 km, with the exception of the eastern states where it is 30 to 80 km. The root mean square difference of temperatures, as a function of the correlation coefficient ρ between two stations is approximated by

$$\text{rmsd} = s_t \sqrt{2(1 - \rho)}, \qquad (15.3)$$

where s_t is the standard deviation of the hourly temperature (estimated as 5 K for Hanscom AFB). For stations 150 km apart, with $\rho = 0.91$ (Equation 15.1), the rmsd should be approximately 2 K.

15.1.2.4 Runway Temperatures. At airports the desired length of the landing strip or runway is directly related to air temperature. Any discrepancy, therefore, between free air temperature over runways and shelter temperatures is important in establishing safe aircraft payloads and runway lengths. It had been thought, on days when insolation is strong, that the free air temperature over airfield landing strips is significantly higher than standard shelter temperature over the surrounding grassy areas. Results of observations, however, over four airstrips (Easterwood Airport, Hearne Air Force Satellite Field and Bryan Air Force Base in Texas, and an auxiliary naval airstrip near Houma, Louisiana) have shown that the air between 0.3 and 6 m above a landing strip is about 0.5 K cooler than indicated by the shelter thermometer over adjacent grassy areas. The relative smoothness of the runway surface is the physical cause of daytime flow of air from grass to runway. During the transition from flow over the rough grassy surface the wind speeds up and entrains the cooler air immediately above the runway. When a daytime equilibrium state is established, there will be a large lapse rate close to the ground. This is the effect over both concrete and blacktop airstrips with surrounding grass having only a slightly modifying effect.

In exceptional cases the free air temperature over the runway exceeds the shelter temperature but by no more than 0.5 K when averaged over 10 min, 1 K when averaged over 1 min with a dry soil environment, and 0.25 K (5-min mean) with a swamp environment. Thus the standard method of temperature measurement in a properly exposed shelter over grass provides a representative temperature for the estimations of runway length and aircraft payloads.

15.1.2.5 Temperature Extremes. A knowledge of the occurrence of hot and cold temperature extremes is important for the design of equipment and the selection of material that will be exposed to the natural environment. The hourly temperature observations at most locations are not normally distributed around the mean monthly values. Departures from a normal distribution are largest in the temperate and northerly latitudes during the winter months when the temperature distributions are substantially bimodal. Thus the straightforward method for determining the frequency distribution of hourly temperatures is to obtain a representative sample of observations for each location and compute the distributions. Estimates of the frequency distribution from such data can be made using the Blom formula given by

$$\hat{P}(T) = \frac{n_T - 3/8}{N + 1/4}, \qquad (15.4)$$

where $\hat{P}(T)$ is the estimated cumulative probability of the temperature T, n_T is the number of observations equal to or less than T, and N is the overall sample size. Since, representative samples of data are not easily obtained for regions outside North America, an objective method has been developed by Tattelman and Kantor [1977] so that the frequency distribution of surface temperature can be estimated at all locations from data in climatic summaries that are available for most locations throughout the world.

Because the warmest temperatures in the world are found at locations where the monthly means are high and the mean daily range is large, Tattelman et al. [1969] developed an index using these values. The index is expressed by

$$I_w = \overline{T} + (\overline{T}_{max} - \overline{T}_{min}), \qquad (15.5)$$

where I_w is the warm temperature index, $\overline{T}$ is the monthly mean, $\overline{T}_{max}$ is the mean daily maximum, and $\overline{T}_{min}$ is the mean daily minimum temperature (K − 273) for the warmest month. The index was related to temperature occurring 1%, 5% and 10% of the time during the warmest months at a number of locations; it appears in the following regression equations for estimating monthly 1%, 5% and 10% warm temperature extremes [Tattelman and Kantor, 1977]:

$$\hat{T}_{1\%} = 0.676 I_w + 10.657, \qquad (15.6)$$

$$\hat{T}_{5\%} = 0.733 I_w + 5.682, \qquad (15.7)$$

$$\hat{T}_{10\%} = 0.762 I_w + 2.902. \qquad (15.8)$$

where $\hat{T}$ is the estimated temperature in (K − 273) occurring 1, 5, and 10% of the time, respectively. The same principle can be used to estimate cold temperature extremes. The cold temperature index is

$$I_c = \overline{T} - (\overline{T}_{max} - \overline{T}_{min}), \qquad (15.9)$$

where I_c is the cold temperature index, $\overline{T}$ is the monthly mean, $\overline{T}_{max}$ is the mean daily maximum, and $\overline{T}_{min}$ is the mean daily minimum temperature (K − 273) for the coldest months. The corresponding regression equations [Tattelman and Kantor, 1977] are

$$\hat{T}_{1\%} = 1.069 I_c - 7.013, \qquad (15.10)$$

$$\hat{T}_{5\%} = 1.084 I_c - 3.050, \qquad (15.11)$$

$$\hat{T}_{10\%} = 1.082 I_c - 0.704. \qquad (15.12)$$

This technique has been used by Tattelman and Kantor [1976a,b] to map global temperature extremes using locations for which monthly climatic temperature summaries are available. Estimates of the 1% warm and cold temperature extremes for the Northern Hemisphere are shown in Figures 15-4 and 15-5.

Most extreme high temperatures have been recorded near the fringes of the deserts of northern Africa and southwestern U.S. in shallow depressions where rocks and sand reflect the sun's heat from all sides. In the Sahara, the greatest extremes have been recorded toward the Mediterranean coast, leeward of the mountains after the air has passed over the heated desert. The highest temperature on record is 331 K at Al Aziziyah, Libya (32°32′N, 13°1′E, elevation 112 m). Northern Africa and eastward throughout most of India is the hottest part of the world, Large areas

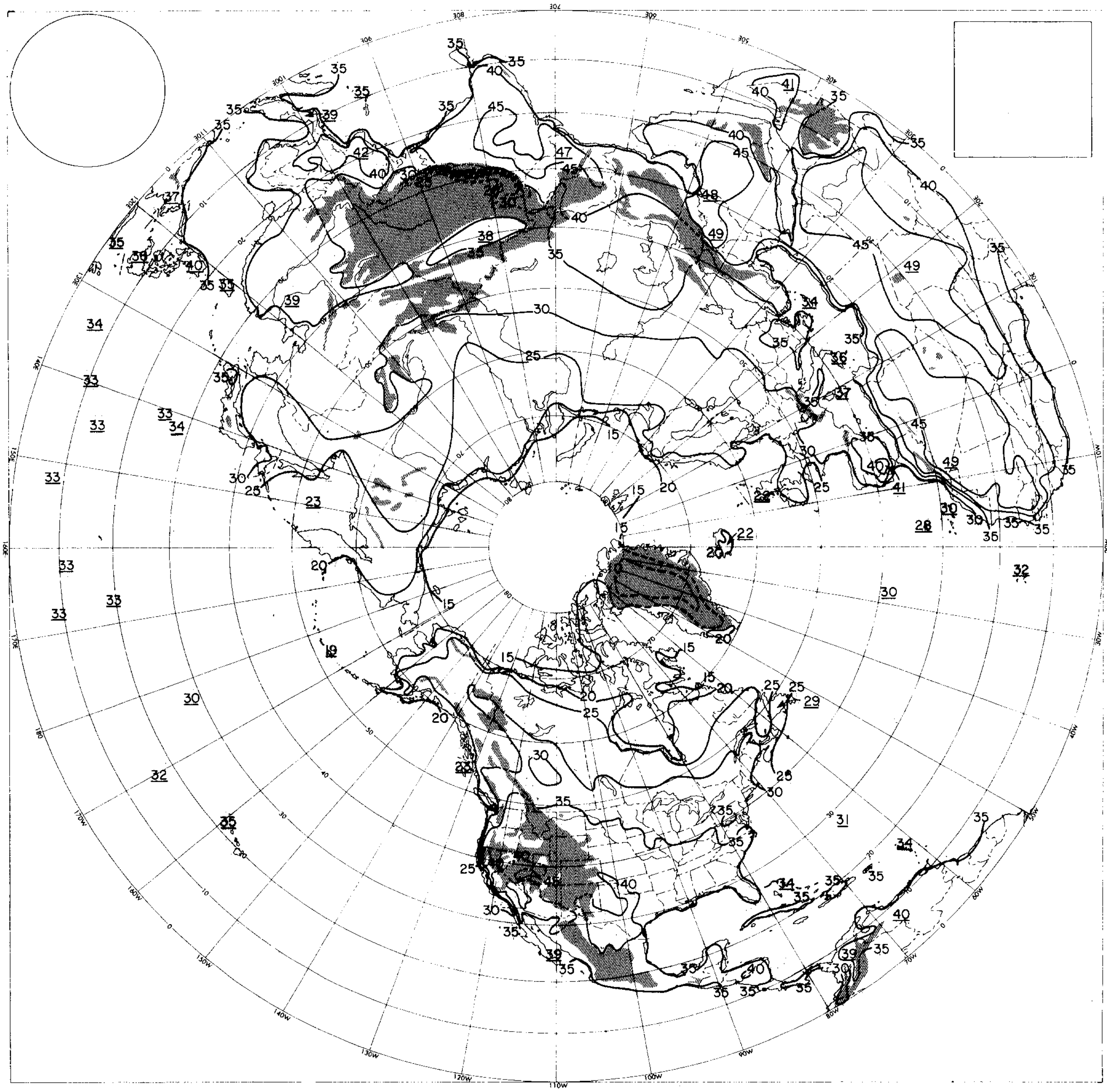

Figure 15-4. Temperature equaled or exceeded 1% of the time during the warmest month (K −273) [Tattelman and Kantor, 1976a].

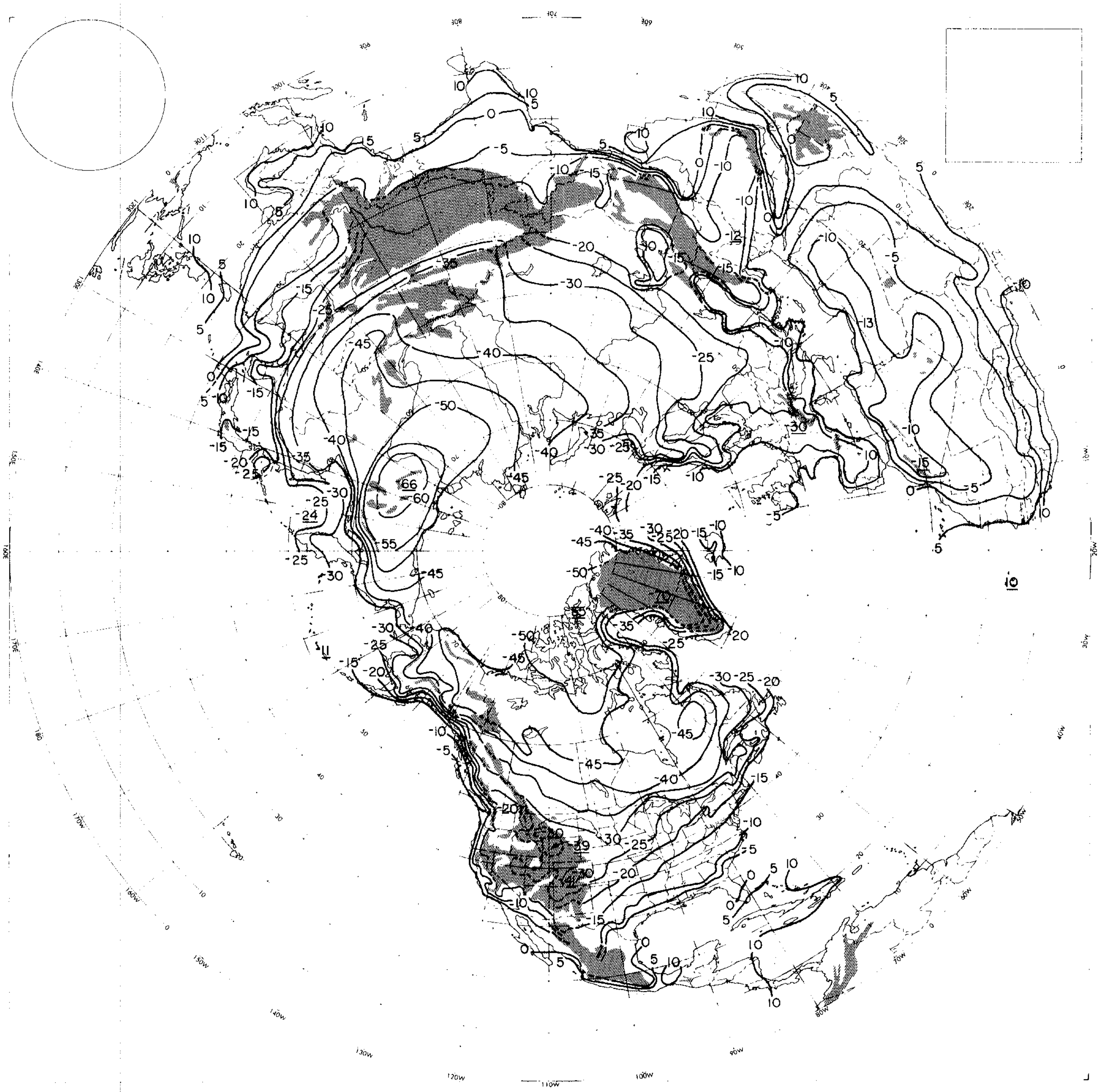

Figure 15-5. Temperature equaled or colder 1% of the time during the coldest month (K − 273) [Tattleman and Kantor, 1976a].

attain temperatures greater than 316 K more than 10% of the time during the hottest month. Sections of northwest Africa experienced temperatures greater than 322 K as much as 1% of the time during the hottest month of the year. Regions in Australia and South America have temperatures at and above 311 K much of the time, but do not experience temperatures greater than 316 K more than 1% of the time during the hottest month. The southwestern U.S. and a narrow strip of land in western Mexico are exceptionally hot. A substantial part of the area experiences temperatures equal to or greater than 316 K for 1% of the time in the hottest month. Death Valley, within this area, has temperatures equal to or greater than 322 K for 1% of the time in the hottest month and it once had a record temperature of 330 K.

Geographic areas of extreme cold include the Antarctic Plateau (2700 to 3600 m in elevation), the central part of the Greenland Icecap (2500 to 3000 m), Siberia between 63°N and 68°N, 93°E and 160°E (less than 760 m elevation) and the Yukon Basin of Northwest Canada and Alaska (less than 760 m elevation). The generally accepted record low temperature (excluding readings in Anarctica) is 205 K in Siberia.

15.1.2.6 The Gumbel Model. For equipment that is either in continuous operation or is on standby status, thereby continuously exposed to all temperatures, the statistic of interest is the extreme temperature that is likely to occur during a full month, season, year, decade, or whatever period is considered to be the useful lifetime of the equipment.

Many extreme values have been estimated effectively by a model that has become known as the *Gumbel* distribution. Let us assume the annual highest temperature (T_i) has been recorded for each of N years (i = 1,N) with average $\bar{T}$ and standard deviation s_t. The Gumbel estimate of the cumulative probability P_T of the annual extreme high temperature (T) is then

$$P_T = \exp[-\exp(-y)], \qquad (15.13)$$

where

$$y = \bar{y} + \frac{\sigma_y}{s_t}(T - \bar{T}), \qquad (15.14)$$

where, to five decimal places

$$\bar{y} = 0.57722 \text{ and } \sigma_y = 1.28255. \qquad (15.15)$$

(There are other estimates to the Gumbel distribution. This one is preferred for its simplicity as well as degree of accuracy.) The quantity y is referred to as the *reduced variate*. If one is interested in the cold temperature, these formulas hold with the T and $\bar{T}$ reversed in Equation (15.14).

If the lifetime of a piece of equipment is intended to be n years, then the cumulative probability $P_T(n)$ that the temperature T will not be exceeded in the n years is

$$P_T(n) = \exp[-\exp(-y + \ell n\ n)] \qquad (15.16)$$

where y is given by Equation (15.14). Assuming, for example, that we want to estimate the temperature T that has only a 10% probability or risk of being exceeded over n years, we set $P_T(n)$ equal to 0.9 in Equation (15.16) and solve Equation (15.16) for y obtaining

$$y = \ell n\ n - \ell n(-\ell n\ P), \qquad (15.17)$$

which we in turn use in Equation (15.14) to obtain

$$\hat{T} = \bar{T} + \frac{s_t(y - \bar{y})}{\sigma y} \qquad (15.18)$$

The return period is a term sometimes used in association with the extreme. In terms of the cumulative probability P_T of the annual extreme temperature, it is equal to $1/(1-P_T)$ years. The return period is not to be confused with the planned lifetime (n) of the equipment. Roughly speaking, the temperature with the 100-yr return period or the annual 1% (P_T = .99) is approximately the 10% temperature of a 10-year planned life.

The Gumbel distribution with a set of periodic extremes is the easiest model to use, but there are reservations in its application. Theoretically the basic distribution, such as the station temperature taken hourly, should be an exponential type, such as Pearson Type III or Gaussian. However, this condition may not be sufficient because the record may not be long enough to make the annual extreme fit into a Gumbel distribution. The Gumbel distribution is only the limiting form over long times and may not be adequately reached over short periods. It is advisable, therefore, to test the data to determine if the Gumbel distribution is applicable. Figure 15-6 illustrates the use of special-purpose "Extreme Probability Paper" in which the cumulative probability P_T is read on the vertical axis to correspond to T on the horizontal axis. Alongside the scale of P_T is the scale of the reduced variate y, which is uniform on this paper. A Gumbel distribution appears as a straight line.

Let us suppose a set of N extreme temperatures T_i for each of N years (i = 1,N) is ordered from lowest to highest value. The cumulative probability of the ith lowest temperature since it is an extreme is best estimated by

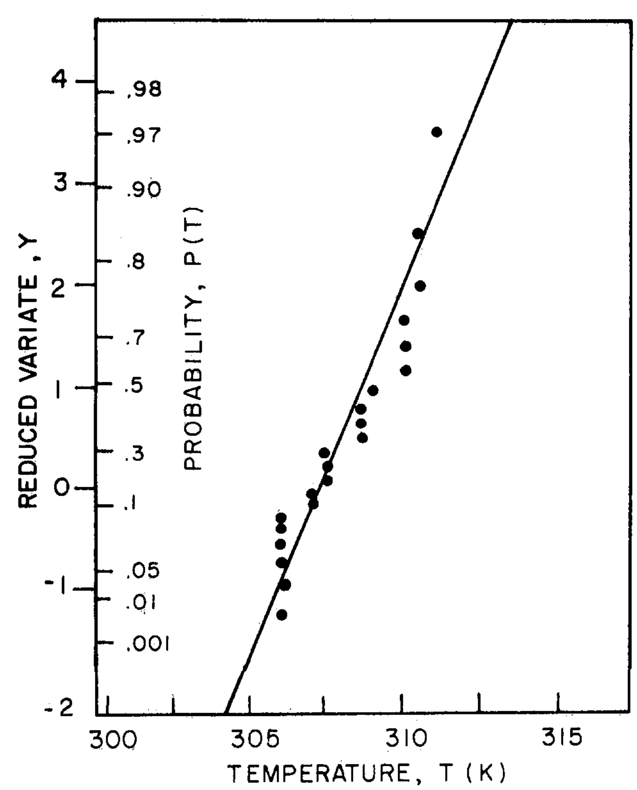

Figure 15-6. a) Annual highest temperature, Hanscom AFB, Mass., 21 ordered values (1944–1964).

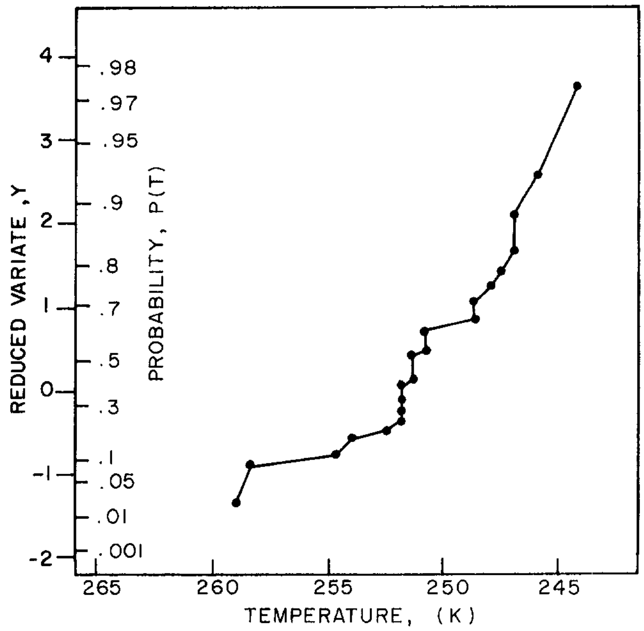

Figure 15-6. b) Lowest temperatures of 22 winter seasons (1943–1965) ordered from warmest to coldest, Hanscom AFB, Mass.

$$\hat{P}_T = \frac{i - 0.44}{N + 0.12} \qquad (15.19)$$

rather than Equation (15.4). Now in the example of Figure 15-6a, we have the plot of the annual highest temperatures of 21 years (1944–1964 at Hanscom AFB, Mass.) ordered from lowest to highest value and having cumulative probability estimates P_T given by Equation (15.19). The mean is $\overline{T}$ = 309 K and the standard deviation is s_t = 1.9 K. The solution of Equation (15.14) gives the straight line plot between y and T as shown. Whether the straight line and therefore the Gumbel distribution adequately fits the distribution is a matter of judgment. If accepted, and it should be in this example, then the 99th percentile (P_T = .99) or the 1% extreme is estimated by Equations (15.17) and (15.18) with n = 1 as 315 K. For a lifetime of 25 years (n = 25) the temperature of 10% risk (P_T = 0.9) is given by Equations (15.17) and (15.18) as 316 K.

As another example, Figure 15-6b shows the plot of the extreme low temperatures of 22 winter seasons (1943–1965) at Hanscom AFB, Mass. The mean is $\overline{T}$ = 251 K and the standard deviation is s_t = 3.68 K. A straight line fit of these data is not satisfactory. Possibly a concave curve would be more appropriate. The Gumbel model is not acceptable in this case, and consequently another model should be tried.

5.1.2.7 Temperature Cycles and Durations. High temperature extremes are inevitably part of a well pronounced diurnal cycle, modified by wind and by moisture content. Typical of a hot climate, the record of Yuma, Arizona (32°51′N, 114°24′W) (Figure 15-7) reveals a mean diurnal temperature range of 15.3 K for the middle 20 days in July.

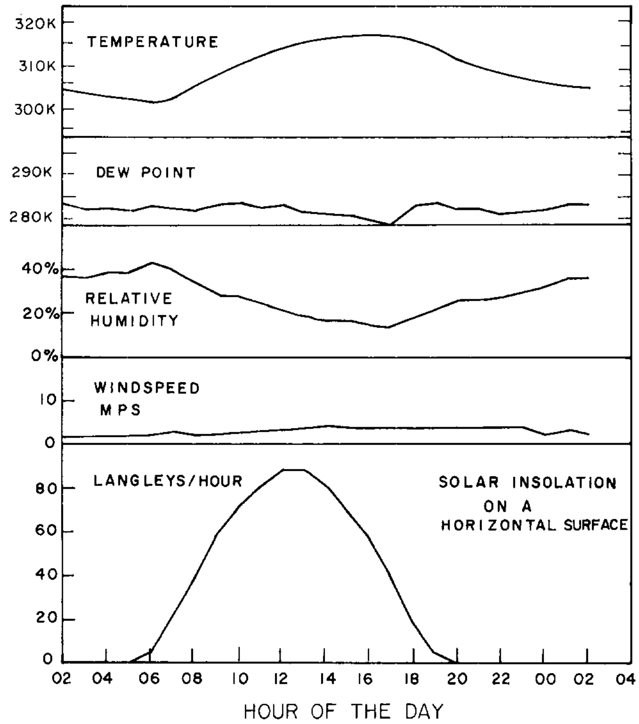

Figure 15-7. Yuma, Arizona typical July diurnal cycles when maximum daily temperature equals or exceeds 317 K (based on 1961–1968 data).

The dewpoint has a median of 287 K with a small diurnal range. Relative humidity, consequently, has a large-amplitude diurnal cycle. Wind speed at anemometer levels of 6 to 8 m above ground averages approximately 4 m/s with little diurnal range. Solar insolation, on the other hand, has a large diurnal range with a maximum clear-sky value of 88.2 L/h and a minimum value of zero from 2000 LST in the evening till 0500 LST in the morning. For the hottest areas on earth (for example, Sahara Desert) Table 15-4 presents the associated cycles of temperature, relative humidity, windspeed and solar insolation when the afternoon temperature in the middle of a 5-day period reaches 322 K which occurs about 1% of the time in the hottest month.

Death Valley, California is also one of the hottest areas but is close to 60 m below sea level resulting in extreme absorption of solar radiation before it reaches the ground. Consequently its maximum clear-sky solar insolation of 82.5 L/h is less than that shown in Figure 15-7. Solar insolation I increases with elevation roughly in accord with the exponential model given by

$$I = I_1 e^{-a(p-p_1)}, \qquad (15.20)$$

where p and p_1 are, respectively, atmospheric surface pressures for a given station and another reference station at roughly the same latitude I_1 is the solar insolation at the reference station, and the value for a is dependent on the location. For Yuma and Death Valley, where the mean

Table 15-4. Diurnal cycles of temperature and associated other elements for days when the maximum temperature equals or exceeds the operational 1% extreme temperature (322 K) in the hottest month in the hottest area.

	Time of Day (h)											
Item	1	2	3	4	5	6	7	8	9	10	11	12
	Temperature (K)											
Hottest Day	308	307	307	306	306	305	306	308	311	314	316	317
1 day before or after	309	308	307	306	306	305	306	309	311	313	315	317
2 days before or after	307	307	306	306	305	305	306	308	310	312	314	315
	Other Elements											
Relative Humidity (%) (dp = 266 K)	6	7	7	8	8	8	8	6	6	5	4	4
Windspeed (m/s)	2.7	2.7	2.7	2.7	2.7	2.7	2.7	2.7	2.7	4.3	4.3	4.3
Solar Radiation (L/H)	0	0	0	0	0	5	23	43	63	79	90	96
	Time of Day (h)											
Item	13	14	15	16	17	18	19	20	21	22	23	24
	Temperature (K)											
Hottest Day	320	321	321	322	321	321	319	315	314	312	311	310
1 day before or after	318	320	320	321	320	319	317	315	313	311	310	309
2 days before or after	316	317	319	320	319	318	317	314	312	311	310	309
	Other Elements											
Relative Humidity (%) (dp = 266 K)	3	3	3	3	3	3	3	4	5	6	6	6
Windspeed (m/s)	4.3	4.3	4.3	4.3	4.3	4.3	4.3	4.3	4.3	4.3	4.3	2.7
Solar Radiation (L/H)	96	90	79	63	43	23	5	0	0	0	0	0

atmospheric surface pressures are about 1006 mb and 1020 mb respectively, $a = 0.00461\ mb^{-1}$.

The hottest locations in the Sahara Desert are relatively high (about 300 m above sea level) with atmospheric pressure about 977 mb. Thus Equation (15.20) yields an estimate for the peak solar insolation at these elevations of about 100 L/h. Most countries, however, including the U.S., Canada, and the United Kingdom, have adopted a peak figure for solar insolation for operational and design purposes of 96 L/h.

Heavy clouds and precipitation reduce the incident solar insolation. At a few stations the National Weather Service has taken records of incoming solar insolation. Table 15-5 gives the results of processing such data from Albuquerque, N.M. It presents estimates of the probabilities with which daily incoming solar insolation equals or exceeds the given amount in June. In contrast, Table 15-6 gives corresponding results for the insolation at Caribou, Maine where there is much more frequent cloudiness and precipitation.

The operability of equipment in a cold climate is very much dependent on the *duration* of extreme cold. Unlike the hot extremes, cold extremes are usually accompanied by very small diurnal ranges, if any. The direct approach for determining the duration of cold temperature is by an analysis of hourly data. Such data are available for many stations in North America but are not generally available for other regions of the world. Data from 108 stations in the U.S. and Canada have been analyzed [Tattelman, 1968] to obtain information on the longest period of time during which the temperature remained at or below eight "threshold" values (from 273 K to 220 K) during a 10-yr period. Figure 15-8 from that report shows the results for a threshold

Table 15-5. Probability of daily solar insolation equaling or exceeding given amounts for given number of consecutive days in June, at Alburquerque, N.M. Station elevation is 1620 m. Peak clear sky solar insolation was observed at 910 L/day.

Insolation	No. of Consecutive Days					
L/Day	1	2	4	8	15	30
850	0.03					
800	0.24	0.06				
750	0.49	0.28	0.09			
700	0.71	0.54	0.31	0.11		
650	0.81	0.70	0.52	0.29	0.09	
600	0.90	0.84	0.77	0.52	0.29	0.08
550	0.935	0.90	0.81	0.65	0.44	0.20
500	0.955	0.93	0.87	0.75	0.57	0.33
450	0.971	0.95	0.91	0.82	0.67	0.43
400	0.985	0.972	0.946	0.87	0.81	0.65
350	0.9933	—	0.973	0.945	0.902	0.82
300	0.9946	—	0.980	0.958	0.928	0.86
250	0.9975	—	—	0.980	0.963	0.932
200	0.999	—	—	—	—	0.970

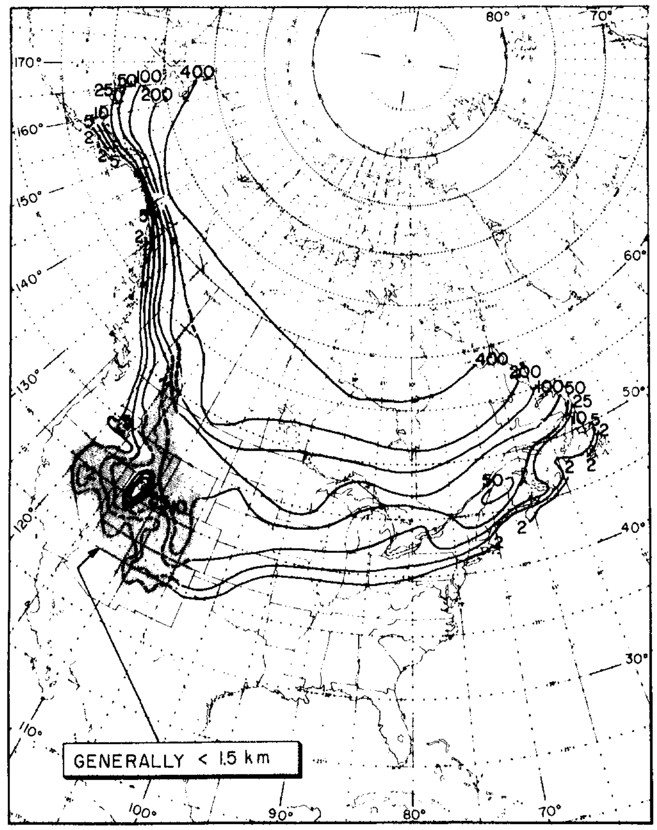

Figure 15-8. Longest duration (h) of temperature ≤ 250 K in ten winters [Tattelman, 1968].

Table 15-6. Probability of daily solar insolation equaling or exceeding given amounts for given number of consecutive days in June, at Caribou, Maine. Station elevation is 190 m. Peak clear sky solar insolation was observed at 843 L/day.

Insolation	No. of Consecutive Days					
L/Day	1	2	4	8	15	30
850						
800	0.019					
750	0.085	0.02				
700	0.20	0.057				
650	0.31	0.13	0.02			
600	0.40	0.20	0.05			
550	0.47	0.26	0.086			
500	0.55	0.33	0.13	0.024		
450	0.59	0.40	0.18	0.037		
400	0.66	0.50	0.26	0.075		
350	0.72	0.56	0.33	0.12	0.02	
300	0.78	0.67	0.47	0.22	0.062	
250	0.82	0.72	0.54	0.30	0.10	
200	0.88	0.80	0.66	0.42	0.22	0.05
150	0.921	0.87	0.77	0.59	0.37	0.13
100	0.965	0.943	0.90	0.79	0.63	0.40
90	0.975	0.96	0.92	0.84	0.72	0.51
80	0.980	0.962	0.93	0.86	0.75	0.56
70	0.987	0.978	0.956	0.912	0.83	0.70
60	0.9931	—	0.971	0.947	0.903	0.82
50	0.9961	—	—	0.977	0.95	0.90
40	0.99906	—	—	—	—	0.97

temperature of 250 K. The report also presents the expected (approximately 50% probability) duration of the temperature at or below six "threshold" temperatures (from 273 K to 232 K) during a single winter season. Figure 15-9 shows the single winter results for a threshold value of 250 K.

Estimates of duration have been made using data that consisted mainly of daily, monthly and annual average maximum and minimum, and monthly and annual absolute maximum and minimum, for some 35 to 50 years at Siberian, Yukon and Alaskan stations. The mean January temperature in eastern Siberia (Verkhoyansk and Oimyakon) is 225 K. Table 15-7 presents estimates of the lower 20% of the average temperature (averaged for durations ranging from one hour to 32 days), the maximum temperature for the durations shown, and the minimum temperature for the same durations.

The duration of temperature anywhere, hot or cold, is of general interest. In the midlatitude belt the temperatures of Minneapolis, Minn. are typical (Figure 15-10). The January probability distribution of all hourly temperatures has a 1% value of 244 K, and a 50% or median value of 263 K. That is, the range from the lower 1% to the median is 19 K. The 24-h averages, as expected, have a narrower range, 17 K. The range of monthly averages (768 h) is much narrower, 7 K. Similarly, the July hourly temperatures have

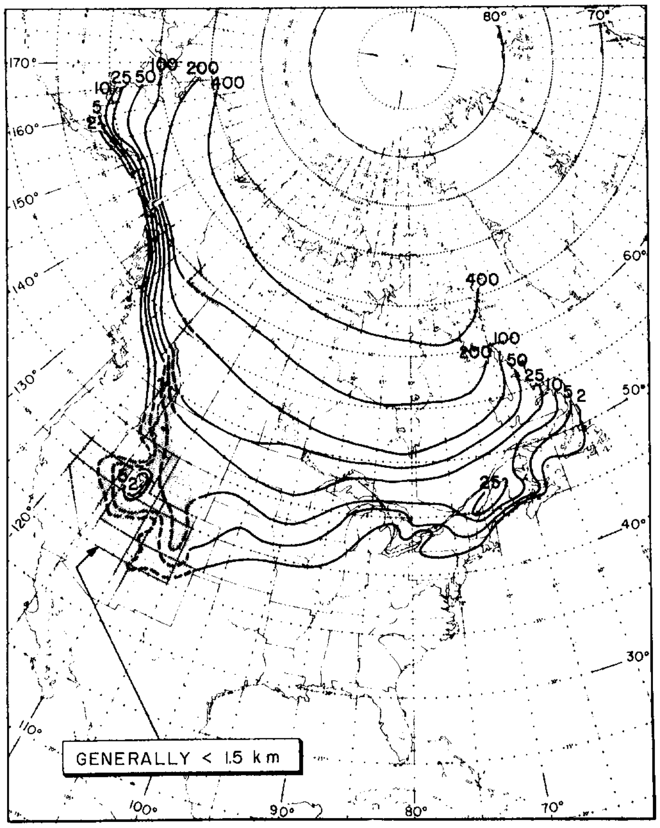

Figure 15-9. Expected longest duration (h) of temperature ≤ 250 K during a single winter season [Tattelman, 1968].

a 12 K range from the 50% value of 295 K to the upper 1% value of 307 K. The 24-h averages have an 8 K range and monthly averages have only a 2 K range. These figures imply a relatively high hour-to-hour correlation. Correlation analysis has provided estimates of 0.982 in the midwinter

Table 15-7. Durations of cold temperatures associated with the 222 K extreme. Each temperature in this table is the maximum, average, or the minimum in an operational time exposure of m hours, with 20% probability of occurrence, during January, in a Siberian cold center.

	Time m(h)									
	1	3	6	12	24	48	96	192	384	768
Maximum Temperature K	222	223	224	225	226	228	230	334	238	241
Average Temperature K	222	222	222	222	222	222	222	223	223	224
Minimum Temperature K	222	222	220	219	217	216	215	213	211	210

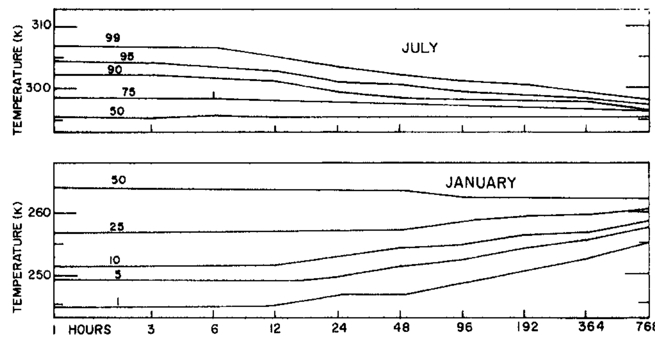

Figure 15-10. The distribution of the averages of consecutive hours of temperature at Minneapolis, Minn. (The upper half is for mid-summer month, from 1 July to 1 August; the lower half is for mid-winter month, 1 January to 1 February. Each curve is labeled with percent probability of occurrence.)

month of January, and 0.919 in the midsummer month of July.

Hourly observations have been taken at Minneapolis for many years, making many useful summaries possible. Figure 15-11 shows a sample distribution (1949–1958) of hourly January temperatures alongside the left axis and the distribution of m-hour minima over the body of the graph, m from 1 hour to 768 hours (1 Jan to 1 Feb inclusive). Figure 15-12 shows the sample distributions of hourly temperatures in January of m-hour maxima. As an example of the usefulness of such a chart, freezing conditions (≤273 K) are shown as 94% frequent for 1-h durations. For 24 consecutive hours this frequency reduces to 83%, for 8 days (192 h) to 42% and for 16 days (384 h) to 10%.

15.1.3 Upper Air Temperature

The temperature data discussed in this section are from direct and indirect observations obtained from balloon-borne

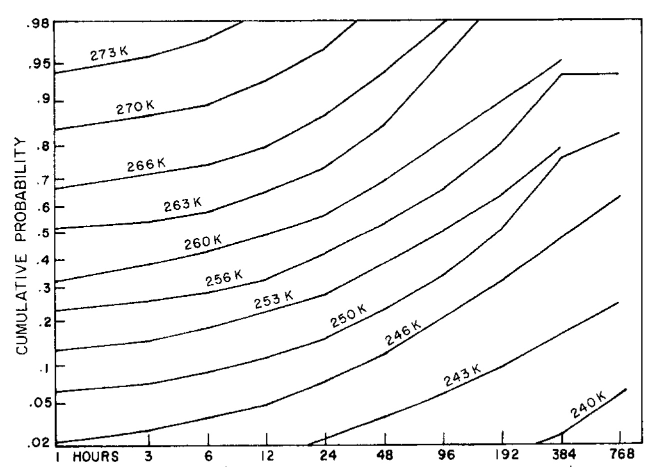

Figure 15-11. The cumulative probability of the M-hour minimum temperature (1 January to 1 February) at Minneapolis, Minn.

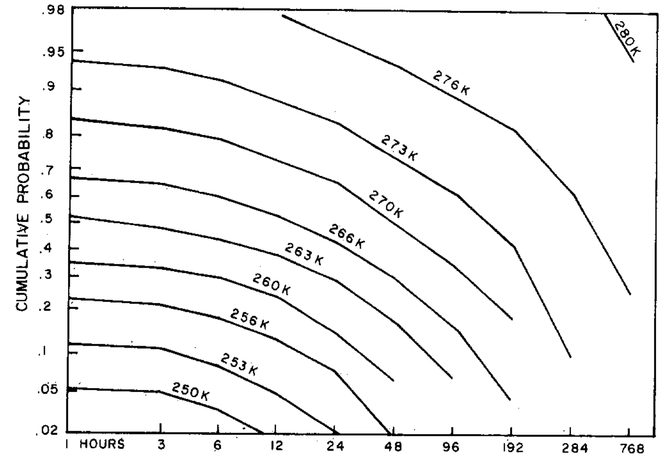

Figure 15-12. The frequency of duration (h) of the temperature (≤ T) in the mid-winter month (1 January - 1 February) at Minneapolis, Minn. (based on 1943–1952 data.)

instruments, primarily radiosondes, for altitude up to 30 km and from rockets and instruments released from rockets for altitudes between 30 and 90 km.

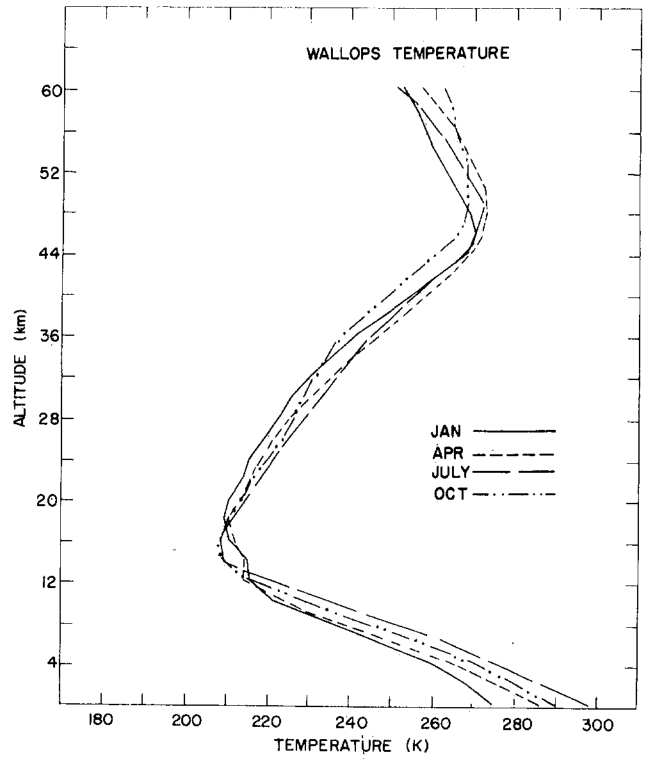

15.1.3.1 Seasonal and Latitudinal Variations. The Reference Atmospheres presented in Chapter 14 provide tables of mean monthly temperature-height profiles, surface to 90 km, for 15° intervals of latitude between the equator and North Pole. These profiles depict both the seasonal and

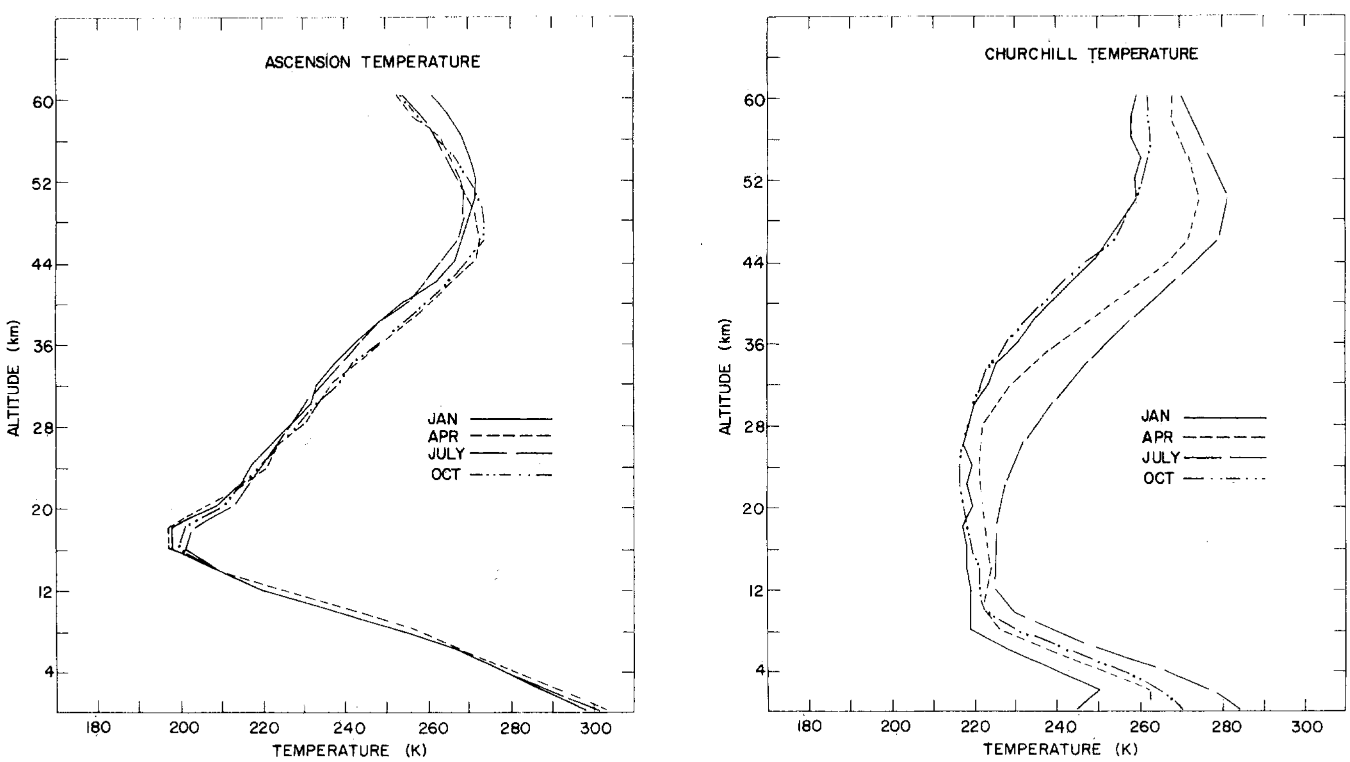

Figure 15-13. Seasonal differences in the temperature-altitude profiles at Ascension Island, Wallops Island, and Ft. Churchill.

Table 15-8a. Median, high, and low values of temperatures for January and July at 30°N.

Altitude (km)	Median (K)	1% High (K)	1% Low (K)	10% High (K)	10% Low (K)	20% High (K)	20% Low (K)
January							
5	262	272	251	267	256	265	258
10	229	239	219	235	223	233	225
15	208	221	198	216	203	214	205
20	208	222	200	216	203	214	204
25	220	231	210	226	216	224	217
30	229	239	218	236	224	234	226
35	240	254	222	248	232	245	235
40	252	270	240	262	249	258	250
45	264	283	253	277	258	272	260
50	266	281	256	276	260	273	262
55	254	272	231	267	243	263	248
60	243	254	223	248	232	246	235
65	231	254	218	242	226	238	228
70	220	235	198	227	204	225	210
75	218	253	197	237	203	227	208
80	209	243	187	230	194	217	197
July							
5	272	278	262	274	266	275	268
10	238	249	227	246	232	242	234
15	204	216	196	211	200	210	200
20	212	223	203	218	206	216	206
25	223	230	216	227	218	226	219
30	234	241	226	238	229	236	231
35	244	254	237	250	240	247	242
40	256	267	247	263	251	261	253
45	266	275	259	272	264	269	265
50	269	282	258	278	262	275	264
55	264	273	247	269	253	267	256
60	247	262	231	255	240	252	243
65	228	240	215	236	219	234	222
70	209	222	186	219	194	214	200
75	200	218	178	214	192	209	196
80	193	207	182	200	189	198	191

Table 15-8b. Median, high, and low values of temperatures for January and July at 45°N.

Altitude (km)	Median (K)	1% High (K)	1% Low (K)	10% High (K)	10% Low (K)	20% High (K)	20% Low (K)
January							
5	250	263	233	257	239	254	242
10	220	233	206	227	212	225	214
15	217	231	202	225	208	222	211
20	215	227	203	222	208	220	210
25	215	233	197	226	205	224	209
30	221	240	209	230	214	226	219
35	233	258	215	251	223	243	226
40	247	272	226	264	236	257	240
45	262	288	240	283	250	271	254
50	265	282	249	274	256	270	258
55	253	275	229	267	239	263	245
60	244	266	220	263	230	257	241
65	235	255	214	246	223	243	228
70	226	246	206	238	211	234	217
75	225	261	197	245	205	235	210
80	216	248	185	237	197	228	202
July							
5	267	277	255	274	259	272	262
10	235	247	222	240	227	239	230
15	216	227	205	222	206	220	212
20	219	233	207	227	213	225	215
25	225	233	216	229	217	228	221
30	234	242	228	239	231	237	232
35	245	254	238	250	241	248	243
40	256	268	250	265	254	263	255
45	268	280	260	276	263	272	265
50	273	283	264	279	268	277	270
55	264	273	249	269	255	267	260
60	247	270	230	264	235	260	238
65	230	245	216	241	223	238	220
70	213	226	188	219	196	216	202
75	195	210	175	205	186	201	190
80	183	203	154	195	163	191	170

latitudinal variations in mean monthly temperatures. The largest seasonal variations in temperature occur at altitudes between 70 and 80 km near 75°N latitude. In this region the mean monthly temperature fluctuates from 230 K in January to 160 K in July. In the upper mesosphere, 60 to 85 km, mean monthly temperatures decrease toward the pole in summer and towards the equator in winter. In the upper stratosphere, 20 to 55 km, conditions are reversed; temperature decreases toward the pole in winter and toward the equator in summer. At altitudes between 15 and 20 km temperature decreases toward the equator in all seasons. Temperature-altitude profiles, surface to 60 km, for the mid-season months at Ascension Island, 8°S, Wallops Island, 38°N, and Ft. Churchill, 59°N, are given in Figure 15-13 and illustrate the magnitude of the seasonal and latitudinal variations in mean monthly temperatures.

5.1.3.2 Distribution Around Monthly Means and Medians. The distributions of observed temperatures around the median values for altitudes up to 80 km in January and July at 30°, 45°, 60° and 75°N are shown in Tables 15-8a to 15-8d. Median, and high and low values that are equaled

Table 15-8c. Median, high, and low values of temperatures for January and July at 60°N.

Altitude	Median	1% High (K)	1% Low (K)	10% High (K)	10% Low (K)	20% High (K)	20% Low (K)
January							
5	240	255	225	249	231	246	234
10	217	231	203	224	209	222	211
15	217	231	203	225	209	222	212
20	215	236	194	226	204	222	208
25	212	241	185	229	197	223	203
30	216	253	203	235	204	225	210
35	221	277	204	259	209	238	214
40	227	300	206	278	211	246	219
45	243	303	219	282	225	255	231
50	251	289	226	280	240	271	245
55	251	283	225	275	233	256	238
60	243	271	210	261	224	253	234
65	238	262	208	258	218	249	222
70	239	264	212	253	219	249	225
75	232	255	180	249	203	246	213
80	223	248	173	243	195	239	204
July							
5	260	271	250	266	254	264	256
10	225	238	214	233	219	231	221
15	225	235	217	231	221	229	223
20	225	233	219	230	222	229	223
25	229	236	222	233	225	232	226
30	239	245	232	243	234	241	235
35	252	258	243	256	247	253	248
40	265	272	259	269	263	268	262
45	277	287	271	283	274	280	275
50	279	290	273	286	277	284	279
55	271	278	257	275	264	273	266
60	259	273	212	265	250	263	253
65	238	259	225	253	230	248	233
70	214	239	202	226	208	222	211
75	190	202	178	196	182	194	186
80	166	180	142	176	153	174	155

Table 15-8d. Median, high, and low values of temperature for January and July at 75°N.

Altitude (km)	Median (km)	1% High (K)	1% Low	10% High (K)	10% Low (K)	20% High (K)	20% Low (K)
January							
5	235	246	222	241	229	238	230
10	214	224	202	219	207	217	209
15	209	219	195	213	201	211	203
20	204	225	179	215	189	210	194
25	205	233	181	221	193	216	198
30	209	255	194	231	198	224	202
35	219	256	199	249	210	236	213
40	229	284	207	256	219	248	224
45	239	281	203	264	224	260	233
50	249	282	201	265	225	259	229
55	255	291	208	262	221	253	226
60	247	303	206	263	213	255	219
65	238	310	186	277	202	263	209
70	242	297	166	277	201	261	207
75	234	289	183	259	201	261	207
80	224	277	165	254	194	240	201
July							
5	254	264	244	259	248	257	250
10	229	238	219	234	223	232	225
15	230	237	225	235	228	233	229
20	230	237	227	235	228	234	229
25	230	240	226	238	227	237	229
30	243	262	233	247	235	246	240
35	256	262	238	260	246	258	250
40	268	275	252	271	260	270	262
45	281	292	268	287	275	284	278
50	284	296	270	291	279	288	280
55	281	288	254	284	270	283	275
60	268						
65	246	(insufficient data above 55 km in summer)					
70	218						
75	189						
80	161						

or more severe 1%, 10% and 20% of the time during these months are given for 5-km altitude increments between the surface and 80 km. Distributions below 30 km are based on radiosonde observations taken in the Northern Hemisphere, and those above 30 km are based on meteorological and experimental rocket observations taken primarily from launching sites in or near North America. The 1% values are considered to be rough estimates as they are based on the tails of the distributions of observed values plotted on probability paper. Estimates of values for altitudes above 50 km are less reliable than those below 50 km because of the paucity of data and larger observational errors at the higher altitudes. Only median temperatures are given above 55 km at 75°N for July due to the small number of observations that are available for the higher altitudes over the polar regions in summer.

In tropical regions, 0° to 15° latitude, the day-to-day variations of temperature are normally distributed about the mean at altitudes up to 50 km. Consequently, a reasonably accurate estimate of the distribution of temperature at a given altitude can be obtained from the standard deviations and

Table 15-9. Standard deviations of observed day-to-day variations in temperatures (K) at Ascension Island (8°S) at altitudes up to 50 km during the midseason months.

Altitude (km)	S. D. of Temperature (K)			
	Jan	April	July	Oct
5	0.8	0.6	0.7	0.6
10	0.8	1.0	0.8	1.1
15	1.6	2.0	1.9	1.5
20	2.2	2.2	2.4	2.1
25	2.2	2.2	2.7	2.1
30	3.1	2.8	3.8	3.6
35	3.7	3.2	3.7	3.8
40	5.2	3.9	3.3	3.5
45	3.6	2.8	3.2	3.3
50	5.8	2.9	3.9	3.0

the monthly means. The standard deviations of observed temperatures around the mean monthly values for the midseason months at Ascension Island, Table 15-9, are typical of the day-to-day variations found in the tropics. Values are not given for altitudes above 50 km as there are too few daily observations on which to base the monthly temperature distributions. The observed standard deviations includes the rms instrumentation errors as well as the actual rms climatic variations. Consequently, the observed variations are somewhat larger than the actual values.

Day-to-day variations of temperature around the annual mean at levels between 50 and 90 km in tropical areas (Table 15-10) were computed from data derived from grenade and pressure-gage experiments at Natal, 6°S, and Ascension Island, 8°S. These data were not uniformly distributed with respect to season or time of day. An analysis of the relatively sparse data that are available for individual months indicates that if the seasonal and diurnal variations are removed from the data, standard deviations around monthly means due to day-to-day changes in synoptic conditions would be roughly 50% of those given in Table 15-10.

5.1.3.3 Distributions at Pressure Levels. The mean January and July temperatures over North America for standard pressure levels up to 10 mb ($\approx$31 km) are presented in Table 15-11. Standard deviations of the daily values around these means are also shown, thereby providing information on seasonal changes in monthly mean temperatures and interdiurnal (day-to-day) variability at various pressure levels and latitudes. Standard deviations are not shown above 100 mb north of 50° latitude because a bimodal temperature distribution exists in the winter stratosphere in arctic and subarctic regions over eastern North America. As a result, the standard deviations do not provide reliable information on the temperature distributions at these levels.

15.1.3.4 Interlevel Correlation of Temperature. The manner in which the correlation between temperatures at two levels decreases (or decays) with increasing separation between the levels is an example of the general problem of correlation decay. Correlation decay is similar for most meteorological elements as the horizontal or vertical distance between the points of observations increases. As yet, no fully satisfactory description of the decay rate, based on fundamental properties or assumptions, is available. Consequently, many empirical models that are valid for specific elements over restrictive ranges have been proposed.

Profiles of correlation coefficient r, of surface temperature with temperature at other altitudes are shown in Figure 15-14 for the midseason months at Ascension Island, Kwajalein, Wallops Island, and Ft. Churchill. At most locations, the correlation between surface temperatures and temperatures at other altitudes decreases rapidly with increasing altitudes, reaching a minimum or becoming negative between 12 and 16 km and then remaining near zero, plus or minus 0.3, from 20 to 60 km. Individual arrays of the mean temperatures, standard deviations and interlevel correlation coefficients for altitudes to 60 km are given in Table 15-12a to 15-12f for the months of January and July at Ft. Churchill, Wallops Island, and Kwajalein. Additional in-

Table 15-10. Standard deviations of observed densities (%) and temperatures (K) around the mean annual values of Ascension Island (8°S)/Natal (6°S).

Altitude (km)	Density S.D. (% of mean)	Temperature S.D. (K)	No. of Observations
50	4.1	6	33
55	4.3	3	33
60	4.8	6	33
65	4.7	7	33
70	6.4	9	32
75	8.6	10	31
80	7.8	10	30
85	10.2	13	29
90	12.3	21	28

Table 15-11. Mean temperature and standard deviation at standard pressure levels over North America.

Mean Temperature and Standard Deviation (K)														
Pressure	20°N		30°N		40°N		50°N		60°N		70°N		80°N	
(mb)	Mean	S.D.	Mean	S.D.	Mean	S.D.	Mean	S.D.	Mean	S.D.	Mean	S.D.	Mean	S.D.
January														
700	280	2	275	5	267	6	256	8	251	8	247	7	245	6
500	264	3	259	4	252	6	242	7	238	7	234	5	232	5
300	236	3	232	3	227	4	221	4	220	4	217	4	214	5
200	217	3	216	5	216	6	219	7	219	7	216	6	213	6
100	198	3	204	4	212	4	218	−5	219	6	216	7	210	6
50	208	3	209	3	213	3	215	4	216	*	213	*	206	*
25	218	2	218	3	216	4	212	5	212	*	208	*	203	*
15	225	2	223	3	221	4	218	6	215	*	211	*	207	*
10	230	2	227	3	224	4	221	−6	217	*	213	*	209	*
July														
700	283	2	283	2	282	3	275	4	270	3	268	4	265	4
500	267	2	267	2	264	3	258	4	255	4	253	4	249	4
300	240	2	240	2	237	3	232	4	229	4	228	4	227	4
200	218	2	218	2	219	3	221	5	224	5	226	5	230	4
100	200	3	203	3	210	3	220	4	226	3	228	2	231	2
50	213	2	215	2	218	3	221	3	226	3	228	3	230	3
25	222	2	222	2	225	2	227	2	229	2	232	2	233	2
15	228	2	228	2	229	2	232	2	235	3	236	3	236	3
10	232	2	233	2	234	2	237	2	239	3	240	3	241	3

*Not normally distributed.

formation useful in design studies is given by Cole and Kantor [1980].

15.1.4 Speed of Sound vs Temperature

The speed of sound is primarily a function of temperature. An equation for computing the speed of sound and the limitations of such computations are presented in Chapter 14. Figure 15-15 shows the relationship between temperature and the speed of sound. It can be used with the various temperature presentations given in this section to estimate the probable speed of sound for various altitudes and geographical areas.

15.1.5 Earth/Air Interface Temperatures

The earth/air interface is either a land, snow, or water surface. At many locations, the physical structure of the interface is overwhelmingly complex. The land surface can be covered with seasonally varying vegetation of great diversity, and even without plant cover there is normally a considerable variability produced by small-scale terrain features, differences in soil moisture and cultivation. A snow surface is markedly affected by aging. The physical conditions of water in a shallow puddle are quite different from the open ocean. All these conditions reflect themselves in the micro-climatological aspects of natural or unnatural surfaces.

As discussed in Section 15.1.2, the use of ordinary thermometers to measure surface temperature, will result in meaningful values only in the rare cases of a flat, uniform, and homogeneous surface. In general, area averages of temperature obtained by an integrating method over certain defined sections will be more representative than any one of a multitude of widely varying point values. Bolometric temperature measurements from an airplane cruising at low altitude provide a more reasonable approach to the problem of surface temperature determination than a series of thermometric point measurements. Table 15-13 lists some results of bolometric measurements from an airplane. The data illustrate the great horizontal variability of surface temperature even when effects on the scale of less than 6 m linear dimension are averaged out.

The processes that determine the temperature of the earth/air interface and the surface characteristics that influ-

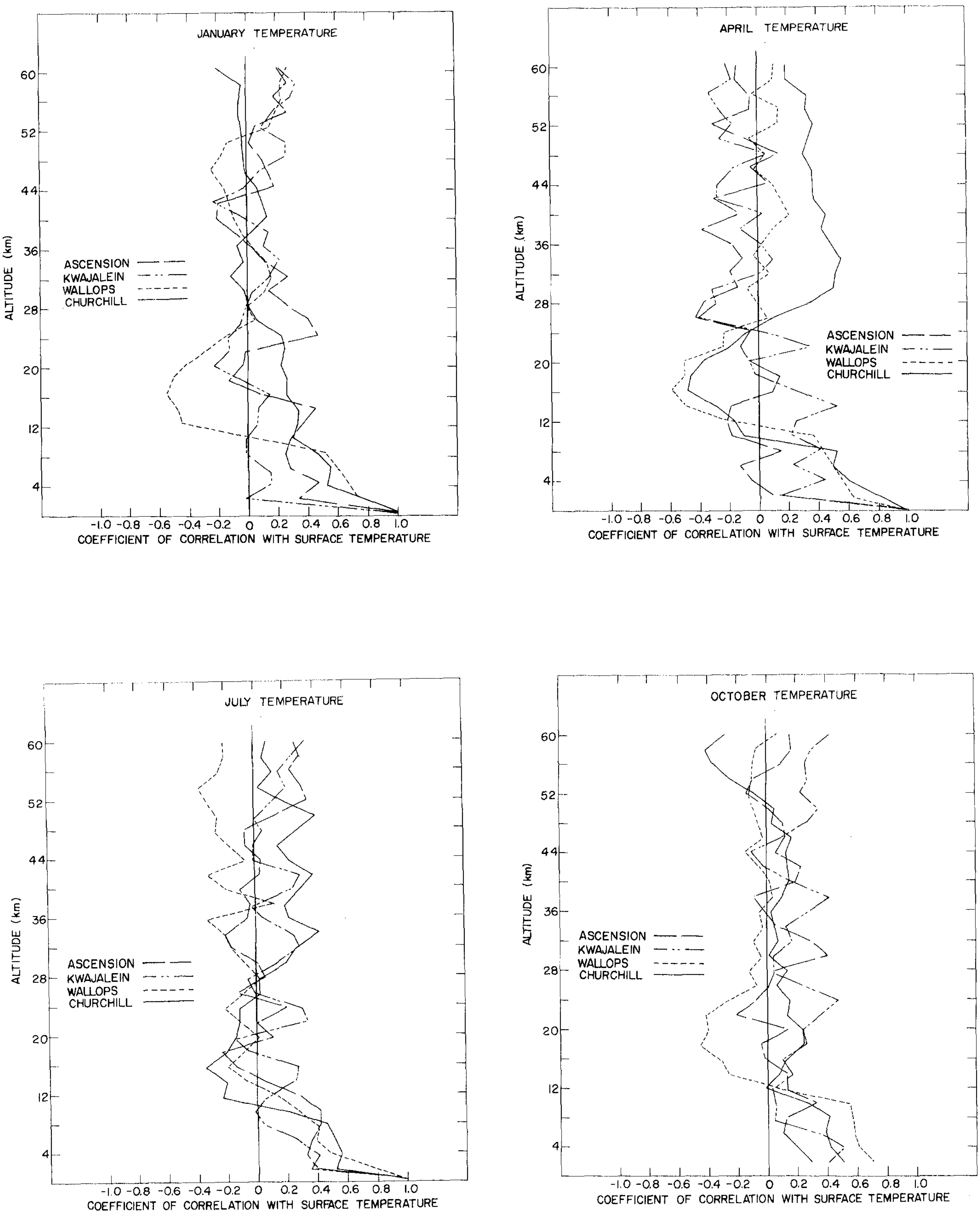

Figure Figure 15-14. Vertical profiles of interlevel coefficients of correlation of surface temperature with temperature at other altitudes up to 60 km for the mid-season months at Ascension Island, Kwajalein, Wallops Island, and Ft. Churchill.

ence these processes may be separated into the following four classes:

1. radiative energy transformation (or net radiation intensity), which depends upon the albedo and selective absorption and emission;
2. turbulent heat transfer into the air (by both convective and mechanical air turbulence);
3. conduction of heat into or out of the ground, which depends upon the thermal admittance of the soil; and
4. transformation of radiant energy into latent heat by evaporation, which depends upon the dampness of the surface or available soil moisture at the ground level.

The aerodynamic roughness of a natural surface strongly influences the momentum exchange between ground and air flowing past it. The momentum exchange establishes the low-level profile of mean wind speed. The mechanical turbulence produced by surface roughness also determines to a certain degree the relative amount of heat transported into or from the air at mean ground level. Other conditions being equal, an increase in roughness and hence mechanical turbulence will cause lowering of maximum surface temperature during daytime and raising of minimum surface temperature during nighttime. For ordinary sandy soil, under average conditions of overall airflow and net radiation on summer days in temperate zones, the diurnal range of surface temperature is about 17 K if the roughness coefficient is 0.06 mm or 14 K if it is 6.35 mm (roughness coefficient, also called roughness "length," is $\varepsilon/30$ where ε is the average height of surface irregularities).

A special and rather extreme case of the influence of surface characteristics is represented by forests. The trees intercept solar radiation and the heat absorbed is given off into the air that is trapped between the stems. Although deep snow may lie on the ground, daytime temperatures in wooded areas in spring can reach 289 K.

The thermal admittance (Section 15.1.6) of most soils depends on porosity and moisture content. Because both the thermal conductivity and heat capacity of soils increase with soil moisture, the thermal admittance may be significantly affected by humidity variations during rainy or wet weather periods, whereas the normal diffusivity may remain unaltered. These effects are difficult to assess, however, because the dampness of the surface is also a major factor in the utilization of solar energy for evaporation. If soil moisture is readily available at the earth's surface, part of the net radiation that would have been used for heating air and ground is used instead for latent heat of evaporation. Table 15-14 lists observed temperatures in the air and soil at levels close to the earth/air interface.

Engineers must consider the effect of albedo and color or net radiation in artificially changing surface or ground temperature. In India, a very thin layer of white powdered lime dusted over a test surface made ground temperatures up to 15 K cooler; the effect was felt at a depth of at least 20 cm.

Another effective method of controlling surface temperature is shading. Thin roofs (metal, canvas), however, may attain a temperature so high that the under surface acts as an intense radiator of long-wavelength radiation, thus acting to warm the ground. In hot climates, multilayer shades with natural or forced ventilation in the intermediate space, or active cooling of the outer surface by water sprinkling, can be used to cool the ground with some success. Table 15-15 compares temperature measurements of various material surfaces with corresponding air and soil temperatures.

15.1.6 Subsoil Temperatures

The thermal reaction of the soil to the daily and seasonal variations due to the earth's rotation and its revolution about the sun of net radiation is governed by the *molecular thermal conductivity* of the soil, k, and by the *volumetric heat capacity* of the soil, $C = \rho c$ (where ρ is the density and c is the heat capacity per unit mass). For a cyclic forcing function of frequency n, the quotient $(nk/C)^{1/2}$ (which has the physical units of velocity) determines the downward propagation or *amplitude decrement with depth* of the soil-temperature response. The product $(nk\,C)^{-1/2}$, which has the physical units of degrees divided by Langleys per unit time (1 L/s equals 4.186×10^4 W/m^2), governs the amplitude of the temperature profile in time at the soil surface. The ratio k/C is the *thermal diffusivity* (physical units of length squared per unit time). The expression $(kC)^{1/2}$ defines *thermal admittance* of the soil.

The continuous flow of heat from the earth's hot, deep interior to the surface is the order of 10^{-5} L/min. This is very small compared with a solar constant of 2 L/min, average net-radiation rates of 0.2 L/min, and induced soil-heat fluxes in the uppermost several feet of the earth's crust of 0.1 L/min. Only for depth intervals in excess of about 30 m must the heat flow from the earth's interior be considered, inasmuch as it results in vertical temperature gradients of the order of 2.5 to 25 K/km.

Table 15-16 gives experimental data on thermal admittance and theoretical values of the *half-amplitude depth interval* based on experimental thermal diffusivity data for diverse ground types. The smaller the thermal admittance, the larger the surface-temperature amplitude for a given forcing function. This latter inverse proportionality is valid only when turbulent heat transfer into the atmosphere is negligible.

In a simple theoretical model of thermal diffusion, an *effective atmospheric thermal conductivity* K is introduced. For air, K is many times larger than the molecular thermal conductivity of the air. For the same forcing function, the surface-temperature amplitudes at two different kinds of ground follow the ratio

$$\frac{(TAR)_2 + (K/k)^{1/2}_{air}}{(TAR)_1 + (K/k)^{1/2}_{air}} \qquad (15.21)$$

Table 15-12a. Ft. Churchill—Correlation of January temperatures (K) from surface to 60 km.

KM Kilometers above Sea Level
MEAN Average of Observed Values
STDV Standard Deviation of Values Times 10
N Number of Values at Each Altitude

KM	.035	2	4	6	8	10	12	14	16	18	20	22	24	26	28	30	32	34	36	38	40	42	44	46	48	50	52	54	56	58	60
MEAN	244	250	240	228	219	219	219	218	218	217	219	218	219	217	218	219	223	225	230	233	238	243	248	252	255	258	258	259	257	257	258
STOV	75	58	49	43	45	52	61	70	75	78	63	69	70	98	96	88	85	89	109	125	166	171	187	173	160	148	143	147	146	138	127
N	50	50	50	50	50	50	50	50	46	40	30	29	23	45	48	50	51	51	51	51	51	51	51	51	51	51	51	51	49	46	36
2	72	**																													
4	53	84																													
6	55	75	82																												
8	46	23	17	47																											
10	30	3	−4	13	85																										
12	32	16	9	19	73	94																									
14	34	21	12	23	68	89	98																								
16	25	18	10	17	56	81	94	98																							
18	26	23	13	10	45	71	85	90	95																						
20	22	14	8	1	38	61	73	78	83	94																					
22	24	14	17	4	30	51	59	59	65	80	93																				
24	22	16	2	−5	9	28	33	28	40	62	84	98																			
26	6	−1	0	−1	17	44	55	58	66	76	80	94	96																		
28	0	0	7	1	9	33	45	48	62	74	79	92	94	96																	
30	−1	4	14	10	4	19	29	33	53	66	72	86	83	87	95																
32	−11	−3	11	−1	−22	−17	−13	−13	7	19	39	59	71	56	73	84															
34	−1	10	21	8	−23	−29	−29	−29	−15	−5	18	37	50	32	50	64	88														
36	−6	1	16	4	−24	−35	−37	−37	−31	−19	18	30	34	12	29	44	74	85													
38	5	1	8	−2	−18	−28	−34	−35	−30	−17	9	15	21	−1	13	27	60	78	92												
40	13	6	6	−2	−14	−27	−34	−37	−37	−29	−3	0	6	−19	−10	1	37	61	78	92											
42	9	1	4	−2	−15	−32	−42	−46	−50	−46	−16	−16	−10	−39	−29	−16	26	51	70	84	93										
44	7	−1	−1	−8	−22	−39	−49	−52	−59	−55	−33	−35	−23	−53	−46	−36	3	34	55	72	82	92									
46	0	−6	−6	−15	−30	−44	−53	−56	−63	−59	−36	−39	−32	−52	−47	−41	−3	25	46	60	74	83	93								
48	−1	−11	−10	−21	−33	−47	−58	−61	−65	−62	−42	−41	−35	−52	−46	−41	−3	24	43	55	67	78	89	96							
50	−1	−11	−17	−29	−33	−44	−52	−53	−57	−52	−36	−36	−35	−45	−42	−40	−14	11	27	39	52	59	73	81	87						
52	−3	−13	−21	−31	−29	−37	−44	−44	−48	−50	−32	−34	−35	−43	−43	−46	−22	−1	13	22	36	44	59	68	76	92					
54	−5	−12	−20	−30	−25	−31	−37	−37	−43	−51	−41	−46	−46	−47	−49	−54	−34	−13	1	8	22	32	47	56	63	79	93				
56	−5	−14	−22	−32	−23	−23	−26	−25	−33	−41	−41	−45	−44	−34	−38	−49	−41	−24	−14	−7	4	13	28	36	47	67	81	92			
58	−4	−14	−20	−28	−16	−15	−17	−15	−21	−36	−43	−46	−49	−28	−33	−45	−45	−34	−31	−27	−20	−9	10	18	34	59	74	85	95		
60	−20	−23	−24	−36	−18	−14	−19	−17	−24	−31	−49	−51	−50	−38	−38	−49	−44	−40	−32	−27	−22	−5	12	22	32	50	61	75	81	87	

**Multiply tabular values by 0.01 to obtain correlation coeffecients.

Table 15-12b. Ft. Churchill—Correlation of July temperatures (K) from surface to 60 km.

KM Kilometers Above Sea Level
MEAN Average of Observed Values
STDV Standard Deviation of Values Times 10
N Number of Values at Each Altitude

KM	.035	2	4	6	8	10	12	14	16	18	20	22	24	26	28	30	32	34	36	38	40	42	44	46	48	50	52	54	56	58	60
MEAN	284	277	265	252	238	228	224	225	225	225	226	227	229	231	235	238	242	247	252	257	262	268	274	278	279	280	278	276	274	271	269
STDV	53	37	40	47	49	25	49	22	23	22	20	18	16	24	21	25	24	32	30	30	35	37	34	31	39	41	43	45	39	38	43
N	28	28	28	28	28	28	28	28	28	28	28	27	27	28	28	28	28	28	28	28	28	28	28	28	28	28	26	25	25	21	20
2	49	**																													
4	53	89																													
6	49	87	95																												
8	44	82	90	96																											
10	19	35	42	42	55																										
12	-24	-66	-69	-76	-73	-3																									
14	-22	-69	-73	-74	-74	-12	83																								
16	-36	-82	-84	-84	-82	-32	69	78																							
18	-22	-75	-71	-69	-66	-33	-46	-63	-90																						
20	-15	-66	-56	-52	-50	-28	27	45	72	91																					
22	-13	-71	-65	-61	-59	-36	43	54	81	93	97																				
24	-13	-65	-61	-53	-54	-37	37	52	76	80	81	85																			
26	1	-37	-39	-37	-39	-18	27	42	54	53	48	55	62																		
28	1	-32	-36	-37	-33	-6	29	44	50	48	38	44	49	92																	
30	19	-20	-16	-15	-19	-14	19	27	34	25	14	25	37	82	77																
32	26	-9	-17	-11	-12	-12	15	33	28	27	16	27	31	78	76	82															
34	41	-4	-10	-11	-12	-6	22	27	26	24	9	21	17	64	67	78	84														
36	22	-20	-21	-23	-24	-6	32	32	28	17	4	14	27	56	54	71	62	72													
38	19	-23	-28	-33	-33	-13	17	29	32	25	17	23	23	68	73	66	63	64	66												
40	30	-8	-18	-21	-19	-8	5	12	34	41	34	35	32	68	70	58	56	63	49	69											
42	39	15	7	1	2	10	6	5	17	17	7	11	6	52	63	57	60	64	38	54	77										
44	23	11	-1	-6	-1	7	18	9	17	11	-6	-4	0	45	54	46	51	59	47	44	62	80									
46	15	-10	-8	-18	-16	-7	9	-1	16	15	4	6	2	47	50	41	38	51	55	61	51	42	61								
48	29	15	13	12	12	10	0	-10	0	1	-9	-7	0	37	40	38	48	55	51	41	45	38	52	71							
50	40	25	23	26	20	14	4	4	-6	-10	-22	-18	0	37	34	49	63	60	57	38	33	38	53	45	80						
52	20	9	3	5	-1	9	22	26	15	-5	-27	-19	-3	42	42	59	70	58	54	40	25	47	56	40	64	90					
54	2	-8	-11	-9	-12	9	27	37	31	12	-9	-1	10	46	51	55	67	54	52	47	26	50	53	49	65	78	93				
56	12	-7	-12	-7	-9	4	24	34	29	11	-13	-3	8	43	51	57	69	64	57	54	34	54	63	52	68	81	91	95			
58	6	-25	-16	-6	-8	6	11	39	44	35	22	24	38	57	59	61	72	67	43	52	43	46	49	37	55	71	80	87	93		
60	9	-9	4	6	7	19	2	14	29	19	5	7	26	50	58	54	55	58	36	48	41	47	56	46	60	66	69	77	81	90	

**Multiply tabular values by 0.01 to obtain correlation coefficients

Table 15-12c. Wallops Island—Correlation of January temperatures (K) from surface to 60 km.

KM Kilometers above Sea Level
MEAN Average of Observed Values
STDV Standard Deviation of Values Times 10
N Number of Values at Each Altitude

KM	.015	2	4	6	8	10	12	14	16	18	20	22	24	26	28	30	32	34	36	38	40	42	44	46	48	50	52	54	56	58	60
MEAN	275	269	260	248	235	222	216	215	211	210	211	214	216	220	223	226	231	236	242	249	255	262	268	270	269	266	263	260	258	256	252
STDV	54	86	79	69	53	33	55	39	44	45	35	35	38	45	54	59	60	63	61	79	95	89	82	80	63	47	66	74	77	90	106
N	44	44	44	44	44	44	44	44	43	43	43	43	43	44	44	44	44	44	44	44	44	44	44	44	44	44	44	44	40	34	19
2	74	**																													
4	66	96																													
6	61	87	96																												
8	52	79	88	94																											
10	5	10	14	17	42																										
12	−44	−46	−56	−62	−55	13																									
14	−47	−65	−73	−76	−74	−13	74																								
16	−54	−72	−78	−79	−79	−10	63	89																							
18	−49	−79	−82	−83	−81	−20	42	72	82																						
20	−41	−60	−59	−56	−57	−14	28	51	58	72																					
22	−27	−42	−41	−42	−48	17	19	28	37	60	81																				
24	−13	−32	−28	−27	−31	−8	−1	2	12	34	52	64																			
26	7	−19	−19	−14	−18	−7	−2	−6	−9	10	37	48	73																		
28	0	−19	−17	−15	−15	6	0	−3	−12	9	37	42	60	86																	
30	11	−25	−22	−17	−17	0	−5	−4	−12	14	35	38	52	79	83																
32	15	−19	−18	−15	−19	−11	−3	1	−7	11	21	13	31	60	63	82															
34	13	14	−19	−20	−23	−18	11	6	−6	6	3	−9	8	30	29	55	80														
36	3	−15	−23	−29	−33	−30	15	8	7	11	−3	−13	−2	16	15	31	58	81													
38	−4	2	−5	−11	−7	−9	4	−10	−4	−3	−25	−36	−24	−22	−26	−26	−2	30	60												
40	−10	1	−5	−9	−2	0	5	−13	−9	−10	−29	−42	−29	−28	−32	−31	−14	19	46	89											
42	−12	5	5	9	14	8	−3	−28	−20	−27	−43	−44	−23	−29	−29	−30	−17	6	29	68	79										
44	−16	3	5	10	12	8	3	−28	−17	−26	−35	−37	−29	−21	−21	−22	−6	3	26	54	63	85									
46	−23	−1	3	7	9	10	−2	−21	−12	−21	−30	−36	−28	−22	−21	−29	−12	−2	19	52	63	74	87								
48	−17	1	5	18	10	7	−14	−18	−14	−23	−33	−43	−34	−21	−14	−22	2	2	19	42	49	62	69	85							
50	−14	−7	−5	1	1	4	−3	−2	4	−10	−30	−38	−32	−21	−21	−15	16	20	33	45	40	42	49	61	76						
52	15	10	9	13	16	3	−7	−6	−5	−14	−37	−47	−40	−23	−16	−11	10	25	41	47	33	32	26	33	40	66					
54	20	11	10	11	15	6	−7	−4	2	−9	−23	−34	−34	−10	−3	0	15	17	32	25	8	10	16	12	18	36	80				
56	23	8	5	8	11	6	−12	−7	2	−5	−7	−15	−26	−1	0	1	14	11	23	12	0	3	8	10	21	29	58	82			
58	23	23	22	24	28	21	−8	−14	−9	−17	−19	−20	−37	−15	−13	−14	1	−5	7	2	−2	1	9	22	29	33	51	71	89		
60	27	19	22	21	29	51	−3	−23	−19	−29	−18	−9	−35	1	−4	−4	14	−5	10	13	7	3	20	32	35	43	38	59	77	95	

**Multiply tabular values by 0.01 to obtain correlation coefficients

Table 15-12d. Wallops Island—Correlation of July temperatures (K) from surface to 60 km.

KM Kilometers Above Sea Level
MEAN Average of Observed Values
STDV Standard Deviation of Values Times 10
N Number of Values at Each Altitude

KM	.015	2	4	6	8	10	12	14	16	18	20	22	24	26	28	30	32	34	36	38	40	42	44	46	48	50	52	54	56	58	60
MEAN	297	286	275	264	251	236	220	210	209	212	216	220	223	226	229	233	237	241	246	251	256	262	267	270	271	270	267	264	260	256	251
STDV	34	21	16	14	20	22	22	27	29	23	16	17	16	24	25	30	28	30	27	27	32	37	43	42	38	38	40	47	55	62	88
N	37	37	37	37	37	37	37	37	37	37	37	37	37	37	37	37	37	37	37	37	37	37	37	37	37	37	37	37	34	30	18
2	75	**																													
4	47	68																													
6	36	53	84																												
8	38	48	69	67																											
10	25	37	48	51	81																										
12	12	29	27	27	48	80																									
14	−8	−18	−26	−11	−28	−7	18																								
16	−22	−48	−39	−46	−55	−50	−25	36																							
18	−10	−25	−14	−24	−35	−47	−32	31	67																						
20	0	−5	−11	−20	−11	−33	−32	17	48	57																					
22	−13	−11	−8	−5	−4	−15	−9	7	42	50	68																				
24	−22	−12	−3	−4	3	12	25	13	22	11	41	48																			
26	−10	−13	17	22	24	31	25	6	10	1	7	32	48																		
28	1	−1	21	19	33	41	27	−3	13	−7	14	35	46	70																	
30	−8	−8	17	8	18	32	25	−5	8	−18	−2	10	33	49	76																
32	−18	−6	23	10	11	17	20	−11	16	2	10	22	54	44	61	72															
34	−22	−19	15	11	28	37	27	−11	9	−15	7	14	45	64	62	60	63														
36	−32	−23	4	−3	13	25	29	4	31	14	27	50	65	62	67	54	61	68													
38	11	−14	17	25	29	28	6	−1	10	9	−2	19	34	61	62	56	47	49	44												
40	−20	−16	17	17	14	18	8	−32	−11	−20	−26	−6	17	27	23	40	47	50	30	49											
42	−33	−28	1	−1	−5	1	15	−10	22	0	−8	16	16	6	21	48	49	42	32	19	70										
44	−6	11	35	37	30	39	41	6	−2	−14	−8	11	29	40	55	52	58	48	38	38	47	53									
46	−18	0	41	41	31	27	20	12	5	−2	−4	13	25	50	54	45	48	51	41	35	30	35	82								
48	−26	−13	18	31	21	25	13	13	−1	−13	−2	16	38	38	53	48	56	42	34	40	34	34	60	66							
50	−25	−15	8	13	23	32	21	−7	−5	−10	2	22	43	51	56	55	55	52	39	42	42	34	48	51	81						
52	−31	−32	−12	−16	9	10	14	−5	9	6	29	40	51	45	49	42	47	52	43	26	27	40	31	30	43	66					
54	−37	−32	−10	−16	9	8	14	−17	6	3	27	44	57	52	45	39	53	57	50	24	32	41	26	23	28	54	88				
56	−23	−16	−7	−18	15	10	15	−23	−1	5	42	39	64	37	30	19	46	47	45	22	26	20	18	3	13	32	66	86			
58	−20	−15	5	6	36	26	17	−17	−9	1	41	44	44	48	41	10	38	56	50	22	29	17	29	19	28	36	61	77	87		
60	−20	−7	8	1	50	48	35	−42	−22	−13	41	56	63	65	72	50	54	79	77	30	37	31	40	25	36	63	86	90	90	95	

**Multiply tabular values by 0.01 to obtain correlation coefficients

Table 15-12e. Kwajalein—Correlation of January temperatures (K) from surface to 60 km.

KM Kilometers Above Sea Level
MEAN Average of Observed Values
STDV Standard Deviation of Values Times 10
N Number of Values at Each Altitude

KM	.008	2	4	5	8	10	12	14	16	18	20	22	24	26	28	30	32	34	36	38	40	42	44	46	48	50	52	54	56	58	60
MEAN	301	288	279	267	255	241	224	208	195	192	206	212	217	221	225	228	232	237	242	247	253	257	262	267	271	272	272	271	268	265	263
STDV	14	13	13	13	14	14	15	16	15	46	28	26	23	30	27	30	36	36	37	42	42	38	42	48	63	64	51	41	44	49	58
N	42	42	42	42	42	42	42	42	42	42	42	42	41	40	+1	42	42	42	42	42	42	42	42	42	42	42	42	42	41	38	34
2	-3	**																													
4	15	39																													
6	11	15	48																												
8	-1	-20	23	28																											
10	-2	8	47	43	70																										
12	5	13	44	52	48	85																									
14	5	-4	22	43	60	71	80																								
16	14	10	-13	6	19	8	15	28																							
18	6	3	-16	-34	-41	-57	-52	-63	1																						
20	-23	-18	-12	0	4	1	-9	-5	-21	10																					
22	-13	-3	-15	-27	-21	-21	-27	-34	-33	33	37																				
24	-14	3	-12	7	-5	-26	-21	-7	-19	16	3	31																			
26	-4	-15	-1	-18	-2	-7	-18	-15	8	11	-28	-11	6																		
28	0	4	5	-9	1	-12	-18	-21	4	17	-9	-3	15	51																	
30	3	-1	9	-26	1	-16	-29	-19	1	25	-6	-6	-8	50	53																
32	16	-3	24	-13	0	-2	-14	-19	-2	24	-1	6	1	28	32	39															
34	20	19	-11	-25	-22	-23	-26	-29	43	29	-27	-20	-30	34	6	29	39														
36	11	31	6	-17	-10	-16	-27	-38	27	38	0	-1	-25	19	19	29	37	47													
38	13	-9	-7	-28	6	3	-10	-19	17	26	25	-8	-39	24	-1	30	26	57	54												
40	-1	-1	-32	-40	-8	-12	-19	-28	19	24	-16	2	-2	23	8	18	21	44	29	47											
42	-22	32	-3	-8	-7	-13	-18	-32	26	24	-4	-3	5	8	34	24	30	33	34	24	51										
44	-1	7	-33	-23	-22	-25	-22	-29	19	29	-3	-2	-11	18	14	25	9	51	15	43	54	64									
46	7	-20	-22	-43	-10	-24	-30	-19	-10	16	-6	-2	8	36	1	41	15	35	-4	32	7	8	37								
48	25	-10	-12	-22	-3	-21	-21	-16	26	23	-25	-26	4	32	32	33	38	58	28	49	33	35	42	53							
50	27	8	8	-7	-7	-9	-12	-22	26	11	-26	-43	-33	20	21	32	32	48	43	48	30	36	39	17	63						
52	9	20	13	4	-6	-6	-11	-22	18	18	5	-31	-32	6	27	33	21	49	45	55	24	35	32	6	53	77					
54	17	12	-9	-4	-8	-7	-26	-34	15	13	2	1	-24	3	14	7	11	39	42	38	31	24	30	1	44	54	64				
56	28	22	25	-9	2	-7	-21	-27	-4	21	-2	12	-8	7	14	31	20	29	32	30	36	25	26	19	35	29	46	59			
58	33	6	32	-16	-4	-12	-20	-31	1	26	-28	-10	-17	26	25	30	13	23	27	19	16	3	1	16	31	39	48	47	65		
60	21	16	10	-2	-7	-7	-14	-24	13	18	-21	-42	-17	19	14	9	2	32	28	23	11	4	5	2	29	50	64	58	32	71	

**Multiply tabular values by 0.01 to obtain correlation coefficients

Table 15-12f. Kwajalein—Correlation of July temperatures (K) from surface to 60 km.

KM Kilometers Above Sea Level
MEAN Average of Observed Values
STDV Standard Deviation of Values Times 10
N Number of Values at Each Altitude

KM	.008	2	4	6	8	10	12	14	16	18	20	22	24	26	28	30	32	34	36	38	40	42	44	46	48	50	52	54	56	58	60
MEAN	301	286	278	266	254	239	222	206	198	203	210	215	219	222	227	230	233	237	241	248	254	259	262	265	266	268	268	265	261	257	253
STDV	12	8	10	12	14	17	16	17	17	24	17	15	20	20	21	34	31	43	42	55	34	35	37	50	48	49	58	69	65	69	61
N	31	31	31	31	31	31	31	31	31	31	31	30	29	25	30	31	32	32	32	32	32	32	32	32	32	32	32	31	31	30	27
2	33	**																													
4	38	72																													
6	23	66	78																												
8	2	49	44	52																											
10	-4	57	50	52	77																										
12	4	64	52	54	72	94																									
14	22	66	48	57	38	52	66																								
16	26	6	11	0	-39	-30	-20	9																							
18	-7	-11	-26	0	-7	-10	-5	7	-22																						
20	-14	-1	12	22	-7	-11	-15	-20	-15	-37																					
22	32	-4	-6	12	-34	-29	-12	20	40	9	15																				
24	28	18	43	42	0	-6	-3	20	18	2	25	14																			
26	-2	-3	-1	17	26	4	8	31	7	36	-40	10	9																		
28	-7	35	12	25	33	23	24	45	9	6	-38	-20	-19	45																	
30	12	30	19	31	15	8	26	44	7	-6	-15	13	-6	34	47																
32	28	46	32	42	10	24	27	52	5	17	-24	19	22	46	39	52															
34	24	46	43	44	20	27	32	43	5	2	-1	23	5	49	28	42	74														
36	6	32	24	40	23	32	34	39	18	-14	14	29	-10	33	13	38	50	72													
38	-2	23	29	34	31	20	23	25	7	4	-7	10	5	36	29	28	44	55	53												
40	24	16	18	37	29	19	20	44	11	-6	-10	24	34	37	38	36	46	39	38	52											
42	29	14	17	30	16	2	14	39	26	32	-29	33	49	37	10	19	39	24	25	42	49										
44	1	27	24	31	20	31	40	33	2	17	-23	2	23	25	6	26	42	27	27	33	9	49									
46	0	16	23	27	9	15	23	23	1	-5	-8	7	9	20	13	35	30	27	27	44	18	29	76								
48	5	5	9	21	4	-4	1	18	22	0	-23	39	-18	53	20	39	32	43	54	44	36	36	36	61							
50	-1	-4	-8	17	13	3	5	12	12	24	-29	25	-21	60	29	21	19	23	32	21	15	24	33	46	79						
52	11	-22	-1	7	10	7	6	6	-1	25	-29	0	-1	36	0	6	4	14	9	16	12	18	31	48	48	64					
54	21	-5	5	7	12	16	21	31	-11	33	-38	1	8	24	1	25	21	25	25	16	26	27	42	43	43	42	76				
56	17	1	2	11	17	22	24	35	-19	33	-51	0	-2	36	25	27	27	18	15	18	41	30	47	42	53	55	59	77			
58	25	20	23	44	9	12	11	37	2	18	-34	20	14	28	50	38	40	28	28	28	46	35	40	53	65	62	47	55	76		
60	34	26	21	43	4	23	21	48	9	18	-22	21	20	24	44	34	36	24	37	22	38	36	43	46	43	50	46	59	72	89	

**Multiply tabular values by 0.01 to obtain correlation coefficients

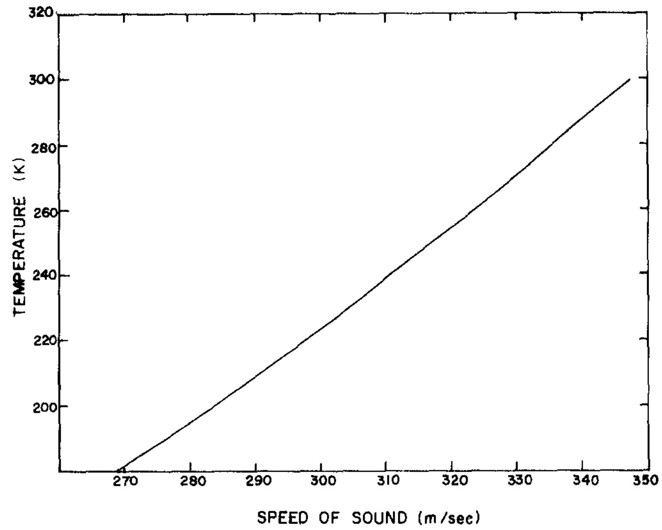

Figure 15-15. Speed of sound vs temperature (K).

where TAR represents the ratio of the thermal admittance of the ground to that of air. For diurnal cycles of net radiation, the ratio $(K/k)_{air}$ is the order of 10^4.

The most extreme surface temperature oscillation occurs over feathery snow where the amplitude may reach approximately four times that over still water or sandy soil, and is at least 100 times as large as that over the turbulent ocean. An amplitude ratio of about 3.5 can be expected for surface temperature over dry vs moist sand surfaces. Theoretically, the penetration of thermal "oscillations" into the soil is inversely proportional to the frequency of the "oscillations" [Lettau, 1954b]. The best insulator is still air or any porous material with air-filled pores, such as feathery snow; materials such as leaf litter have similar insulating properties [Geiger, 1957].

Much information is available on soil-temperature variations in various climatic zones. Table 15-17 gives annual and daily temperature cycles in different soil types. In addition to the type of ground, certain meteorological factors such as rainfall and melting snow have marked effects on the soil temperature. Snow cover is a leading factor in protecting the soil from severe frost. On one extreme occasion with an air temperature of 255 K, the temperature was 272 K under a 13 cm snow cover, whereas on bare soil it was 251 K.

The soil-temperature variations illustrated in Figure 15-16 were obtained at a station cleared of pine trees but in generally wooded country. Topsoil and brown sandy loam (0 to 0.6 m) changed to brown sand and gravel that varied from medium (0.6 to 2 m), to coarse (2 to 4 m), and again to medium (4 to 18 m). The water level was at 15 m. The figure illustrates the amplitude decrease and phase retardation of the annual cycle with depth. Amplitudes of weather disturbances with periods of several days, as illustrated by the temperature curve of the 0.75-m level, decrease with depth more rapidly than the annual amplitudes. Qualitatively, this agrees with the theoretical prediction of an amplitude decrement proportional to the square root of the length of the period of oscillation. The actual half-amplitude depth interval of the annual cycle can be estimated from Figure 15-16 as being nearly 3 m, which is much larger than the depth inferred from experimental values of thermal

Table 15-13. Bolometric records of area (approximately 37 m^2) surface temperature from an airplane cruising at approximately 370 m along a constant flight path, April 1944 [condensed from Albrecht, 1952].

Surface Temperature (K) — Bolometric Data										
Day	Hour	Sun's Elevation (degree)	Sky Cover	Standard Shelter Temp. at Airport K	Baltic Sea	Sand Beach	Down Land	City	Woods	Opening in Woods
9	13 to 14	40.4	10/10	282	275	285	287	281	280	281
11	10 to 20	−1.6	1/10	283	275	280	275	276	276	278
16	19 to 20	−1.8	9/10	287	277	281	280	280	277	275
20	05 to 06	0.5	1/10	275	278	271	267	272	270	266
29	14 to 15	42.1	4/10	280	280	319	315	290	289	296
				Wind Speed m/s	Woods	Clear Cutting in Woods		Dry Peat	Swamp	Pond
7	19	—	4/10	0.5	275	271		267	273	274
20	20	—	2/10	1.5	273	272		269	273	273
26	20	—	3/10	2.6	275	270		272	272	274
Albedo values as determined by Albrecht:					5%	8%		8%	7%	5%

Table 15-14. Temperature of the air 10 cm above, and of the soil 0.5 cm below, the earth/air interface measured by thermocouples [Davidson and Lettau, 1957].

	Temperature (K) at Mean Local Time								
Condition	0400	0600	0800	1000	1200	1400	1600	1800	2000
*Air	287.7	289.8	296.0	300.7	303.7	304.7	305.0	301.9	297.5
*Soil	290.6	290.9	296.0	304.1	308.6	309.2	306.8	302.3	298.5
**Air	281.1	282.5	291.5	297.9	301.7	303.0	301.1	296.1	292.3
**Soil	284.8	284.6	291.4	303.1	310.8	310.3	304.3	297.8	293.8

*Mean soil moisture in 0 to 10 cm layer 10% wet weight basis.
**Mean soil moisture in 0 to 10 cm layer about 4% wet weight basis.

diffusivity. The discrepancy may be caused by seepage or downward migration of rain water and the accompanying advection or transfer of heat. This process could increase the apparent or effective thermal diffusivity for annual soil-temperature variations by factors of 4 to 8 times the experimental values obtained in soil of constant moisture. The data in Table 15-17 are more in line with experimental findings than the curves in Figure 15-16. The limitation of Table 15-17 is that the data are for clearly defined and nearly ideal soil types that are seldom matched by actual ground conditions.

Factors that must be investigated and assessed for any one set of soil-temperature observations are (1) type and state of compaction of the soil, (2) moisture content and seepage of the soil during the test, (3) position of the water table during the test, (4) type and color of surface cover, (5) amount and nature of traffic over the site, and (6) local climatic conditions.

Subsoil temperature information is useful in computing thermal stresses and loads. Some examples are the determination of the depth to which a structure should be buried when proximity to natural isothermal conditions is desired to conserve on the air conditioning load, or to dissipate heat generated by power cables. The determination of frost penetration depths is usually the principal concern.

Table 15-15. Comparison of air and soil temperature with surface temperatures of materials exposed on a tropical island with normal trade winds. Air and material surface temperatures at 1.2 m above, soil temperature at 2.5 cm below, the earth/air interface. Exposed surface area about 930 cm^2 [Draeger and Lee, 1953].

	Temperature (K)		
	Highest	Average	
Material	Recorded	Max.	Min.
Air (1.2 m)	302	301	299
Soil (2.5 cm)	307	307	299
Wood	314	310	298
Aluminum	313	309	298
Galvanized Iron	318	311	298
Black Iron	324	315	298
Concrete Slab	310	307	298

15.1.7 Degree-Day and Temperature-Wind Combinations

A *degree-day* is a unit adopted to measure the departure of the daily mean temperature from a given standard. In the United States the number of *heating degree-days,* on any one day, is the number of Fahrenheit degrees of the 24-h mean temperature below 65°F (291 K). Cumulated, day by day, over the heating season, the total number of degree days becomes an index of heating fuel requirements. In such cumulation, the days on which the mean temperature exceeds 65°F (291 K) are ignored. When the centigrade scale is used, the base is usually 19°C (292 K). The United States Army Corps of Engineers computes "freezing-degree days" as the departure of the daily mean temperature from 32°F (273 K), a negative departure when above 32°F (273 K). The National Weather Service supplies "normal degree-days," both monthly and annual totals. A few examples of the 30-year annual normals are 9274(F°) for Fargo, N.D., 5634(F°) for Boston, Mass. and 108(F°) for Key West, Florida.

The *wind-chill* concept was introduced in 1939 by the famous antarctic explorer, Paul Siple, to measure the cooling effect of low temperature and strong wind combined. The wind-chill index is the equivalent temperature, in a normal walk (1.9 m/s) in calm air, corresponding to the combination of actual air temperature and windspeed. It can be related to the heat loss H from a nude body in the shade. H is given by

$$H = (10\sqrt{V} + 10.45 - V)(306 - T_a), \quad (15.22)$$

where H is the heat loss in kilogram calories per square meter of body surface per hour, T_a is the air temperature (K), and V is the windspeed (m/s). Neutral skin temperature is roughly 306 K. For windspeeds greater than 1.9 m/s the wind-chill index (T_{wc}) in K is given closely by

Table 15-16. Physical thermal parameters of diverse ground types [Lettau, 1954b].

Ground Type	Thermal Admittance Ratio (TAR), Ground to Air	Half-Amplitude Depth Interval (theoretical)	
		Annual Cycle (m)	Diurnal Cycle (m)
SOILS			
Quartz sand, medium-fine dry	110	1.0	0.05
8% moisture	230	1.6	0.08
22% moisture	360	1.5	0.08
Sandy clay, 15% moisture	280	1.3	0.07
Swamp land, 90% moisture	340	1.0	0.05
ROCKS			
Basalt	350	1.8	0.09
Sandstone	380	2.2	0.12
Granite	440	2.5	0.13
Concrete	440	2.3	0.12
SNOW, ICE, AND WATER			
Feathery snow	10	0.67	0.04
Packed snow	100	1.4	0.07
Still water	280	0.82	0.04
Ice	320	1.4	0.07
Turbulent ocean	10^3 to 10^5	61 to 610	3 to 30

$$T_{wc} = (306 - H/22). \tag{15.23}$$

This formula gives only an approximation because of individual body variations, incoming radiation, and other factors affecting heat loss from the body. The formula is not not used, or needed, with wind speeds less than 6 km/h (2 m/s).

Extreme temperature-wind combinations are frequently important in thermal equilibrium design problems, requiring estimates of the maximum steady wind speeds likely to be

Table 15-17. Annual and daily temperature cycles. Annual values are averages for the years 1939 through 1940 at Giessen, Germany [Kreutz, 1943]. Daily values are averages of clear weather, 10 through 12 August 1893, Finland, after Homen [Geiger, 1957].

	Temperature (K)					
	Annual Means			Daily Means		
	Loam	Sand	Humus	Swamp Land	Sandy Heath	Granite Rock
Surface	282.1	282.3	283.1	289.6	298.0	297.6
1.0 m above	283.8	284.3	284.3	—	—	—
0.6 m above	—	—	—	284.5	287.0	293.4
Surface Amplitude	283.5	283.7	284.4	283.4	290.0	283.2
	Half-Amplitude Depth Interval (m)					
Depth	1.8	1.6	1.4	0.05	0.08	0.15

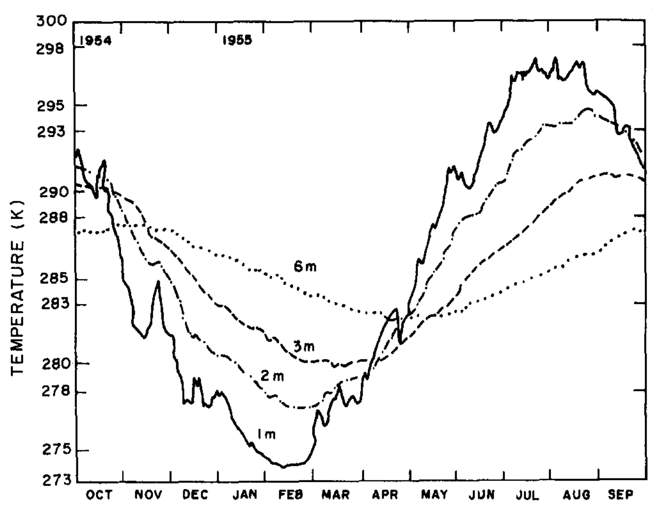

Figure 15-16. Variations of soil temperature at indicated depths; North Station, Brookhaven, Long Island, October 1954 through September 1955, [after Singer and Brown, 1956].

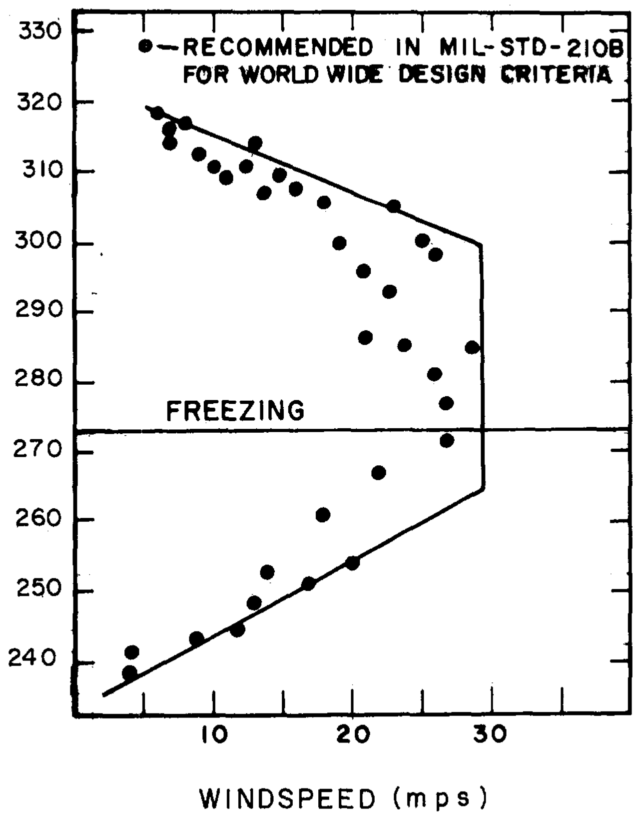

Figure 15-17. Extremes of temperature in combination with windspeed. Windspeeds, in general, were observed 12 to 30 m above the surface. The 35 observations were taken over a 5-year period at some 22 stations widely scattered in the United States. The envelope is for the recommended U.S. design criteria.

encountered at various temperatures. Figure 15-17 was prepared from 4 years of 6-hourly and 1 year of hourly data for 22 stations in the United States [Sissenwine and Court, 1951]. It shows maximum steady (5-min) wind speeds that occurred with temperatures in the range from 236 K to 319 K during this period. The stations used in this study were selected as representative of climatic areas in the United States. Mountainous stations were unrepresentative of generally operational areas and were not among those selected. Also, the high winds of hurricanes and tornadoes were omitted from the figure.

The wind speeds of Figure 15-17 occurred at anemometer heights, usually at 12 to 30 m above ground level during the years of observation. The wind speeds at the 3-m level are approximately 20% less and even 50% less for the extreme low temperature (less than 252 K).

The combination of values of temperature and windspeed, recommended for extreme U.S. thermal equilibrium design criteria, are shown by the envelope in Figure 15-17. This recommendation is not valid in mountainous areas or in Death Valley. For the latter the criteria are the same as for world-wide criteria, as plotted in Figure 15-17.

15.2 ATMOSPHERIC DENSITY UP TO 90 KM

The density data discussed in this section are from direct and indirect observations obtained from balloon-borne instrumentation for altitudes up to 30 km, and measurements from rockets and instruments released from rockets for altitudes between 30 and 90 km.

15.2.1 Seasonal and Latitudinal Variations

The Reference Atmospheres presented in Chapter 14 provide tables of mean monthly density-height profiles, surface to 90 km, for 15° intervals of latitude between the equator and the North Pole. Densities at altitudes between 10 and 90 km are highest during the months of June and July and lowest in December and January at locations north of 30° latitude. In tropical and subtropical areas seasonal variations are relatively small with highest densities at levels above 30 km occurring in the spring and fall.

Mean monthly density profiles, surface to 60 km, observed during the midseason months at Ascension Island, 8°S, 14°W, Wallops Island, 38°N, 75°W, and Ft. Churchill, 59°N, 94°W, are plotted in Figure 15-18. Densities are shown as percent departure from the *U.S. Standard Atmosphere, 1976*. The individual mean monthly profiles cross or converge near 8 km and between 22 and 26 km. Both are levels of minimum density variability. The level near 8 km is considered an isopycnic level because mean monthly densities depart from standard by no more than 1% or 2% regardless of the geographical location or season. Between 22 to 26 km, however, there is a marked seasonal variability, even though there is very little longitudinal or latitudinal variability during individual months. Seasonal differences in the density profiles at the same three locations are shown in Figure 15-19. The minimum seasonal variability of the mean monthly values, 1% to 2%, occurs at 8 km, and the maximum seasonal variability occurs above 60 km. The seasonal variations are largest at Ft. Churchill and are smallest at Ascension Island.

15.2.2. Day-to-Day Variations

The density at a specific altitude may differ from the seasonal or monthly mean at that altitude due to day-to-day changes in the weather pattern. The distribution of observed densities in January and July at the most climatically extreme locations for which data are available near 30°, 45°, 60° and 75°N are shown in Table 15-18a to 15-18d for altitudes up to 80 km. Median, and high and low values that are equaled or more severe 1%, 10%, and 20% of the time are given as percent departures from the U.S. Standard Atmosphere at 5-km altitude increments. The 1% values for altitudes

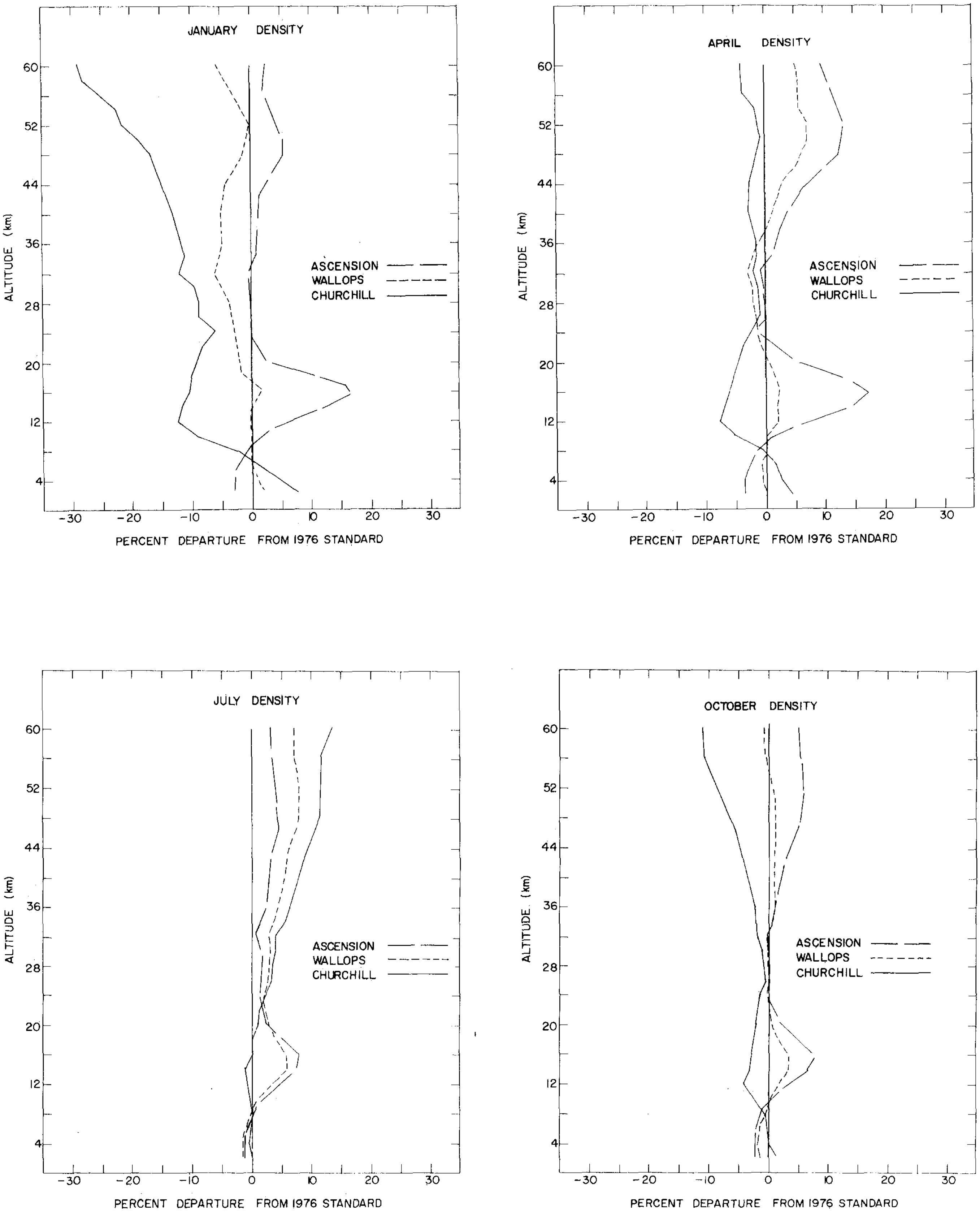

Figure 15-18. Latitudinal differences in the density-altitude profiles for the mid-season months at Ascension Island, Wallops Island, and Ft. Churchill.

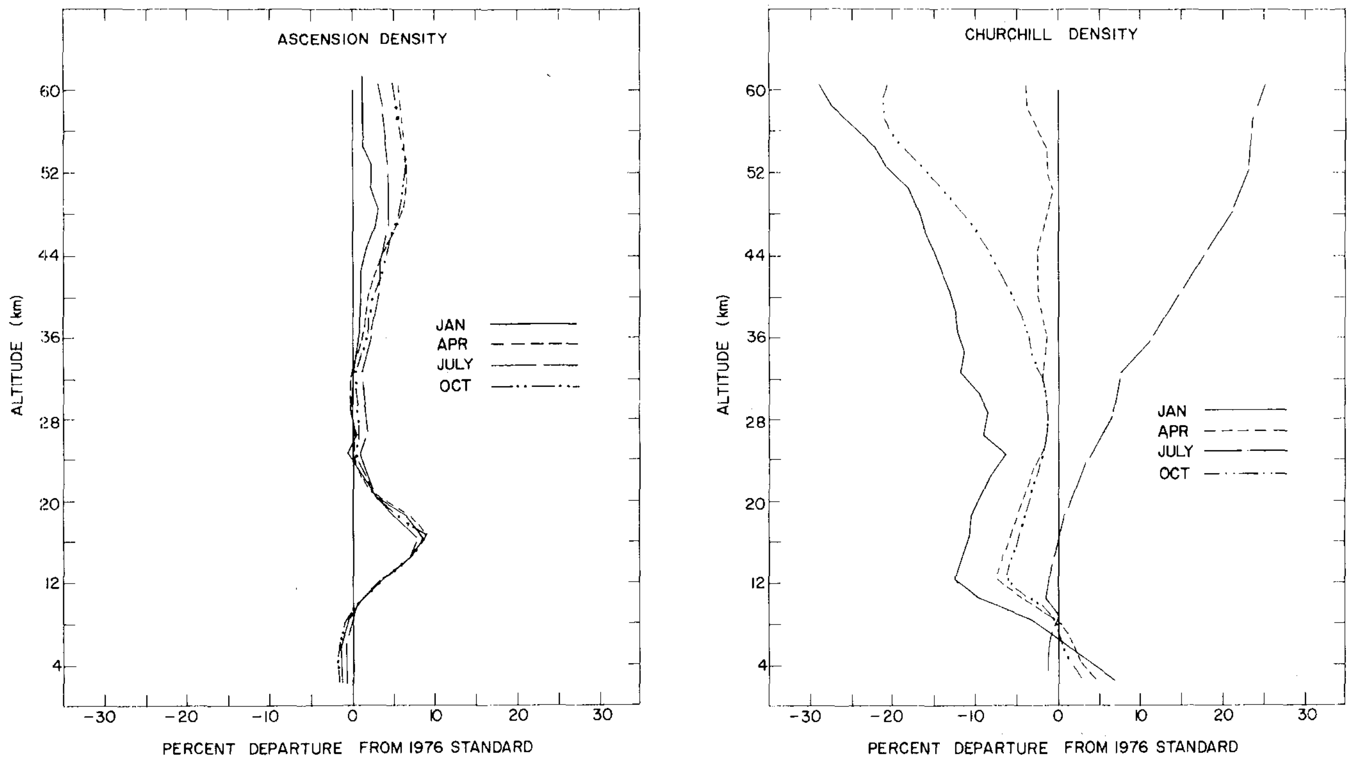

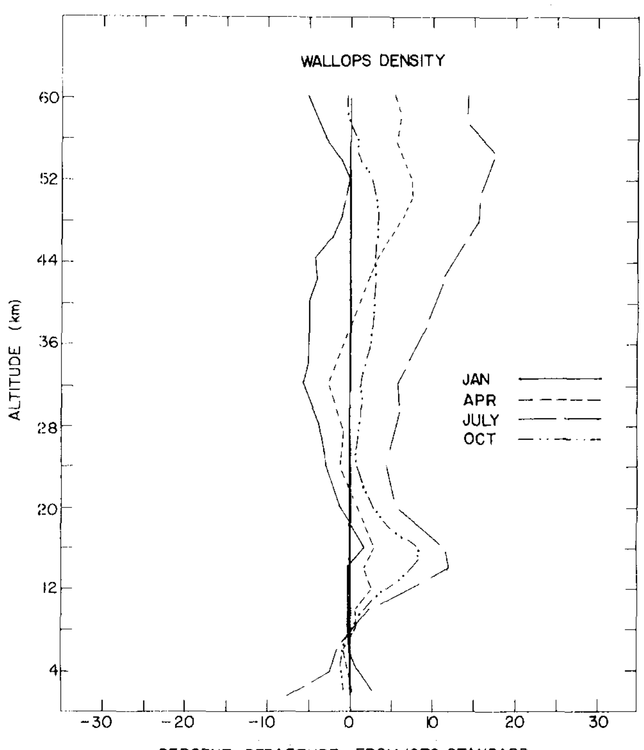

Figure 15-19. Seasonal differences in the density-altitude profiles at Ascension Island, Wallops Island, and Ft. Churchill.

above 30 km are considered rough estimates as they are based on the tails of the distributions of observed values plotted on probability paper. Estimates above 60 km are less reliable than those at lower levels because of the paucity of data and larger observational errors at the higher altitudes. In tropical regions the monthly density distributions are nearly normal for altitudes up to 50 km. Consequently, reasonable estimates of the distributions of density in the tropics can be obtained from monthly means and standard deviations. Standard deviations of the observed densities around the mean monthly values at Ascension, given in Table 15-19, are typical of the day-to-day variations found in the tropics [Cole and Kantor, 1980].

15.2.3 Spatial Variation

The rate of decay of the correlation coefficient between densities at two points with increasing horizontal separation is directly related to the scale of the major features of the weather patterns that are experienced at a specific latitude and altitude. Figure 15-20 provides information on the decay of density correlations with distance near 60°N for altitudes up to 60 km. The decay in density correlations below 20 km are based on an interpretation of data from studies of the spatial correlations of pressure, temperature, density and wind at radiosonde levels at locations between 30° and 70°N

Table 15-18a. Median, high, and low values of densities given as percentage departure from U.S. Standard Atmosphere 1976 for January and July at 30°N.

Altitude (km)	Median (% of Std)	1%		10%		20%		U.S. Std Density (kg/m^3)
		High	Low	High	Low	High	Low	
January								
5	−1	+1	−3	0	−2	0	−2	7.3643 − 1
10	+1	+4	−3	+3	−1	+2	0	4.1351
15	+7	+15	−1	+12	+4	+10	+5	1.9476
20	+3	+7	−2	+5	+1	+4	+2	8.8910 − 2
25	−2	+4	−6	+3	−4	+1	−2	4.0084
30	−4	+2	−10	−2	−8	−3	−6	1.8410
35	−3	+3	−12	0	−8	−1	−6	8.4634 − 3
40	−1	+2	−10	+1	−7	0	−5	3.9957
45	0	+8	−10	+3	−7	+2	−5	1.9663
50	+1	+12	−8	+7	−4	+5	−2	1.0269
55	0	+9	−10	+5	−6	+3	−4	5.6810 − 4
60	−2	+12	−15	+5	−9	+2	−6	3.0968
65	−4	+21	−25	+13	−13	+7	−6	1.6321
70	−5	+16	−26	+9	−17	+6	−12	8.2828 − 5
75	−7	+21	−25	+13	−15	+8	−10	3.9921
80	−4	+21	−22	+15	−13	+8	−7	1.8458
July								
5	−3	0	−5	−1	−4	−2	−4	7.3643 − 1
10	+1	+3	−1	+2	0	+2	0	4.1351
15	+16	+20	+11	+17	+13	+17	+14	1.9476
20	+8	+11	+14	+10	+5	+9	+6	8.8910 − 2
25	+4	+9	0	+7	+2	+6	+3	4.0084
30	+3	+7	−1	+5	+1	+4	+2	1.8410
35	+6	+10	+2	+8	+3	+7	+4	8.4634 − 3
40	+9	+15	+2	+11	+5	+10	+7	3.9957
45	+12	+19	+4	+14	+7	+13	+9	1.9663
50	+13	+23	+6	+17	+8	+15	+10	1.0269
55	+11	+20	+2	+15	+5	+13	+7	5.6810 − 4
60	+13	+14	−1	+21	+3	+19	+7	3.0968
65	+15	+43	−6	+38	0	+30	+6	1.6321
70	+15	+32	−9	+23	+1	+20	+8	8.2828 − 5
75	+10	+24	−11	+20	−6	+15	+1	3.9921
80	+6	+22	−15	+17	−6	+14	+1	1.8458

latitude [Bertoni and Lund, 1964]. Information on the spatial correlations at altitudes above 20 km is from a study by Cole [1979]. In that paper, data from constant pressure maps for 5.0, 2.0 and 0.4 mb levels were used together with nearly simultaneous rocket observations at several pairs of stations near 60°N to determine the rates of decay of density correlation at levels between 30 and 55 km. As Figure 15-20 indicates, the rate of decay in density correlation with distance decreases substantially with altitude. At 10 km, for example, zero correlation is attained at about 2000 km at 50 km, zero correlation is attained at more than twice that distance, or 4450 km. This analysis indicates the presence of disturbances with wavelengths of roughly 18 500 km at 50 km, close to planetary wavelength number one at 60°N. Information from Kantor and Cole [1979] on the correlations between densities at points up to 370 km apart in tropical regions is provided in Table 15-20, for levels between 10 and 60 km.

The rms difference between the densities at two points can be estimated by

Table 15-18b. Median, high, and low values of densities given as percentage departure from U.S. Standard Atmosphere 1976 for January and July at 45°N.

Altitude (km)	Median (% of Std)	1%		10%		20%		U.S. Std Density (kg/m^3)
		High	Low	High	Low	High	Low	
January								
5	0	+4	−3	+3	−2	+2	−1	7.3643 − 1
10	−2	+6	−10	+3	−6	+1	−4	4.1351
15	−3	+4	−12	+1	−8	−1	−6	1.9476
20	−2	+2	−8	0	−6	−1	−5	8.8910 − 2
25	−2	+2	−8	0	−6	−1	−5	4.0084
30	−5	+1	−17	−2	−13	−4	−9	1.8410
35	−6	+2	−20	−2	−16	−4	−12	8.4634 − 3
40	−8	+5	−23	0	−17	−4	−13	3.9957
45	−9	+8	−22	+2	−16	−3	−14	1.9663
50	+8	+11	−20	+4	−16	−3	−14	1.0269
55	−9	+9	−25	+2	−18	−4	−16	5.6810 − 4
60	−12	+7	−28	0	−23	−7	−20	3.0968
65	−14	0	−38	−5	−34	−10	−28	1.6321
70	−15	+2	−38	−9	−30	−12	−26	8.2828 − 5
75	−16	−3	−38	−9	−30	−12	−26	3.9921
80	−23	−2	−42	−8	−36	−10	−30	1.8458
July								
5	−2	+1	−5	−1	−4	−1	−3	7.3643 − 1
10	0	+3	−4	+2	−2	+1	−1	4.1351
15	+8	+17	+2	+15	+4	+13	+5	1.9476
20	+6	+11	0	+8	+2	+7	+3	8.8910 − 2
25	+7	+10	+4	+9	+5	+8	+6	4.0084
30	+7	+12	0	+9	+2	+8	+4	1.8410
35	+9	+16	0	+12	+3	+10	+6	8.4634 − 3
40	+13	+21	+4	+16	+3	+14	+10	3.9957
45	+15	+26	+6	+20	+10	+18	+12	1.9663
50	+17	+31	+9	+25	+12	+21	+14	1.0269
55	+17	+32	+8	+25	+11	+22	+14	5.6810 − 4
60	+19	+30	+4	+26	+10	+24	+13	3.0968
65	+20	+40	+4	+35	+10	+30	+13	1.6321
70	+20	+37	0	+32	+9	+27	+12	8.2828 − 5
75	+19	+40	−2	+30	+7	+26	+11	3.9921
80	+14	+32	−4	+30	+4	+25	+9	1.8458

$$\sigma_{xy} = \sqrt{\sigma_x^2 + \sigma_y^2 - 2r_{xy}\,\sigma_x\,\sigma_y}, \qquad (15.24)$$

where σ_{xy} is the estimated rms difference between densities at points x and y, $\sigma_x^2$and $\sigma_y^2$are the variances of density around the monthly mean values, and and r_{xy} is the correlation coefficient between the densities at points x and y. For short distances (up to 550 km) σ_x^2 and σ_y^2 can usually be assumed to be equal.

The estimated rms difference between densities that are observed simultaneously at locations 90, 180 and 360 km apart in the tropics are presented in Table 15-21 for altitudes between 10 and 60 km. For a given month, the rms differences provided in Table 15-21 can be considered to represent variability around the mean monthly density gradients, which are given in Table 15-22 [Cole and Kantor, 1975] for the indicated latitudinal differences. Longitudinal difference remain near zero in tropical areas. Information on the spatial variability of density is useful in determining how accurately a density observation taken 75 to 500 km from the point of

Table 15-18c. Median, high, and low values of densities given as percentage departure from U.S. Standard Atmosphere 1976 for January and July at 60°N.

Altitude (km)	Median (% of Std)	1% High	1% Low	10% High	10% Low	20% High	20% Low	U.S. Std Density (kg/m³)
				January				
5	+1	+6	−3	+4	−1	+2	0	7.3643 − 1
10	−6	+3	−15	+2	−15	−3	−10	4.1351
15	−9	−2	−15	−5	−12	−6	−11	1.9476
20	−8	−1	−15	−5	−11	−6	−10	8.8910 − 2
25	−7	+3	−16	−2	−12	−4	−10	4.0084
30	−10	+7	−32	+2	−18	−2	−15	1.8410
35	−12	+8	−35	−3	−27	−3	−19	8.4634 − 3
40	−15	+10	−36	+5	−30	−4	−20	3.9957
45	−21	+12	−39	+5	−34	−10	−24	1.9663
50	−26	+14	−43	+3	−36	−15	−29	1.0269
55	−32	+9	−48	−10	−39	−20	−35	5.6810 − 4
60	−36	+4	−54	−12	−40	−25	−39	3.0968
65	−36	−5	−50	−16	−46	−27	−42	1.6321
70	−37	−12	−54	−25	−49	−32	−43	8.2828 − 5
75	−35	−10	−53	−24	−47	−30	−42	3.9921
80	−28	−11	−53	−17	−47	−21	−40	1.8458
				July				
5	−2	+2	−5	+1	−4	0	−3	7.3643 − 1
10	0	+7	−8	+4	−5	+2	−3	4.1351
15	0	+6	−7	+3	−4	+2	−2	1.9476
20	+3	+7	−2	+6	0	+5	+1	8.8910 − 2
25	+5	+8	+1	+7	+2	+6	+3	4.0084
30	+7	+12	−1	+9	+2	+8	+4	1.8410
35	+10	+18	0	+14	+3	+12	+7	8.4634 − 3
40	+15	+23	+5	+19	+10	+17	+12	3.9957
45	+20	+28	+7	+25	+13	+23	+16	1.9663
50	+25	+35	+10	+30	+16	+28	+22	1.0269
55	+27	+35	+11	+30	+16	+29	+22	5.6810 − 4
60	+28	+42	+11	+39	+16	+33	+22	3.0968
65	+35	+50	+11	+44	+18	+39	+28	1.6321
70	+42	+52	+12	+46	+20	+44	+30	8.2828 − 5
75	+44	+58	+12	+52	+20	+48	+35	3.9921
80	+40	+56	+10	+50	+18	+44	+30	1.8458

vehicle reentry represents the conditions encountered in the reentry corridor.

15.2.4 Statistical Applications to Reentry Problems

The relatively large number of available radiosondes and meteorological rocket observations permit a detailed analysis of the characteristics of atmosphere density profiles at altitudes below 60 km. Arrays of means and standard deviations of density at 2-km intervals of altitude from the surface to 60 km, together with interlevel correlation coefficients between levels have been developed for tropical, temperate and arctic regions [Cole and Kantor, 1980]. Tables 15-23a to 15-23f contain statistical arrays of density for the months of January and July at Kwajalein (9°N), Wallops Island (38°N), and Ft. Churchill (59°N).

Variations in the range or deceleration of free falling objects or ballistic missiles that arise from day-to-day changes in atmospheric density can be estimated from Tables 15-23a to 15-23f. The integrated effect, E, of mean monthly density on the trajectory or impact point of a missile can

Table 15-18d. Median, high, and low values of densities given as percentage departure from U.S. Standard Atmosphere 1976 for January and July at 75°N.

Altitude (km)	Median (% of Std)	1%		10%		20%		U.S. Std Density (kg/m³)
		High	Low	High	Low	High	Low	
January								
5	+2	+6	−1	+5	0	+4	+1	7.3643 − 1
10	−8	+2	−18	−3	−13	−5	−10	4.1351
15	−10	−1	−18	−6	−14	−8	−13	1.9476
20	−12	−1	−22	−6	−17	−8	−15	8.8910 − 2
25	−15	−2	−28	−8	−20	−10	−18	4.0084
30	−21	−4	−36	−9	−26	−16	−24	1.8410
35	−25	0	−43	−10	−32	−16	−30	8.4634 − 3
40	−29	+4	−48	−9	−38	−16	−38	3.9957
45	−33	+8	−52	−6	−45	−16	−39	1.9663
50	−38	+4	−56	−8	−48	−20	−42	1.0269
55	−44	+5	−65	−10	−56	−23	−50	5.6810 − 4
60	−46	0	−70	−16	−60	−32	−55	3.0968
65	−47	+1	−66	−27	−62	−35	−58	1.6321
70	−48	−1	−69	−21	−62	−35	−60	8.2828 − 5
75	−45	−10	−65	+25	−57	−35	−53	3.9921
80	−40	−8	−55	−24	−50	−34	−45	1.8458
July								
5	1	+4	−2	+3	−1	+2	0	7.3643 − 1
10	−4	+5	−12	+3	−10	0	−7	4.1351
15	−4	+2	−9	0	−7	−2	−6	1.9476
20	+1	+6	−4	+4	−2	+3	−1	8.8910 − 2
25	+1	+10	−8	+6	−3	+5	−2	4.0084
30	+7	+13	+2	+10	+5	+8	+6	1.8410
35	+12	+25	+3	+18	+8	+16	+10	8.4634 − 3
40	+19	+27	+6	+23	+13	+21	+16	3.9957
45	+25	+35	+10	+30	+18	+28	+21	1.9663
50	+27	+40	+10	+35	+20	+32	+24	1.0269
55	+32	+42	+10	+39	+20	+35	+25	5.6810 − 4
60	+37							3.0968
65	+48	(Insufficient data above 55 km in summer)						1.6321
70	+60							8.2828 − 5
75	+67							3.9921
80	+64							1.8458

be determined for a specific location by computer "flights" through mean monthly or seasonal density profiles if the proper influence coefficients, C_i, for the missle at various levels are given. For example, we can write

$$E = \Sigma C_i \bar{\rho}_i \qquad (15.25)$$

where $\bar{\rho}_i$ is the mean monthly density at the ith level. The influence coefficients depend upon aerodynamic characteristics, reentry angle, and the speed of the vehicle. The integrated standard deviation in range or deceleration σ_{int}, due to day-to-day variations from the mean seasonal or the mean monthly density profile can be obtained from

$$\sigma^2_{int} = \Sigma_{ij} C_i \sigma_i r_{ij} \cdot C_j \sigma_j, \qquad (15.26)$$

where σ^2_{int} is the integrated variance for all layers being considered, C_i and C_j are influence coefficients at the ith and jth levels, σ_i and σ_j are the standard deviations of density at the two levels, and r_{ij} is the correlation coefficient between densities at the two levels. In these computations density is assumed to have a Gaussian distribution at all levels. As a

Table 15-19. Standard deviations (%) of observed day-to-day variations in density around the monthly mean at Ascension Island (8°S).

Altitude (km)	S.D. of Density (% of Monthly Mean)			
	Jan	Apr	July	Oct
5	0.4	0.3	0.3	0.4
10	0.4	0.4	0.4	0.4
15	0.8	0.7	0.8	0.7
20	1.5	1.3	1.8	1.3
25	1.3	1.3	1.2	1.3
30	1.2	1.2	1.4	1.2
35	1.8	1.8	1.4	1.2
40	2.3	2.1	1.8	1.8
45	2.3	2.3	2.6	2.3
50	2.7	2.5	2.6	2.7

result, the error in the CEP (the circle within which 50% of the events are expected to occur) will be generally less than 10%.

15.2.5 Variability with Time

Studies based on radiosonde observations have shown that there are no significant diurnal variations in density at altitudes up to 30 km. The analysis of meteorological rocket observations, however, indicates the presence of a significant diurnal oscillation in density at altitudes between 35 and 60 km. The phases and amplitudes of the diurnal oscillation at these altitudes are best defined in the tropics.

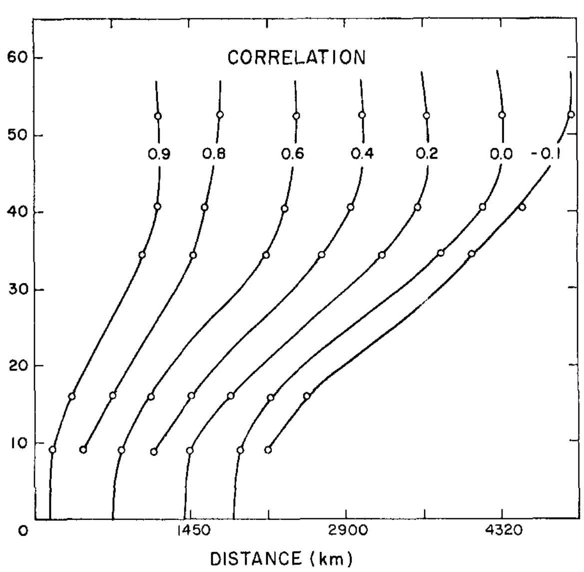

Figure 15-20. Decay of density correlations with distance at various altitudes in midlatitudes.

Table 15-20. Correlation coefficients between densities at points up to 370 km apart in the tropics.

Altitude (km)	Correlation Coefficient		
	90 km	180 km	370 km
10	0.97	0.95	0.90
20	0.98	0.97	0.92
30	0.98	0.97	0.92
40	0.98	0.97	0.92
50	0.98	0.97	0.92
60	0.98	0.97	0.92

The decrease in the number of available observations above 60 km and the larger random observational errors at the higher altitudes make it difficult to obtain reliable estimates of the magnitude of the diurnal variations at altitudes between 60 and 90 km.

The 50-km densities from a series of soundings taken at Ascension during a 48-h period in April 1966 [Cole and Kantor, 1975] are plotted versus local time in Figure 15-21. Densities are given as percent departure from those for the 1976 U.S. Standard Atmosphere. The crosses represent averages of observations taken within two hours of each other. Harmonic analysis of the eight average values produced the solid curve when the first and second harmonics for the 48-h period were added together. An F-test indicates that the second harmonic, which represents the diurnal oscillation in density, has an amplitude of slightly less than 4% (a range of almost 8%) and is significant at the 1% level; it reduces the observed variance by 91%. Maximums occur at 1600 and minimums near 0400 local time. From this analysis it is apparent that the diurnal oscillation is the dominant short-period fluctuation at 50 km.

The rms differences between density observations taken from 1 to 36 hours apart also provide a measure of the rate of change in density with time at a given altitude. Computed rms values from the Ascension series mentioned above are shown as a function of time in Figure 15-22 for altitudes from 35 to 60 km. The number of pairs of observations available for each time interval is also shown. Since at time T = 0 the rms change in space is zero, an estimate of the random observational error can be obtained from the observations themselves by extrapolating curves in Figure 15-22 back to zero hours. This procedure indicates that the random rms errors are approximately 1% at 35 and 40 km, and 1.5% to 2.0% at altitudes between 45 and 60 km.

If there are no well-defined periodic oscillations within a 24-h period, the rms variability would be expected to increase smoothly with time until it reached a value representing the climatic or the day-to-day variability around the monthly mean. However, a well-defined 24-h oscillation can be seen (Figure 15-22) in the rms density variations at

Table 15-21 Estimated rms differences (% of mean) between densities at locations 90, 180, and 360 km apart during the midseason months in the tropics.

Altitude (km)	90	January 180 km	360	90	April 180 km	360	90	July 180 km	360	90	October 180 km	360
10	0.10	0.13	0.18	0.10	0.13	0.18	0.10	0.13	0.18	0.10	0.13	0.18
15	0.13	0.17	0.25	0.11	0.14	0.21	0.16	0.20	0.30	0.16	0.20	0.30
18	0.50	0.61	1.00	0.34	0.42	0.68	0.30	0.37	0.60	0.34	0.42	0.68
20	0.28	0.34	0.56	0.28	0.34	0.56	0.24	0.29	0.48	0.24	0.29	0.48
25	0.28	0.34	0.56	0.28	0.34	0.56	0.24	0.29	0.48	0.26	0.32	0.52
30	0.30	0.37	0.60	0.30	0.37	0.60	0.28	0.34	0.56	0.30	0.37	0.60
35	0.34	0.42	0.68	0.30	0.37	0.60	0.30	0.37	0.60	0.36	0.44	0.72
40	0.40	0.49	0.80	0.44	0.54	0.88	0.48	0.59	0.96	0.44	0.54	0.88
45	0.46	0.56	0.92	0.40	0.49	0.80	0.60	0.73	1.20	0.52	0.64	1.04
50	0.56	0.69	1.12	0.54	0.66	1.08	0.72	0.88	1.44	0.54	0.66	1.08
55	0.66	0.81	1.32	0.56	0.69	1.12	0.84	1.03	1.68	0.78	0.96	1.56
60	0.84	1.03	1.68	0.66	0.81	1.32	1.00	1.22	2.00	0.82	1.00	1.64

all altitudes between 40 and 60 km with maximums at 12 and 36 hours and a minimum at 24 hours. An analyses of meteorological rocket observations taken at Kwajalein (9°N) and Ft. Sherman (9°N) show similar results [Kantor and Cole, 1981]. The diagram in Figure 15-22 and the results of similar studies show that in the tropics an observation 24 hours old is more representative of actual conditions than one 12 hours old.

The observed rms variations of density with time lags of 1, 2, 4 and 6 hours are shown in Figure 15-23 for levels between 60 and 90 km at Kwajalein. This information, from Cole et al. [1979], is based on a July 1978 series of high-altitude ROBIN falling sphere flights at Kwajalein. The first profile represents the estimated rms observational error.

The rms variations of density with time at the 50-km level are shown in Figure 15-24 for Wallops Island (38°N) and Ft. Churchill (59°N) for the months of January and July. Unlike the tropics, a 24-h oscillation in density is not apparent from this analysis which is based on eight years of data at Ft. Churchill and ten years at Wallops Island. The diurnal oscillation is relatively small and is probably masked by instrumentation errors and changing synoptic patterns. The rms variability at both locations increases with time until the climatic values of day-to-day variations around the monthly means are reached.

15.3 ATMOSPHERIC PRESSURE UP TO 90 KM

Pressure data provided in this section are based on (1) routine radiosonde observations taken by national weather services and extending to approximately 30 km, and (2) measurements from rockets and instruments released from

Table 15-22. Mean monthly latitudinal density gradients (% change per 180 km) in the tropics.

Altitude (km)	January Gradient (%)	April Gradient (%)	July Gradient (%)	October Gradient (%)
10	0.01	0.02	0.03	0.04
15	0.15	0.17	0.08	0.05
20	0.12	0.23	0.08	0.06
25	0.04	0.14	0.10	0.14
30	0.26	0.13	0.14	0.21
35	0.13	0.22	0.16	0.23
40	0.03	0.16	0.16	0.20
45	0.14	0.01	0.17	0.21
50	0.11	0.09	0.12	0.20
55	0.08	0.12	0.04	0.27
60	0.09	0.04	0.10	0.25

Table 15-23a. Kwajalein—Correlation of January density (kg/m) from surface to 60 km.

KM Kilometers Above Sea Level
MEAN Average of Observed Values
STDV Standard Deviation of Values Times 10
N Number of Values at Each Altitude

KM	.008	2	4	6	8	10	12	14	16	18	20	22	24	26	28	30	32	34	36	38	40	42	44	46	48	50	52	54	56	58	60
*MEAN	1167	969	786	639	516	416	332	261	199	141	934	654	464	342	248	182	133	980	725	538	401	303	230	175	234	105	818	640	504	397	310
	-3	-3	3	-3	-3	-3	-3	-3	-3	-3	-4	-4	-4	-4	-4	-4	-4	-5	-5	-5	-5	-5	-5	-5	-5	-5	-6	-6	-6	-6	-6
STDV	15	5	4	4	5	4	5	5	10	28	15	13	12	18	15	15	17	18	16	18	21	20	23	28	22	28	28	33	34	37	37
N	42	42	42	42	42	42	42	42	42	42	42	42	41	40	41	42	42	42	42	42	42	42	42	42	42	42	42	42	41	38	34
2	17	**																													
4	17	37																													
6	-4	7	22																												
8	-9	-24	2	14																											
10	9	10	17	9	58																										
12	7	17	1	21	44	74																									
14	9	-9	-23	3	23	27	49																								
16	2	7	-36	-11	-7	-10	4	29																							
18	-3	2	-22	-32	-37	-37	-14	-9	52																						
20	-1	9	8	19	7	28	17	7	12	15																					
22	1	-2	-22	-28	-25	1	-4	6	21	38	42																				
24	-30	0	-12	16	-6	-16	-5	27	14	7	5	31																			
26	-6	-4	6	-13	-4	4	-2	11	31	15	-5	14	41																		
28	16	14	10	2	-14	-9	1	-9	23	3	9	16	37	66																	
30	25	4	13	-14	-10	-8	-5	17	17	4	6	8	21	61	67																
32	15	-6	17	-14	-24	-8	-25	0	-4	-2	7	10	14	30	39	51															
34	0	5	-21	-10	-33	-8	-11	10	27	-5	-2	-3	10	30	24	41	48														
36	8	21	-1	3	-32	-7	-12	-2	7	-7	10	3	-6	3	18	31	35	52													
38	10	-9	-3	12	3	33	16	16	-9	-18	32	0	-1	8	5	32	35	61	55												
40	-1	-16	-24	7	-12	16	14	23	-5	-20	0	18	36	-1	8	14	24	45	36	57											
42	-4	14	4	34	-14	7	11	17	-18	-30	6	10	31	-12	24	15	27	33	39	42	70										
44	2	-3	-18	23	-20	8	12	29	-14	-23	9	16	26	-2	13	19	21	49	34	59	72	83									
46	-5	-15	-5	5	-6	4	3	31	-31	-26	6	16	32	3	4	22	22	31	19	44	47	58	72								
48	9	-20	-12	19	-15	-8	-3	29	-28	-30	-8	-4	34	-1	19	14	33	39	26	42	45	54	61	70							
50	3	-1	12	26	-22	-3	-5	5	-32	-37	-4	-11	14	-1	22	25	34	37	52	44	56	64	63	56	67						
52	-3	7	18	40	-17	5	15	9	-43	-42	14	-1	5	-30	3	-1	7	18	40	35	45	64	62	58	58	82					
54	-2	-8	0	28	-16	0	0	6	-41	-43	9	15	5	-34	-14	-16	2	9	32	25	52	60	63	62	53	67	88				
56	-3	-5	24	26	-14	-3	2	11	-40	-35	6	14	2	-31	-16	-18	-3	-7	19	14	42	56	55	62	41	52	79	90			
58	-9	-6	24	14	-19	5	0	12	-40	-28	7	27	4	-18	-11	-20	0	-6	20	14	35	50	55	67	43	62	81	88	92		
60	-27	5	7	27	-20	6	1	7	-37	-29	4	14	4	-25	-20	-32	-1	6	38	14	29	49	51	58	45	64	83	67	80	91	

*Multiply mean by indicated negative power of 10.
**Multiply tabular values by 0.01 to obtain correlation coefficients

Table 15-23b. Kwajalein—Correlation of July density (kg/m) from surface to 60 km.

KM Kilometers Above Sea Level
MEAN Average of Observed Values
STDV Standard Deviation of Values Times 10
N Number of Values at Each Altitude

KM	.008	2	4	6	8	10	12	14	16	18	20	22	24	26	28	30	32	34	36	38	40	42	44	46	48	50	52	54	56	58	60
*MEAN	1170	969	790	642	518	418	334	262	194	134	933	661	473	349	254	187	138	102	754	554	415	313	238	183	142	109	852	669	526	413	321
	-3	-3	-3	-3	-3	-3	-3	-3	-3	-3	-4	-4	-4	-4	-4	-4	-4	-4	-5	-5	-5	-5	-5	-5	-5	-5	-6	-6	-6	-6	-6
STDV	4	3	4	4	4	4	4	8	12	14	12	9	10	18	11	14	10	16	16	21	20	24	26	27	27	34	36	36	37	37	43
N	31	31	31	31	31	31	31	31	31	34	31	30	29	26	30	30	31	31	31	31	31	31	31	31	31	31	31	30	30	29	26
2	51	**																													
4	65	78																													
6	32	56	71																												
8	0	32	27	40																											
10	14	49	35	30	73																										
12	25	35	24	32	19	21																									
14	4	15	16	26	-20	-14	-4																								
16	-36	-34	-35	-34	-50	-61	-39	-1																							
18	-35	-51	-52	-23	-8	-15	-8	4	7																						
20	-24	-29	-9	2	-11	-15	-8	-11	20	6																					
22	-33	-57	-44	-29	-41	-55	-6	15	35	38	56																				
24	-28	-43	-9	-11	-19	-28	-12	-3	29	32	50	30																			
26	-28	-50	-31	-34	7	7	-39	-37	25	46	15	29	38																		
28	-55	-18	-25	-14	14	4	-31	4	32	25	15	14	2	41																	
30	-29	-20	-14	-3	-6	-7	-18	21	12	8	32	31	3	1	52																
32	-22	-21	-17	-19	-24	-1	-12	-17	12	35	31	33	26	36	32	31															
34	-9	4	8	3	4	12	-4	-10	14	13	36	37	5	28	26	24	47														
36	-34	-30	-25	-18	0	-4	-13	-27	31	11	52	45	12	22	15	17	26	62													
38	-38	-31	-17	-15	18	-6	-13	-31	23	27	37	33	37	44	34	13	20	40	54												
40	-34	-58	-50	-44	-6	-41	-6	-33	37	30	45	42	48	37	16	-4	-1	3	41	49											
42	-35	-55	-46	-44	-9	-33	-5	-18	37	45	29	38	48	27	12	-4	5	5	47	45	81										
44	-28	-34	-34	-42	-5	-15	2	-29	24	31	31	29	32	20	14	6	8	9	46	35	66	83									
46	-28	-36	-28	-32	-5	-19	-3	-26	24	26	44	38	33	27	24	16	9	16	50	46	69	74	92								
48	-36	-44	-42	-40	-10	-35	-19	-27	42	29	40	54	18	43	22	8	9	24	57	35	76	73	76	81							
50	-38	-40	-41	-34	2	-19	-8	-29	34	34	32	38	20	39	24	-3	2	16	48	28	75	76	77	77	91						
52	-26	-46	-39	-44	-3	-17	-14	-36	27	32	29	24	26	32	10	-3	-1	13	43	31	78	77	79	79	82	89					
54	-15	-41	-34	-50	-6	-18	-8	-29	20	31	27	19	31	19	3	-7	0	5	36	26	77	79	80	72	70	78	92				
56	-24	-40	-39	-47	-4	-25	-10	-36	20	30	33	24	29	27	19	-6	3	0	33	29	85	81	80	70	76	81	82	87			
58	-29	-38	-32	-29	-20	-47	-16	-27	39	23	44	39	34	15	29	1	13	2	39	29	78	75	69	69	75	77	70	72	87		
60	-51	-51	-43	-36	-10	-30	-10	-32	31	29	54	44	37	20	43	27	13	7	59	44	81	82	75	74	73	77	75	77	87	95	

*Multiply mean by indicated negative power of 10
**Multiply tabular values by 0.01 to obtain correlation coefficients

Table 15-23c. Wallops Island—Correlation of January density (kg/m) from surface to 60 km.

KM Kilometers Above Sea Level
*MEAN Average of Observed Values
STDV Standard Deviation of Values Times 10
N Number of Values at Each Altitude

KM	.015	2	4	6	8	10	12	14	16	18	20	22	24	26	28	30	32	34	36	48	40	42	44	46	48	50	52	54	56	58	60
*MEAN	1292	1029	821	658	524	411	310	227	168	122	874	638	452	331	241	175	128	936	689	509	379	285	216	187	130	102	601	627	486	378	293
	-3	-3	-3	-3	-3	-3	-3	-3	-3	-3	-4	-4	-4	-4	-4	-4	-4	-5	-5	-5	-5	-5	-5	-5	-5	-5	-6	-6	-6	-6	-6
STDV	23	26	16	10	15	35	51	43	41	39	29	40	25	22	23	25	29	36	38	48	50	47	42	44	44	46	47	50	52	55	63
N	44	44	44	44	44	44	44	44	43	43	43	43	43	42	43	43	43	43	43	43	43	43	43	43	43	43	43	43	39	33	16
2	74	**																													
4	66	92																													
6	34	28	53																												
8	-29	-62	-50	25																											
10	-33	-75	-74	-9	86																										
12	-42	-72	-79	-34	61	84																									
14	-39	-79	-83	-31	60	84	92																								
16	-42	-81	-84	-27	63	82	88	97																							
18	-39	-82	-81	-23	63	79	79	92	94																						
20	-37	-76	-72	-9	57	70	67	79	83	92																					
22	-34	-51	-47	-5	33	46	49	49	52	61	72																				
24	-21	-53	-46	2	36	39	40	48	55	69	76	59																			
26	-8	-48	-37	11	38	40	39	44	48	63	70	57	90																		
28	-21	-50	-41	5	45	45	35	41	43	58	62	51	79	83																	
30	-13	-45	-37	11	46	40	34	41	43	55	53	41	65	73	81																
32	-12	-28	-25	-3	21	18	28	33	36	38	29	19	41	46	53	80															
34	-17	-18	-24	-21	9	7	25	23	24	24	10	9	23	20	28	60	86														
36	-27	-17	-25	-32	3	1	23	22	25	20	4	1	14	4	12	38	69	89													
38	-28	-8	-16	-32	-5	-8	9	6	9	3	-12	-12	-2	-16	-13	9	42	71	87												
40	-29	-8	-14	-23	-1	-8	6	3	6	0	-13	-9	-2	-18	-13	9	35	65	81	95											
42	-32	-6	-7	-7	-6	-16	-3	-5	0	-8	-18	1	-3	-17	-12	5	26	51	67	80	87										
44	-34	-7	-5	-1	-6	-13	1	-1	4	-7	-16	3	-12	-22	-19	-2	19	36	53	64	72	89									
46	-30	-6	-2	3	-3	-10	-1	4	8	-3	-13	1	-12	-23	-19	-5	13	30	45	57	66	79	92								
48	-21	-6	-1	4	-1	-8	-2	7	9	-1	-13	-1	-17	-22	-19	-5	8	20	32	42	48	65	79	92							
50	-12	-7	-5	-1	1	0	3	12	13	3	-12	1	-21	-23	-25	-7	1	12	18	24	28	42	60	75	91						
52	-3	0	0	-3	-5	-5	-2	7	7	-3	-18	-10	-29	-31	-30	-13	-8	9	15	19	20	34	48	64	82	94					
54	-1	0	0	-6	-6	-5	-3	7	8	-3	-16	-14	-30	-32	-35	-21	-19	-8	0	3	5	22	42	55	75	88	94				
56	1	6	6	-3	-12	-12	-11	-1	2	-6	-16	-17	-28	-29	-33	-22	-23	-15	-9	-8	-1	13	33	51	74	86	87	95			
58	2	15	15	4	-7	-12	-10	-8	-5	-17	-28	-26	-39	-38	-40	-18	-15	-5	1	4	13	27	44	61	78	88	84	91	96		
60	-6	26	26	-8	-47	-46	-32	-29	-23	-41	-52	-48	-55	-59	-69	-55	-39	-19	-3	10	20	43	59	71	83	92	87	91	93	98	

*Multiply mean by indicated negative power of 10
**Multiply tabular values by 0.01 to obtain correlation coefficients

Table 15-23d. Wallops Island—Correlation of July density (kg/m) from surface to 60 km.

KM Kilometers above Sea Level
MEAN Average of Observed Values
STDV Standard Deviation of Values Times 10
In Percent of Mean Times 10
N Number of Values at Each Altitude

KM	.015	2	4	6	8	10	12	14	16	18	20	22	24	26	28	30	32	34	36	38	40	42	44	46	48	50	52	54	56	58	60
*MEAN	1192	980	798	647	522	420	333	254	184	131	934	673	486	360	264	194	143	106	786	588	441	332	253	195	152	119	933	734	574	451	352
	−3	−3	−3	−3	−3	−3	−3	−3	−3	−3	−4	−4	−4	−4	−4	−4	−4	−4	−5	−5	−5	−5	−5	−5	−5	−5	−6	−6	−6	−6	−6
STDV	14	8	6	5	6	7	9	18	17	14	11	12	12	15	17	18	20	21	22	26	31	32	31	32	36	38	42	42	43	47	33
N	37	37	37	37	37	37	37	37	37	37	37	37	37	37	37	37	37	37	37	37	37	37	37	37	37	37	37	37	34	30	18
2	77	**																													
4	40	72																													
6	26	55	82																												
8	25	39	55	66																											
10	17	32	42	48	73																										
12	0	16	18	20	27	71																									
14	−16	−21	−16	1	−8	11	42																								
16	−26	−31	−22	−16	−22	−10	21	64																							
18	−7	−5	−4	8	−2	−12	−3	47	75																						
20	−1	13	−6	12	7	−2	−3	24	36	61																					
22	−12	11	−9	10	3	3	18	12	21	35	68																				
24	−11	10	0	14	5	18	23	1	−1	13	63	75																			
26	9	17	2	4	−4	−2	9	5	−4	15	38	70	66																		
28	21	34	10	19	8	12	10	−1	1	22	61	77	75	83																	
30	3	7	−16	−9	−18	−4	5	−4	−3	13	53	67	75	70	84																
32	6	18	−2	−1	−13	−8	8	4	10	30	59	73	75	80	84	86															
34	−3	3	−17	−1	−7	−7	−2	0	−1	20	50	63	65	69	71	73	82														
36	5	11	−19	−5	−10	−9	2	13	7	29	51	67	57	71	75	74	83	88													
38	19	10	−19	−3	−12	−19	−12	11	1	30	48	56	50	73	74	73	81	82	90												
40	4	8	−15	−4	−17	−20	−9	2	−2	22	46	58	55	71	70	76	86	87	90	93											
42	2	7	−18	−5	−19	−22	−1	14	10	28	47	59	48	63	67	75	84	82	90	89	95										
44	21	27	−2	6	−7	−9	2	12	−5	16	44	58	48	71	75	68	80	78	87	88	86	89									
46	14	18	−10	−2	−10	−22	−10	13	−4	20	42	54	43	69	68	63	76	79	88	88	84	86	96								
48	7	7	−24	−9	−14	−20	−8	20	4	29	50	58	48	67	69	67	78	79	90	90	86	88	89	92							
50	12	12	−22	−11	−10	−15	−1	14	4	33	52	58	48	70	70	66	78	78	90	90	86	86	85	88	96						
52	11	5	−32	−21	−15	−22	−4	16	8	33	51	55	39	58	61	62	74	77	89	87	82	86	83	87	92	94					
54	8	5	−31	−21	−17	−25	−4	13	8	33	51	58	42	61	61	60	75	78	89	86	83	85	80	84	89	93	98				
56	9	8	−20	−6	−4	−11	−4	12	9	45	69	56	47	56	65	60	75	77	88	85	82	82	81	82	86	93	93	97			
58	12	6	−22	−5	−6	−17	−15	9	6	40	64	53	38	57	65	60	74	81	91	87	85	83	85	88	90	91	93	95	97		
60	−3	−16	−43	−13	−35	−2	35	50	24	31	29	23	32	32	33	45	55	76	85	78	79	78	73	78	83	93	91	91	92	96	

*Multiply mean by indicated negative power of 10
**Multiply tabular values by 0.01 to obtain correlation coefficients

Table 15-23e. Ft. Churchill—Correlation of January density (kg/m) from surface to 60 km.

KM Kilometers Above Sea Level
MEAN Average of Observed Values
STDV Standard Deviation of Values Times 10
N Number of Values at Each Altitude

KM	.035	2	4	6	8	10	12	14	16	18	20	22	24	26	28	30	32	34	36	38	40	42	44	46	48	50	52	54	56	58	60
*MEAN	1446	1078	848	666	511	375	273	201	148	109	806	591	439	312	227	166	120	881	641	471	347	256	191	142	108	814	625	479	372	286	220
	−3	−3	−3	−3	−3	−3	−3	−3	−3	−3	−4	−4	−4	−4	−4	−4	−4	−5	−5	−5	−5	−5	−5	−5	−5	·6	6	−6	−6	−6	−6
STDV	31	19	15	12	24	26	22	20	20	26	30	38	33	65	79	92	108	118	126	129	138	144	153	150	149	151	154	160	163	138	140
N	50	50	50	50	50	50	50	50	46	40	30	29	23	43	46	46	46	46	46	46	46	46	46	46	46	46	46	46	44	41	34
2	72	**																													
4	36	70																													
6	7	8	60																												
8	−6	−36	−8	55																											
10	−25	−49	−22	33	89																										
12	−34	−50	−24	20	71	94																									
14	−46	−55	−25	12	57	81	92																								
16	−49	−49	−19	0	37	63	76	89																							
18	−39	−26	−6	−3	15	32	42	62	85																						
20	−45	−22	3	4	−2	9	17	35	60	91																					
22	−38	−18	6	6	−11	−3	2	18	45	81	96																				
24	−26	21	56	41	−4	−3	1	11	31	72	91	98																			
26	−43	−28	8	21	−2	6	9	26	43	67	83	91	92																		
28	−47	−33	1	18	0	7	10	29	41	61	76	85	86	98																	
30	−43	−30	−1	17	−3	1	1	20	30	51	62	72	76	94	98																
32	−40	−30	−2	16	−4	−2	−4	15	24	43	54	65	69	90	96	99															
34	−34	−25	−4	12	−7	−8	−11	7	14	35	44	55	57	84	92	97	99														
36	−34	−29	7	11	−5	−7	−11	7	14	33	33	44	44	81	89	95	97	99													
38	−29	−29	−11	9	−3	−6	−11	5	11	26	22	32	29	76	85	92	95	97	99												
40	−25	−27	−12	8	−3	−8	−14	1	6	19	12	23	20	69	80	87	91	95	97	99											
42	−28	−29	−11	9	−2	−8	−14	−1	3	13	6	19	23	66	77	85	89	92	94	96	98										
44	−28	−30	−13	4	−5	−10	−14	0	3	10	5	18	20	64	75	82	86	89	90	93	94	98									
46	−32	−32	−13	2	−5	−8	−9	5	8	11	3	16	18	60	71	77	80	82	83	85	87	93	97								
48	−33	−33	−14	0	−2	−3	−4	8	9	10	3	16	18	56	67	71	73	74	75	77	79	87	93	98							
50	−34	−32	−16	−6	−2	−2	−1	10	10	10	7	17	18	47	56	60	61	62	62	64	66	76	84	92	97						
52	−35	−32	−16	−5	−1	−1	1	10	8	6	4	13	12	38	48	51	52	52	52	54	56	68	76	86	93	98					
54	−35	−31	−15	−5	−1	0	2	9	7	2	3	12	11	32	41	45	45	45	45	47	50	62	71	82	89	96	99				
56	−35	−30	−12	−5	−1	1	4	7	5	−2	3	12	12	29	35	39	37	37	36	39	41	54	64	76	86	92	97	99			
58	−32	−40	−35	−15	−4	−4	−3	−2	−7	−14	−12	−3	0	23	29	35	36	37	41	46	51	57	63	73	81	88	93	96	99		
60	−49	−42	−31	−6	1	−1	−1	0	−4	−10	−7	1	10	17	28	37	37	38	44	47	52	57	62	70	76	81	86	90	93	97	

*Multiply mean by indicated negative power of 10
**Multiply tabular values by 0.01 to obtain correlation coefficients

Table 15-23f. Ft. Churchill—Correlation of July density (kg/m) from surface to 60 km.

KM Kilometers Above Sea Level
MEAN Average of Observed Values
STDV Standard Deviation of Values Times 10
N Number of Values at Each Altitude

KM	.035	2	4	6	8	10	12	14	16	18	20	22	24	26	28	30	32	34	36	38	40	42	44	46	48	50	52	54	56	58	60
*MEAN	1236	999	810	654	525	409	306	224	166	122	901	662	487	362	267	197	146	109	813	610	460	349	267	206	161	126	992	765	620	492	389
	-3	-3	-3	-3	-3	-3	-3	-3	-3	-3	-4	-4	-4	-4	-4	-4	-4	-4	-5	-5	-5	-5	-5	-5	-5	-5	-6	-6	-6	-6	-6
STDV	21	12	11	10	10	19	39	24	22	20	16	14	12	15	13	12	12	13	11	14	15	16	18	21	22	23	23	25	27	29	32
N	28	28	28	28	28	28	28	28	28	28	28	27	27	28	28	28	28	28	28	28	28	28	28	28	28	28	26	25	25	20	19
2	55	**																													
4	59	85																													
6	49	74	89																												
8	39	43	61	78																											
10	8	-32	-19	-17	29																										
12	-17	-64	-54	-56	-24	69																									
14	-24	-69	-58	-56	-26	63	92																								
16	-32	-75	-64	-60	-32	56	88	96																							
18	-29	-74	-60	-54	-30	50	78	92	97																						
20	-28	-72	-60	-54	-33	44	71	87	93	98																					
22	-33	-72	-63	-57	-39	39	75	86	91	95	98																				
24	-42	-68	-62	-56	-44	33	71	81	85	87	89	95																			
26	-8	-42	-40	-40	-23	44	58	71	72	73	71	71	63																		
28	-9	-37	-37	-42	-17	51	51	63	61	60	57	56	49	93																	
30	-1	-33	-27	-34	-25	38	50	56	54	53	48	51	50	84	83																
32	-7	-23	-28	-32	-21	38	37	46	43	41	37	39	37	72	82	79															
34	10	-19	-26	-36	-29	34	37	37	36	32	27	28	25	60	72	77	88														
36	-27	-38	-43	-56	-46	18	36	35	34	30	28	33	39	29	41	48	63	67													
38	-34	-29	-44	-56	-45	4	14	26	27	26	29	33	34	29	46	30	63	53	71												
40	-25	-19	-32	-42	-37	-6	6	16	25	25	27	25	22	22	36	15	48	45	52	78											
42	-21	10	-3	-17	-18	-5	-6	-4	-1	-3	-3	-3	1	-5	17	6	42	37	44	64	80										
44	-45	9	-19	-28	-27	-9	-3	-4	-2	-6	-7	-6	3	-23	-3	-12	27	22	52	61	69	85									
46	-51	-28	-29	-40	-39	-18	-7	-6	-2	-3	-2	0	8	-19	-3	-11	26	19	57	68	62	64	85								
48	-42	-17	-18	-21	-31	-30	-15	-17	-12	-14	-16	-14	-5	-23	-9	-14	27	23	50	56	57	60	79	92							
50	-35	-7	-10	-10	-24	-30	-11	-12	-12	-14	-17	-14	-2	-23	-12	-7	33	23	51	51	50	60	78	79	89						
52	-31	9	2	-4	-21	-38	-18	-16	-21	-21	-20	-17	-11	-30	-19	-17	22	14	44	50	50	67	79	76	81	94					
54	-51	-12	-11	-14	-26	-36	-15	-6	-8	-5	-1	1	3	-28	-18	-21	21	9	48	58	56	70	81	81	80	87	95				
56	-44	-8	-10	-13	-23	-37	-24	-17	-16	-13	-8	-8	-7	-42	-29	-34	7	3	44	58	61	71	83	83	80	84	90	96			
58	-49	-10	-26	-24	-28	-24	-17	-19	-16	-17	-14	-13	-15	-43	-31	-41	1	3	37	39	55	71	84	78	76	81	87	92	98		
60	-66	-11	-29	-36	-39	-27	-17	-22	-17	-20	-16	-15	-17	-44	-30	-45	-8	-3	40	41	54	71	85	83	76	74	81	88	95	98	

*Multiply mean by indicated negative power of 10
**Multiply tabular values by 0.01 to obtain correlation coefficients

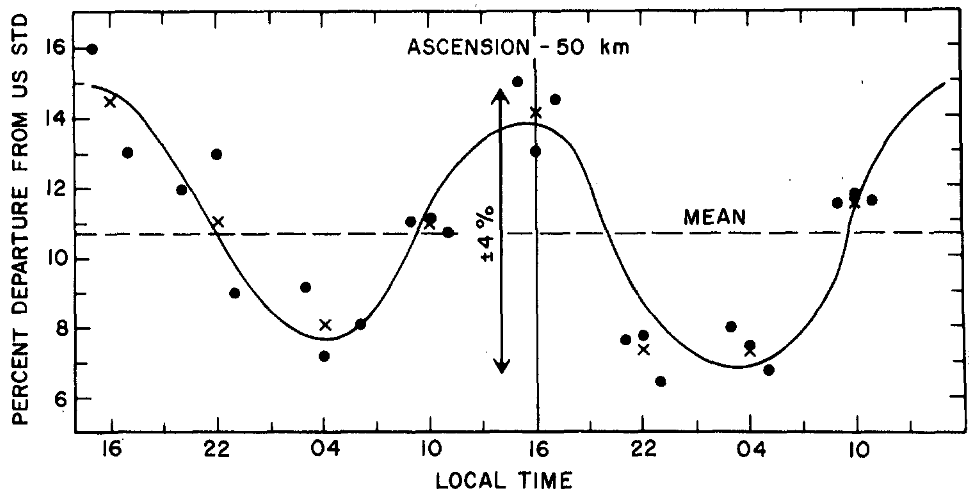

Figure 15-21. Diurnal density (50 km) variation at Ascension Island. (Dots indicate observed values, x's represent 3-h averages, and the solid line depicts the computed diurnal cycle.)

rockets at altitudes between 25 and 90 km. Both data sources are supplemented with pressures derived from measurements made from earth-orbiting satellites. Although atmospheric pressure above radiosonde altitudes is occasionally measured directly, it normally is calculated hydrostatically (as discussed in Chapters 14) from observed temperatures or densities for altitudes above 30 km. These data are intended for use in design problems involving variations in the heights of constant pressure surfaces and/or changes in pressure at specific altitudes.

15.3.1 Sea-Level Pressure

The variations of sea-level pressure normally have little effect on the operation of surface equipment. However, in the design of sealed containers that could possibly explode or collapse with pressure changes, the range of surface pressures likely to be encountered should be considered. Surface pressures vary with the height of the station above sea level as well as with changing weather patterns. Standard atmospheric pressure at sea level is 1013.25 mb, but there

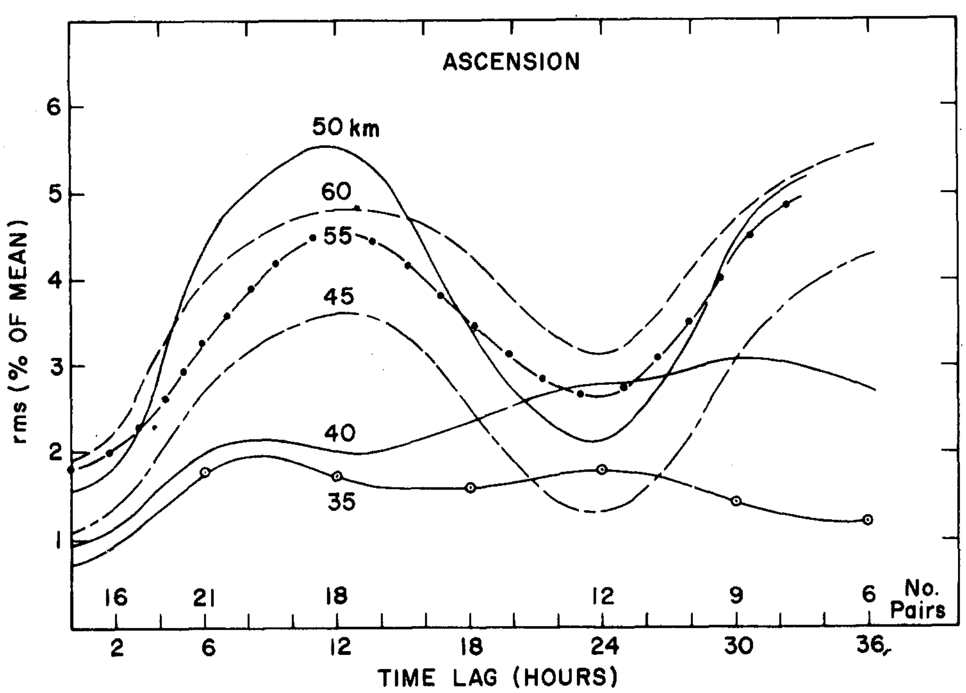

Figure 15-22. Root mean square (rms) lag variability of density with time at Ascension Island.

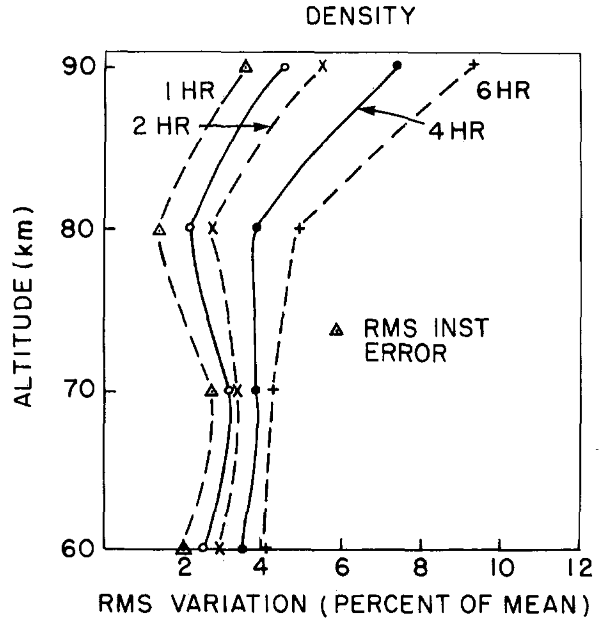

Figure 15-23. The rms variation in density for time lags of 1 to 6 h at Kwajalein.

are sizable variations from this value with both time and location.

Table 15-24 indicates extreme sea-level pressures that may be encountered in the Northern Hemisphere. During the month of January, pressures exceeded 99% of the time are given for areas under the influence of semipermanent cyclones, and pressures exceeded 1% of the time are given in areas under the influence of anticyclones. In the Northern Hemisphere extreme values, excluding tropical cyclones and tornadoes, are most likely to occur in these regions during January. Table 15-25 lists for comparison actual worldwide pressure extremes, including those resulting from storms of tropical origin. Examples of mean sea-level pressures and typical fluctuations are given in Table 15-26 which contains mean sea-level pressures for the four midseason months and the standard deviations of daily values around these means for 16 specific locations in the Northern Hemisphere.

Table 15-24. Sea-level pressures exceeded 99% and 1% of the time in January.

Location	Pressure (mb)
	Exceeded 99% of time
Aleutian low	965
Icelandic low	953
	Exceeded 1% of time
Siberian high	1057
Pacific high	1038
Canadian high	1052

15.3.2 Seasonal and Latitudinal Variations

The Reference Atmospheres presented in Chapter 14 provide tables of mean monthly pressure-height profiles,

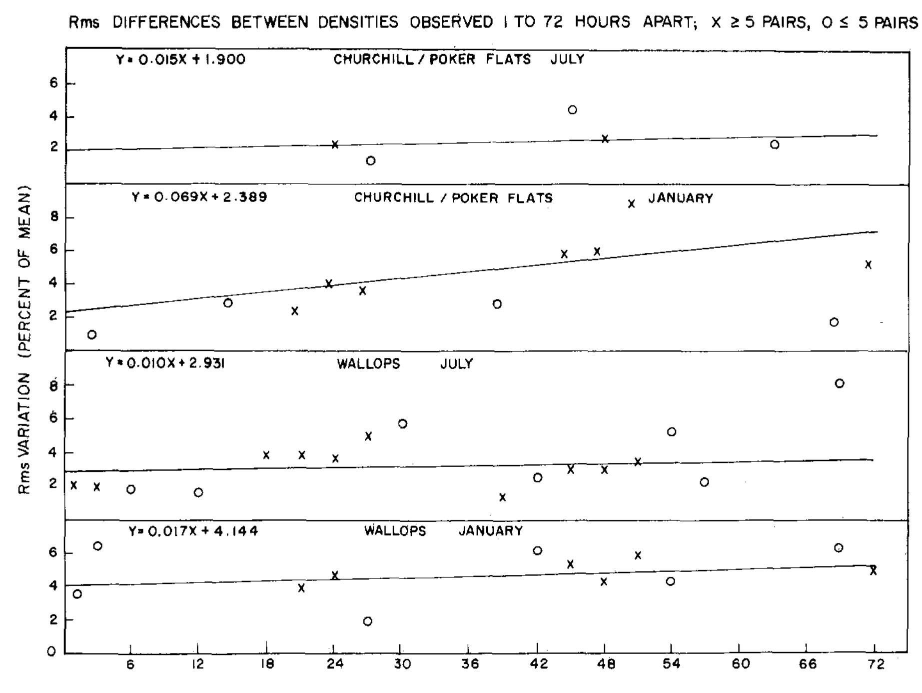

Figure 15-24. Rms differences between densities observed 1 to 72 h apart at 50 km (x ≥ 5 pairs, o ≤ 5 pairs).

Table 15-25. Worldwide pressure extremes.

	Pressure (mb)	Location	Date
LOW			
World	870*	17°N, 138°E, Typhoon Tip [Wagner, 1980]	12 Oct 1979
	876*	13°N, 141°E, Typhoon June [Holliday, 1976]	19 Nov 1975
	877*	19°N, 135°E. Typhoon Ida [Riordan, 1974]	24 Sep 1958
	877*	15°N, 128°E, Typhoon Nora [Holliday, 1975]	6 Oct 1973
No. America	892.3	Matecumbe Key, Florida, hurricane [Riordan, 1974]	2 Sep 1935
HIGH			
World	1083.8	Agata, Siberia [Riordan, 1974]	31 Dec 1968
	1075.2	Irkutsk, Siberia, [Valley, 1965]	14 Jan 1893
No. America	1067.3	Medicine Hat, Alberta [Riordan, 1974]	24 Jan 1897

*Dropsonde measurements

surface to 90 km, for 15° intervals of latitude from the equator to the north pole. These atmospheric models describe both seasonal and latitudinal variation of pressure. Figure 15-25 contain the vertical pressure profiles for the midseason months at each of four latitudes: 15°, 30°, 45° and 60°N. The profiles are displayed as percent departures from the *U.S. Standard Atmosphere, 1976*. Pressures at altitudes between 2 km and 70 or 80 km are highest in summer and lowest in winter over regions poleward of 30°N. In tropical latitudes, seasonal differences are small and do not display a systematic seasonal pattern. Departures from standard generally increase with latitude. Thus, largest seasonal differences are shown at 60°N where mean monthly pressures at 60 to 70 km are nearly 40% greater than standard in July and 30% to 36% less than standard in January. Consequently, July values are roughly twice those in January between 60 and 70 km. Pressures at these levels at 75°N (not shown) are roughly 10% lower than these values in winter and 15% higher in summer.

Table 15-26. Mean monthly sea-level pressures and standard deviations of daily values.

Location		January		April		July		October	
Latitude	Longitude	Mean (mb)	S.D. (mb)	Mean (mb)	S.D. (mb)	Mean (mb)	S.D. (mb)	Mean (mb)	S.D. (mb)
10°N	70°W	1013	2	1012	1	1012	1	1011	1
20°N	70°W	1018	2	1017	2	1018	2	1013	2
30°N	70°W	1022	6	1019	5	1021	3	1018	4
40°N	70°W	1018	10	1017	9	1016	5	1018	8
50°N	70°W	1016	12	1014	10	1011	6	1013	11
60°N	70°W	1008	11	1014	10	1008	7	1008	10
70°N	70°W	1004	11	1014	10	1009	6	1006	10
80°N	70°W	1011	11	1020	9	1011	6	1013	8
10°N	20°E	1012	4	1008	3	1009	2	1009	2
20°N	20°E	1017	4	1011	3	1008	2	1012	2
30°N	20°E	1019	5	1014	4	1012	3	1015	3
40°N	20°E	1018	9	1013	6	1013	3	1016	5
50°N	20°E	1020	12	1013	7	1013	5	1017	8
60°N	20°E	1015	16	1012	10	1011	7	1011	11
70°N	20°E	1004	15	1010	10	1012	7	1005	11
80°N	20°E	1008	15	1016	10	1014	7	1010	10

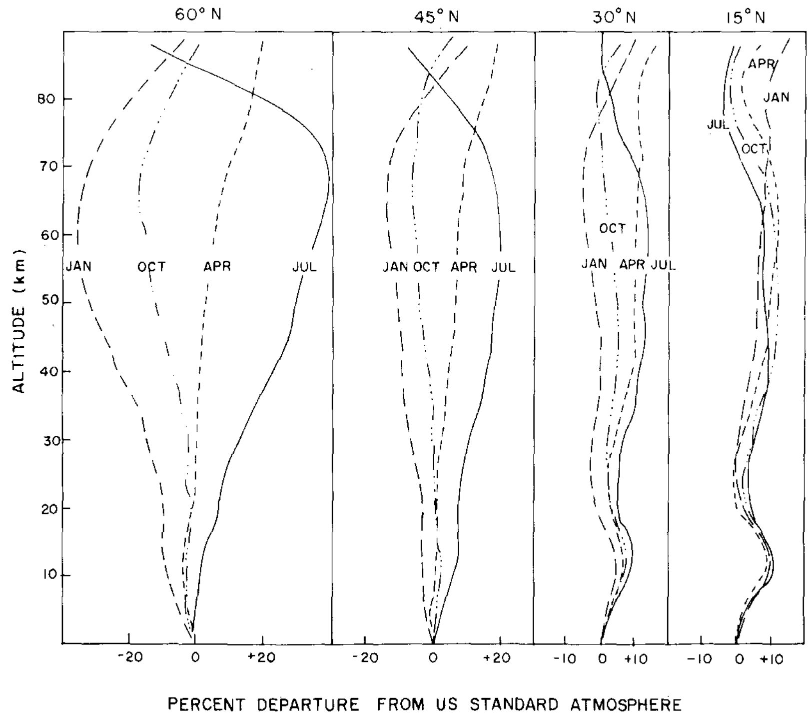

Figure 15-25. Pressure-altitude profiles for midseason months.

Table 15-27. Average height and standard deviation at standard pressure levels over North America, 90 to 100°W.

Average Height and Standard Deviation														
	20°N		30°N		40°N		50°N		60°N		70°N		80°N	
Pressure (mb)	Mean (km)	S.D. (m)	Mean (km)	S.D. (m)	Mean (km)	S.D. (m)	Mean (km)	S.D. (m)	Mean (km)	S.D. (m)	Mean (km)	S.D. (m)	Mean (km)	S.D. (m)
January														
700	3.165	30	3.115	55	3.015	85	2.865	100	2.770	100	2.710	90	2.690	75
500	5.845	40	5.745	85	5.565	125	5.340	145	5.180	150	5.075	140	5.055	125
300	9.595	55	9.425	125	9.150	175	8.825	195	8.585	230	8.425	210	8.380	180
200	12.280	70	12.090	130	11.765	165	11.430	175	11.180	190	10.995	200	10.920	195
100	16.455	55	16.325	95	16.110	110	15.890	145	15.655	175	15.400	195	15.195	190
50	20.540	130	20.500	200	20.415	215	20.280	215	20.075	200	19.775	180	19.440	180
25	24.900	210	24.865	245	24.790	335	24.555	275	24.380	245	23.905	245	23.425	230
15	28.100	245	28.050	335	28.000	365	27.750	365	27.650	350	27.000	335	26.350	305
10	30.600	250	30.550	380	30.500	400	30.250	380	30.150	380	29.500	320	28.750	260
July														
700	3.185	15	3.190	20	3.170	35	3.080	55	3.005	60	2.975	65	2.930	65
500	5.890	20	5.910	25	5.875	50	5.720	85	5.600	90	5.540	90	5.465	95
300	9.675	30	9.705	35	9.630	80	9.405	130	9.215	125	9.125	125	9.010	130
200	12.395	40	12.430	50	12.345	100	12.080	135	11.870	135	11.790	135	11.710	135
100	16.570	45	16.625	50	16.605	65	16.515	80	16.455	85	16.420	80	16.390	75
50	20.765	75	20.865	90	20.940	105	20.975	105	21.005	105	21.045	90	21.050	75
25	25.180	150	25.330	150	25.440	175	25.530	175	25.625	165	25.715	150	25.765	150
15	28.300	170	28.450	170	28.650	175	28.800	175	28.900	175	29.100	170	29.200	165
10	30.800	190	30.950	190	31.200	190	31.400	190	31.550	190	31.750	185	31.950	180

Table 15-28. Departures from mean monthly pressures (%) exceeded less than 5% of the time in January and July. Values below 30 km are based on radiosonde observations. Those values above 30 km are based on rocketsonde observations.

Height	January					July				
(km)	75°N	60°N	45°N	30°N	15°N	15°N	30°N	45°N	60°N	75°N
0	±2.5	±3	±2.5	±1	±0.4	±0.4	±0.5	±1	±1	±1.5
10	7	4	3	2	0.8	0.7	0.8	2	3	4
20	10	10	10	7	4	2	2	3	3	3
30	20	16	14	12	7	4	4	4	5	5
40		25	20	15	8	7	8	8	10	
50		30	25	18	10	10	12	13	14	
60		35	30	20	12	12	14	16	18	
70		30	25	18	10	10	12	15	16	
80		20	16	12	8	8	9	10	10	

15.3.3 Day-to-Day Variations

Changing synoptic situations, which include movements of high and low pressure centers and their associated ridges and troughs, and variations in the energy absorbed directly by the atmosphere, cause day-to-day changes in the height of constant pressure surfaces. Information on the magnitude of day-to-day variations in the heights of such surfaces are provided in this section. Detailed information for specific levels and locations should be requested if conditions appear critical.

Table 15-27 lists monthly mean heights of pressure surfaces in January and July and their standard deviations for middle North America. These data indicate the variation in the mean heights of constant pressure surfaces between 700 and 10 mb with latitude and season, and the estimated distributions of day-to-day variability around the monthly means. Estimated departures from mean monthly pressures, which are equaled or exceeded less than 5% of the time between 15° and 75°N, are shown in Table 15-28 as percentages of the mean January and July values, surface to 80 km.

As can be seen in Table 15-28, day-to-day variability generally increases with latitude and altitude in both January and July, although to a much smaller extent in July. The estimated 5% extremes are largest at 60 to 65 km at all latitudes, reaching ±35% during 60°N winter. Variability appears to decrease above 65 km to a probable minimum value near 85 km. The estimated departures shown in Table 15-28 include some diurnal and semidiurnal fluctuations due to solar influences, particularly since the basic pressure data were not observed at the same time every day. Envelopes of these estimated 95% values should not be used as profiles since such pressures would not necessarily be found at all altitudes at any one given time and/or location. Decreases in atmospheric pressure in one layer, for example, normally are associated with increases in another layer.

Table 15-29. Amplitudes of systematic pressure variations and time of maximum at Terceira, Azores [Harris et al, 1962].

		Diurnal		Semidiurnal	
Pressure Level (mb)	(m)*	Ampl. (mb)	Time (h)	Ampl. (mb)	Time (h)
Sfc	0	0.10	2100	0.50	0948
1000	122	0.10	1904	0.53	0950
950	570	0.12	1824	0.46	0956
900	1033	0.16	1612	0.49	1002
850	1454	0.18	1604	0.47	1002
800	2027	0.20	1612	0.44	1002
750	2569	0.20	1616	0.38	1010
700	3127	0.25	1548	0.37	1002
650	3731	0.18	1608	0.40	1030
600	4365	0.25	1608	0.33	1020
550	5051	0.27	1508	0.33	1034
500	5782	0.28	156	0.29	1032
450	6587	0.27	1424	0.24	1036
400	7449	0.31	1504	0.24	1046
350	8409	0.31	1504	0.20	1046
300	9482	0.32	1444	0.18	1108
250	10708	0.33	1420	0.16	1102
200	12149	0.32	1408	0.14	1110
175	12991	0.32	1352	0.13	1120
150	13948	0.30	1348	0.11	1100
125	15066	0.28	1328	0.11	1124
100	16423	0.26	1304	0.09	1128
80	17776	0.24	1300	0.09	1120
60	19547	0.23	1256	0.07	1124
50	20668	0.21	1256	0.07	1114
40	22077	0.20	1244	0.06	1116
30	24012	0.18	1256	0.05	1110
20	26673	0.16	1256	0.04	1128
15	28005	0.15	1252	0.03	1136
10	30507	0.12	1304	0.01	1204

*Estimated mean annual height

15.3.4 Diurnal and Semidiurnal Variations

Mean hourly sea-level pressures follow a systematic diurnal and semidiurnal periodicity somewhat variable in amplitude and phase according to location and season. The sea-level pressure cycle is generally characterized by minima near 0400 and 1600 hours and maxima near 1000 and 2200 hours local time. The amplitude approaches 1 mb, which is small relative to synoptic changes in middle latitudes. In the tropics only minor synoptic changes occur from day to day, so that interdiurnal pressure changes are small compared to the systematic daily variations in these latitudes.

Upper-air pressures appear to follow a systematic diurnal/semidiurnal cycle similar to that at sea level; however, extremes occur at somewhat different hours. Table 15-29 lists amplitudes and times of occurrence of diurnal and semidiurnal maxima to 10 mb (roughly 30 km) over Terceira, Azores, which provides an estimate of mean annual systematic pressure variations at a maritime location near 40°N. The *semidiurnal* variations at climatically and geographically different locations such as Washington, D.C. and Terceira, Azores, appear to be similar [Valley, 1965]. The *diurnal* maxima and minima, however, that result from solar insolation and terrestrial radiation, may differ considerably in time of occurrence and amplitude at various locations, particularly at or near surface levels.

REFERENCES — CHAPTER 15

Albrecht, F., "Micrometeorologische Temperaturmessungen von Flugzeug aus," *Ber. Deutsch Wetterd, Bad Kissingen,* **38:** 332, 1952.

Bertoni, E.A. and I.A. Lund, "Winter Space Correlations of Pressure, Temperature and Density of 16 km," AFCRL-64-1020, ADA611002, 1964.

Cole, A.E. "Review of Data and Models of the Middle Atmosphere," *Space Research,* **20** 1979.

Cole, A.E. and A.J. Kantor, "Tropical Atmospheres, 0 to 90 km," AFCRL TR-75-0527, ADA019940, 1975.

Cole, A.E. and A.J. Kantor, "Interlevel Correlations of Temperature and Density, Surface to 60 km," AFGL TR-80-0163, ADA090515, 1980.

Cole, A.E., A.J. Kantor, and C.R. Philbrick, "Kwajalein Reference Atmospheres, 1979," AFGL TR-79-0241, ADA081780 1979.

Davidson, B. and H. Lettau (eds.), *Great Plains Turbulence Field Program,* Pergamon Press, New York, 1957.

Draeger, R.H. and R.H. Lee, "Meteorological Data Eniwetock Atoll," *Naval Medical Res. Inst. Memo Rept. 53-8,* Bethesda, Md, 1953.

Geiger, R., *The Climate Near the Ground,* Harvard University Press, Translated by M.N. Stewart et al., 1957.

Gringorten, I.I., "Probability Models of Weather Conditions Occupying a Line or an Area," *J. Appl. Meteorol.,* **18:** 957, 1979.

Harris, M.F., F.G. Finger, and S. Teweles, "Diurnal Variation of Wind, Pressure and Temperature in the Troposphere and Stratosphere over the Azores," *J. Atmos Sci.,* **19:** 136, 1962.

Holliday, C.R., "An Extreme Sea-level Pressure Reported in a Tropical Cyclone," *Monthly Weather Rev.,* **103:** 163, 1975.

Holliday, C.R., "Typhoon June — Most Intense on Record," *Monthly Weather Rev.,* **104:** 1188, 1976.

Kantor, A.J. and A.E. Cole, "Time and Space Variations of Density in the Tropics," AFGL TR-79-0109, ADA074472, 1979.

Kreutz, W., "Der Jahresgang der Temperatur in Verschiedenen Boeden unter Gleichen Witerungs Verhaeltnisser," *Zeitschr, f. angewandte Meteorologie,* **60:** 65, 1943.

Lettau, H., "A Study of the Mass, Momentum and Energy Budget of the Atmosphere," *Archiv fur Meteorologie, Geophysik and Bioklimatologie,* Serie A, **7:** 133, 1954a.

Lettau, H., "Improved Models of Thermal Diffusion in the Soil," *Trans. AGU,* **35:** 121, 1954b.

National Weather Service, "Surface Observations," *Federal Meteorological Handbook 90-1,* Government Printing Office, Washington, D.C., 1979.

Riordan, P., Weather Extremes Around the World, Report ETL-TR-74-5, U.S. Army Engineering Topographic Laboratories, Ft. Belvoir, Va., 1974.

Singer, I.A. and R.M. Brown, "Annual Variation of Sub-Soil Temperatures About a 600-Foot Diameter Circle," *Trans. AGU,* **37:** 743, 1956.

Sissenwine N. and A. Court, "Climatic Extremes for Military Equipment," Env. Protection Br., Rpt. No. 146, Dept. of Army, Washington, D.C., 1951.

Tattelman, P., "Duration of Cold Temperature Over North America," AFCRL-68-0232, AD669567, 1968.

Tattelman, P. and A.J. Kantor, "Atlas of Probabilities of Surface Temperature Extremes: Part I, Northern Hemisphere," AFGL TR-76-0084, ADA027640, 1976a

Tattelman, P. and A.J. Kantor, "Atlas of Probabilities of Surface Temperature Extremes: Part II, Northern Hemisphere," AFGL TR-77-0001, ADA038237, 1976b.

Tattelman, P. and A.J. Kantor, "A Method for Determining Probabilities of Surface Temperature Extremes," *J. Appl. Meteorol.,* **16:** 175, 1977.

Tattelman, P., N. Sissenwine, and R.W. Lenhard, Jr., "World Frequency of High Temperature," AFCRL-69-0348, AD696094, 1969.

Valley, S. (ed.), *Handbook of Geophysics and Space Environments,* AFCRL, 1965.

Wagner, A.J., "Weather and Circulation of October 1979," *Monthly Weather Rev.,* **108:** 119, 1980.

WMO, "Proceedings of the World Climate Conference, Geneva, 12–23 Feb 1979," WMO Report No. 537, 1979.